Abstract

After the general introduction, characteristics of the world-wide distribution of the current origin for polar magnetic disturbances was examined systematically: positive bay, sharp negative bay, broad negative bay and giant pulsation are studied with special reference to the distribution of their equivalent current systems. Some remarks are also given for the peculiarity of the current system responsible for gaint pulsations (Chapter 1).

In comparison with the geomagnetic nature in polar disturbances, the world-wide patterns of *foEs* and *h'E* are shown in the next chapter. When examined in the light of world-wide pattern, the distribution of ionospheric activity (increase in *foEs*) is found to be quite similar to the geomagnetic activity around the auroral zone. There is also an evidence for a systematic fall of *h'Es* throughout the night in the auroral zone (Chapter II).

The subsequent chapter is devoted to the description of the world-wide charateristics of aurora, with reference to its altitude distribution pattern, which revealed itself to have strong resemblance to that of *h'Es*. From the resemblance, the origin of the two phenomena is first concluded to be common, and is suggested to be due to the effect of incoming corpuscular stream which penetrate into the level of the two disturbance phenomena (Chapter III).

A brief summary of the statistical results reached in the preceding chapters is given in the next chapter and the problems which are left unsolved in Part I (Chapter I-V) are also summarized. They include the problem of altitude effect on the disturbance phenomena, which is later solved in Chapter VIII (Chapter IV).

Subsequent chapters belong to Part II of the present paper, in which the numerical relations among the upper atmosphere disturbance phenomena are mostly discussed. To make clear the problems which will be dealt with in Part II, the physical quantities concerned are examined and selected for establishing inter-relations among the disturbance quantities. Then, the most important of them are concluded to be the magnitude of horizontal disturbance vector in geomagnetic field, maximum electron number density and the height of the level of the maximum density in *Es* layer or cloud and auroral zenith luminosity of λ5577 (Chapter V).

In introducing to part II, the relationship between the maximum number density of electrons in *Es* (n_{max}) and auroral zenith luminosity of λ5577 (J (5577)) are examined

with some references to the luminosity of NG based on the data at Syowa Station, the Japanese Antarctic Base. From the examination, it is established here that in an equilibrium state in aurora, $J(5577)$ is proportional to the second power of n_{max}, with a proportionality constant 5×10^{-10} KR/ (electrons/cm^3)^2, such as $J(5577) = 5 \times 10^{-10} n^2_{max}$.

The dependence of the proportionality constant on the altitude of disturbances is also examined. Further, from the dependence on altitude is obtained the dependence of effective thickness of auroral display on altitude, which in connection with the altitude dependence of effective recombination coefficient, is found to result in only a little altitude effect on the proportionality constant (Chapter VI). The study is further extended to the relationship between the magnitude of horizontal disturbance vector in geomagnetic field ($|\triangle \boldsymbol{H}|$) and auroral zenith luminosity of λ5577 ($J(5577)$). It is found that $J(5577)$ is proportional to the second power of $|\triangle \boldsymbol{H}|$ in an equilibrium state, as so is in J-n_{max} relation. But there is a number of factors which modify appreciably the relationship. A consideration, in which the factors are assumed to act on the proportionality constant in terms of a factor due to integration in some cases and of a factor due to impedance effect in the ionosphere in some others, is developed (cf. Chapters VII and VIII). It is concluded from the consideration above that simple relation holds between $|\triangle \boldsymbol{H}|$ and $J(5577)$ such as, $J(5577)_{in\ KR} = 3 \times 10^{-3}\ |\triangle \boldsymbol{H}|^2_{in\ \gamma}$ in the case of isolated bay disturbances, and the relations in cases of severe storms, *SSC**s, giant pulsations and short period pulsations can be interpreted as some modifications of the "standard" relationship. In addition, some remarks are given on a sort of giant pulsations which seems to have no related and ionospheric phenomena of appreciable magnitude (Chapters VII and VIII).

In Chapter IX are given summaries and discussions on the conclusions reached in Chapters VII and VIII. On the relationship between $|\triangle \boldsymbol{H}|$ and $J(5577)$, the factors which affect the relation, namely, the altitude effect, the effect of integration, the impedance effect and the change in electric field (Chapter IX) are discussed. By using the numerical relations among the disturbance quantities, an attempt is made to interpret the world-wide characteristics of the disturbance phenomena around the auroral zone. Then, it is shown that almost all the magnetic, the ionospheric and the auroral phenomena, except a sort of giant pulsations, may be reasonably attributable to the anomalous ionization with simultaneous excitation of the upper atmosphere particles due to the incoming of electrons with the energy ranging from 500 ev to 10 kev. The electric field in auroral forms is also studied in connection with some observational evidences which may indicate a possibility of its existence in the lower ionosphere during severe magnetic disturbances (Chapter X). In concluding, some of the important results obtained, with the problems which remained unsolved in the present paper, are summarized in Chapter XI.

GENERAL INTRODUCTION

It has been known for a long time that geomagnetic disturbances and the auroral displays have certain essential features in common, and the explanation of their physical mechanism is one of the oldest problems in geophysics[1-6]. The fact that the magnetic disturbances and auroral displays are concentrated around the auroral zone, has long led to the belief that the phenomena are caused by high-speed charged corpuscles guided towards the regions by the action of the earth's magnetic field. These ideas have received strong support from laboratory experiment with "Terrela" as first performed by BIRKELAND[7].

A direct proof of the entry of high-speed corpuscles into the upper atmosphere has been first obtained by the asymmetrical broadening of H_α (λ6562) line in the aurora by MEINEL[8] and GARTLEIN[9]. MEINEL had noted that the asymmetrical broadening is observed only when the direction of observation is along the magnetic lines of force. He concluded from his observation that, during a moderate aurora, the shift may correspond to a mean energy of incoming protons of 2 kev, with a maximum 10 kev, and that during intense auroral displays energy amounts up to 60 kev has been recorded. Recent development of rocket technique has made it possible to examine the nature of incoming particles directly and in full detail. DAVIES, BERG and MEREDITH[10] have found that with the aid of the data of four aerobee rockets which through the auroral rays, the most part of incoming particles are electrons with energy higher than 10 kev. The same kind of result have been obtained at about the same time by MCILWAIN[11], by using IGY rockets II 6.26 F and II 6.27 F. His results are summarized in Table 1.

Table 1. Incoming particles during auroral display.

Rocket	Object	Flux	Energy range
II 6.26 F	Auroral glow of	$2.5\times10^{6}\ e^{-E/30}$ protons/sec cm^2 sterad.	80-250 kev
	about intensity 1	$2.5\times10^{9}\ e^{-E/5}$ electrons/sec cm^2 sterad.	3-30 kev
II 6.27 F	Bright active	0.75 J is due to monoenergetic	
	auroral arc	electrons with energy of about 6 kev	
		5×10^{10} electrons/sec cm^2 sterad. (peak)	

Other kinds of evidences were presented in the ionospheric observations in high latitudes. As early as 1932, ionospheric storms accompanying magnetic storms and

auroral displays were found at Tromsö during the Second Polar Year. In particular. it was sometimes found that a strong absorption region was formed in the lower E layer, while the electron density in the ionospheric $F2$ region was generally reduced. The research of the abnormal ionization in the lower E layer in the polar region has been futher developed by OBAYASHI and HAKURA[12,13]. They have made an extensive analysis of ionospheric blackout, which is an outstanding feature in the polar ionosphere, and concluded that, some kinds of high-energy corpuscles are invading the polar region causing polar-cap blackout before the onset of magnetic storms, and that the blackout region moves to concentrate along the auroral zone as the magnetic storm proceeds.

In addition to the ground observation on earth storm, new knowledge on the physical condition of the earth's outer atmosphere has been brought out from direct observations by artificial satellite[14,15,16]. The first Explorer satellite, launched in 1958, showed that a large number of charged particles are trapped around the earth by its magnetic field above 1000 km. The deep space probes established the existence of two Van Allen radiation zones, the inner zone extending from about 1000 to 6000 km at low latitudes, the outer zone extending out to 6 earth radii or more in the equatorial plane. The characteristics of the radiation zones may be summarized as follows (Table 2).

Table 2 Observed particles in the radiation belts.

	Outer zone	Inner zone
height	1000-6000 km	1000 km
majority of particles	10^{11} electrons/cm^2 sec 20 kev 100 protons/cm^2 sec 60 Mev	10^9 electrons/cm^2 sec 20 kev 2×10^4 protons/cm^2 sec 40 Mev

The outer zone, descending from a maximum height around the equatorial plane approximately along the geomagnetic lines of force as the latitude increases, approaches the earth surface at about 50–55° in geomagnetic latitude just outside of auroral zone. Moreover, a strong evidence for a geomagnetic effect of the trapped particles in the outer zone was given by the Pioneer IV probe, launched during the period after several days of marked auroral activity, which showed much greater intensity of low energy electrons in the outer radiation zone than pioneer III, launched after a rather quiet geomagnetic period. The facts suggest that the Van Allen radiation zones, at least outer zone, are intimately related to the entry of high-energy corpuscles into the auroral zone, and it appears likely that the zone may have a rôle of a reservoir of charged particles.

Many evidences have been found, as stated above, to substantiate the belief that magnetic storms associated with ionospheric disturbances and auroral displays in the polar regions result from the entry of solar corpuscular stream into the auroral zone under the action of earth's magnetic field. There still remain, however, many unsolved problems for understanding the whole physical process of generation of the earth storms. One of the most fundamental problems may concern with the physical state of the lower ionosphere in the auroral zone, during magnetic disturbances associated with auroral displays.

The present study mostly concerns with the interaction of impinging corpuscles with the earth's upper atmosphere, and the mechanism of polar earth storm due to the energy flow of the corpuscles into the upper atmosphere in the auroral zone. At first the world-wide distribution pattern of various kinds of disturbances, *i.e.*, geomagnetic and ionospheric disturbances and auroral displays, with special reference to their altitude dependence will be dealt with. The result may give us information on the magnitude of energy and flux density of impinging corpuscular stream and on the mechanism of spatial distribution of the energy flow into the upper atmosphere in the polar region. Secondly the study concerns with the inter-relations among auroral displays, ionospheric disturbances and geomagnetic storms in the auroral zone, since it seems that problems have been not yet quantitatively established, though a number of studies on individual phenomena have been reported[19,20,21,22].

Auroral displays and anomalous ionization in the lower ionosphere may be attributable to excitation and ionization respectively of the earth's upper atmosphere due to the impinging corpuscles, and the anomalous ionization consequently may cause an additional electric current in the lower ionosphere which may result in geomagnetic disturbances. The corpuscular stream, however, may consist at least of two components, namely protons and electrons, and these two kinds of particles may have respective energy spectra. In addition, flux density of each particle group may also be a significant point in relation with the intensity and the height of ionization and auroral displays. For the purpose of attacking this problem, a number of data on geomagnetic disturbances, ionospheric disturbances and auroral displays in the northern and in the southern polar regions have been examined for the period during the International Geophysical Year.

As for the second point of the problems, that is, the inter-relations among the upper atmosphere disturbance phenomena, special synthetic observations of the earth's storm were carried out at Syowa Station (69° 00′S, 39° 35′E) near the auroral zone in Antarctica.

The present study consists of two parts. The one concerns the morphological aspect of upper atmosphere disturbance phenomena, which may indicate the characteristics of impinging corpuscular stream, and in the second part, the inter-relations of the disturbance phenomena in the polar region will be dealt with as quantitatively as possible.

PART I

I. WORLD-WIDE CHARACTERISTICS OF POLAR MAGNETIC DISTURBANCES

1. Early studies of polar magnetic disturbances

The systematic study on the morphology of magnetic storms had been commenced by CHAPMAN and his colleagues[23,24,25] in 1913, and has been extended by many investigators[26,27,28]. In their analysis, the average features of sudden commencements, *SSC*, the storm time variation *Dst* and the disturbance daily variation *SD* have been established. However, there have been left some ambiguities concerning the physical meaning of the statistical characteristics deduced from the mathematical average of the disturbance quantities. In fact, it was one of the most fundamental questions that, what represents the most elementary process of polar magnetic storms, the mathematical average or the individual disturbance. In 1948, NAGATA[29] and VESTINE[30] examined detailed aspect of individual disturbance field for some typical magnetic storms, and pointed out that the disturbance field does not always appear in the idealized form which is derived from the early statistical study (Fig. 1.). This study was further extended by FUKUSHIMA[31], who finally concluded that polar magnetic storms are composed of a number of elementary disturbances, such as shown in Fig. 2, which is the most elementary pattern of the disturbance, shown by a simple doublet field type current-system centered around the auroral zone. His results showed that the elementary disturbances, regional in space and enduring short in time, are the most fundamental disturbances in the polar regions.

2. A trial classification of polar magnetic disturbances

As FUKUSHIMA has pointed out, the polar elementary storm can be represented by an equivalent current system of simple dipole type, which takes place intermittently or successively with a short duration, along the auroral zone. The distribution pattern of the occurrence probability, however, is not yet clear enough for the examination of inter-relations among the world-wide pattern of disturbance phenomena, though it reveals itself to be one of the most important problems in connection with the spatial distribution of impinging corpuscular stream. But it seems necessary to re-examine

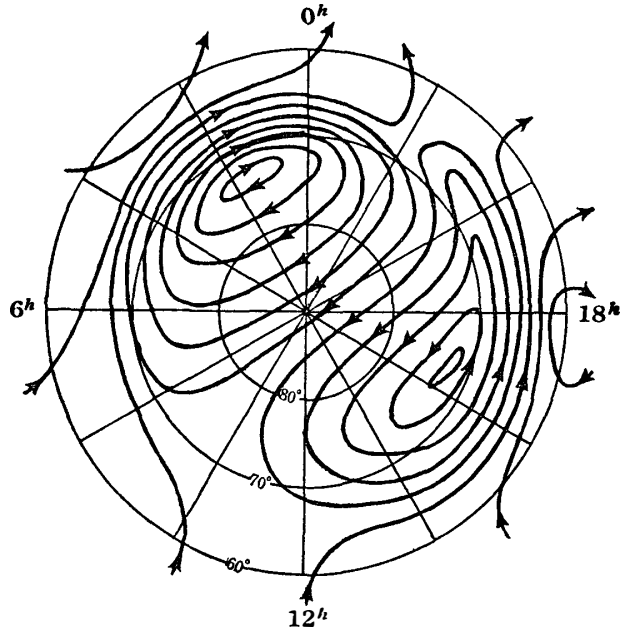

Fig. 1. The mean equivalent current-system for polar magnetic storms during the Second International Polar Year (electric current between adjacent stream lines is 2.9×10^4 amp.). After NAGATA.

the characteristics of polar elementary storm, before the distribution pattern is studied, because the so-called polar elementary storm may consist of physical process more elementary, or may include other kinds of disturbance in it. An attempt then was made for a trial classification which concerns mostly with the magnitude of time derivative of disturbance field and their dependence on local time.

One may notice at a glance of magnetograms recorded at high latitudes that the geomagnetic variation of fairly large amplitude, whose duration is from several minutes to a few hours, shows characteristic sharpness of the onset of the variation. It may be considered that the so-called polar elementary storm has its commencement of sharpness which depends on the local time when it occurs. Fig. 3 shows the average curves for time derivatives on the magnitude of geomagnetic horizontal vectors, observed at Syowa Station in the southern auroral zone, during March, June, September and December in 1959. It is obvious in the figure that, an average $|d\boldsymbol{H}/dt|$ has a fairly definite pattern, showing large values around local midnight, with two maxima in equinox and with broad one in June and December solstice.

An important problem here will be whether or not each of the values $|d\boldsymbol{H}/dt|$ can be classified into certain goups, since this problem ought to be examined in connection with other, *i.e.,* ionospheric and auroral phenomena. The study of the total occurrence frequency may be an answer to this question. The distributions of total occurrence frequency of each value are shown in Fig. 4. It seems that the values may be divided into two groups; namely sharp ($d\boldsymbol{H}/dt > 30\gamma$/min) and broad group ($d\boldsymbol{H}/dt < 30\gamma$/min), the later of which include the so-called positive bays whose

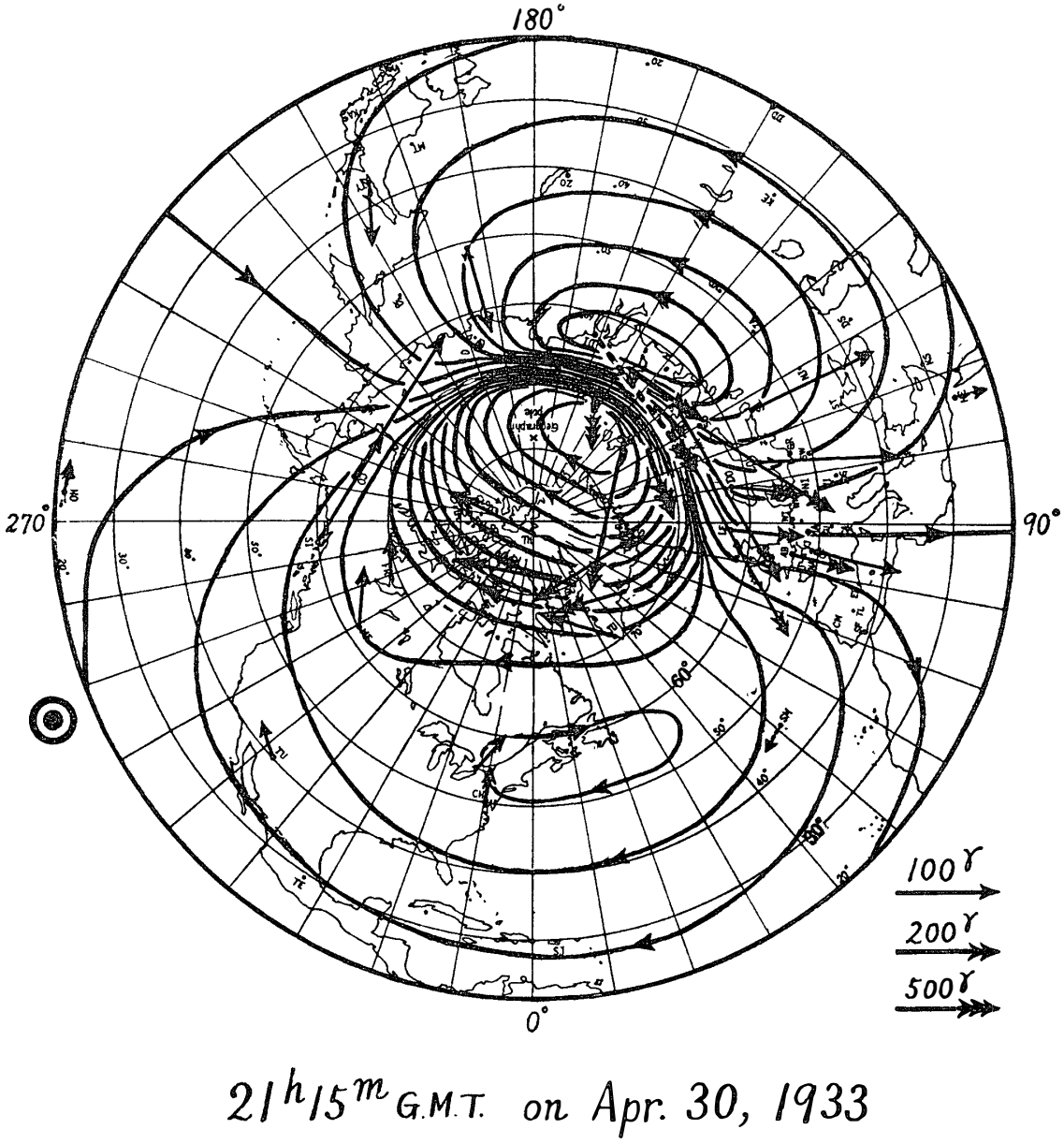

Fig. 2. The equivalent current-system for a polar magnetic storm. After FUKUSHIMA.

occurrences are mostly concentrated in the evening, as seen in Fig. 3. Then, the results bears out a conclusion that the polar magnetic storms are composed at least of three kinds of disturbance, that is, the sharp negative group, the broad negative group and the broad positive group.

In addition to these three kinds of disturbance, characteristic pulsative variations are found frequently on the magnetograms at high latitude stations. They may be the so-called giant pulsations, or other kinds of pulsative variation, the study of which has been developed recently in connection with the oscillation of earth's magnetic field in the earth's outer atmosphere[32,33].

These four kinds of disturbance, mentioned here, have their own characteristic

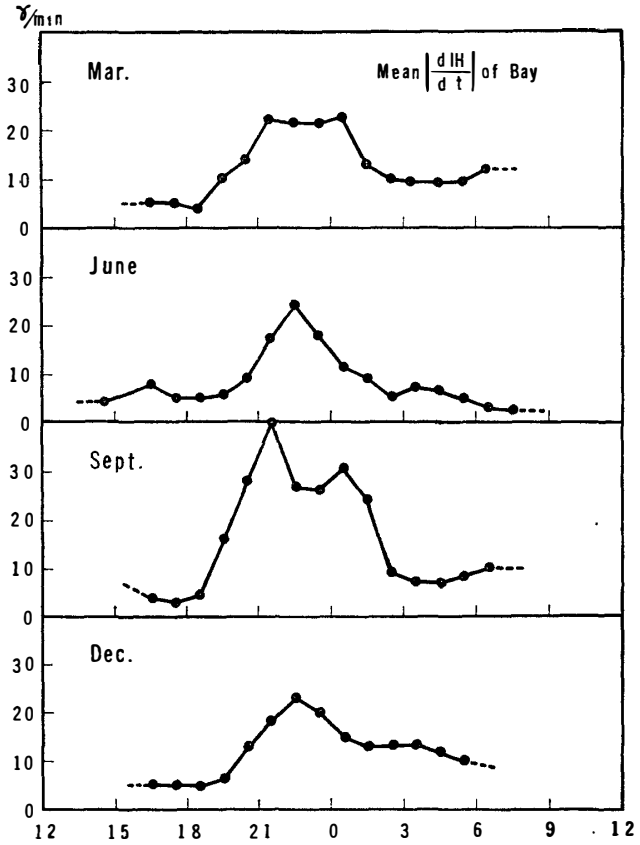

Fig. 3. The local time changes in mean time derivatives of geomagnetic horizontal disturbance vector of bay disturbances ($d\boldsymbol{H}/dt$) at Syowa Station.

feature, for example, in the local time dependence, in the spatial distribution of magnitude and in the duration of occurrence.

For the purpose of establishing the characteristics of the disturbances, further examination by means of distribution pattern will be useful especially with respect to the relationship with the ionospheric and auroral phenomena. From this standpoint, the distribution patterns of them will be dealt with in the next paragraph.

3. Occurrence probability of polar magnetic disturbances

The geomagnetic activity is generally predominant in night time at high latitudes (Fig. 5), and the type of disturbances may be classified into four groups as has been already stated in the preceding paragraphs. An example of traces on magnetograms of the four kinds are illustrated in Fig. 6.

As for the occurrence frequency of each group at Syowa Station, positive group mostly occurs from evening to night, while the majority of the disturbances around midnight are sharp negative group, and broad negative group is concentrated in the morning (Fig. 7). The mean values of $|d\boldsymbol{H}/dt|$ for positive bay group and for broad negative bay group is approximately equal to each other and are to be a few tens of

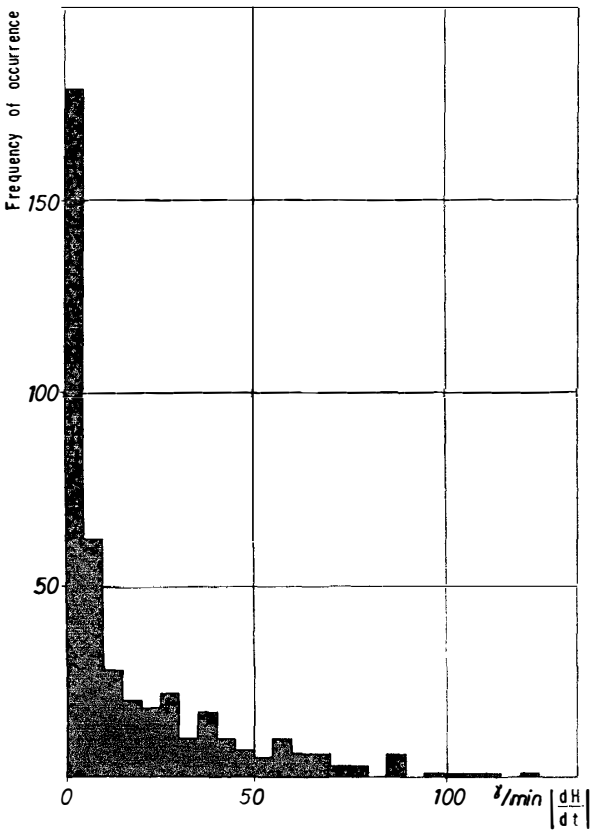

Fig. 4. The distribution of occurrence frequency with respect to the magnitude of the time derivative (dH/dt).

gammas per minute, while in the case of sharp negative bays, it sometimes amounts up to about 300 gammas per minute.

As already established by FUKUSHIMA, polar elementary disturbance may be attributable to an equivalent current-system of simple dipole type, with the main axis being approximately along the auroral zone. The centre region of the overhead current-system, where the current seems to be generated, is rather regionally limited in small linear dimension. This area will be called hereafter as a magnetically activated area in the polar region. Examples of the simple current-system responsible for sharp negative bay, broad negative bay and positive bay are given in Fig. 8.

In order to confirm such an occurrence probability of polar disturbances as obtained at Syowa Station, the world-wide distribution pattern of activated area is examined. A number of data on polar storms at the stations well distributed around in northern high latitudes, have been collected for this purpose. The stations whose data are used in this analysis are ginven in Table 3 and Fig. 9, for the period of analysis covering from January to July 1958 during the IGY.

On examining the world-wide data of polar storms, it has become evident that the occurrence probability of activated area of the three kinds of group shows a considerable local time inequality of occurrence in addition to the characteristic dependence on

Fig. 5. The local time change of mean geomagnetic activity normalized to the equivalent amplitude, at Syowa Station.

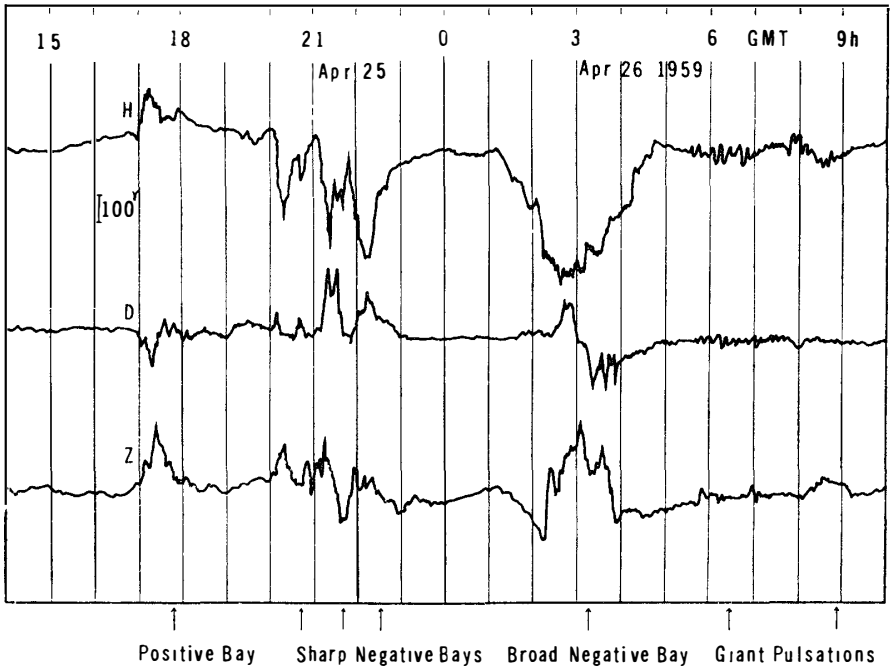

Fig. 6. Examples of four kinds of polar magnetic disturbances, positive bay, sharp negative bay, broad negative bay and giant pulsation, observed at Syowa Station.

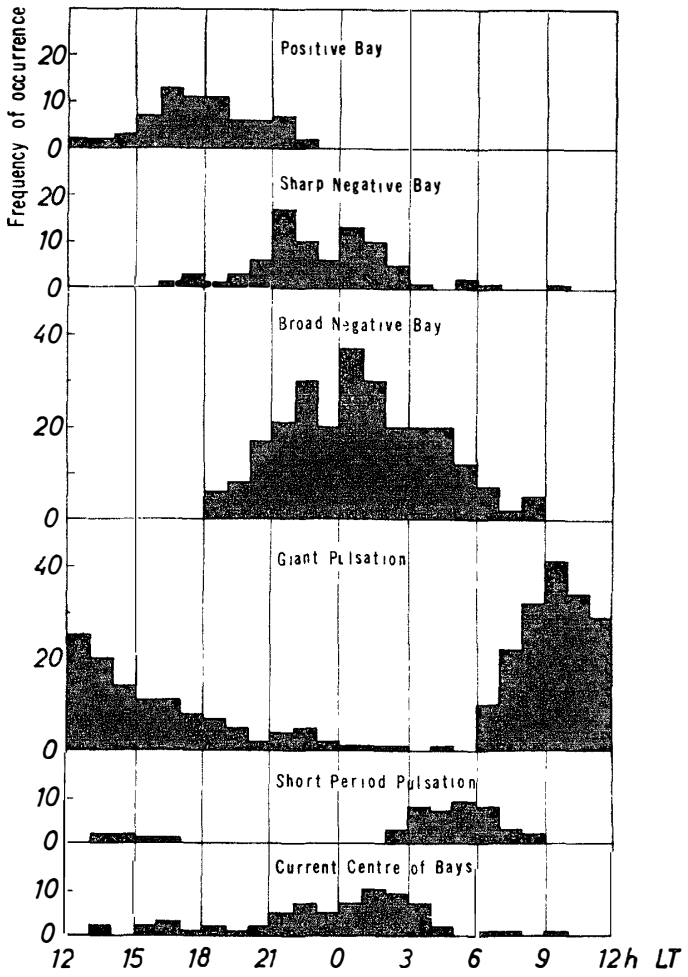

Fig. 7. The local time distribution of occurrence frequencies of polar magnetic disturbances. The histograms for positive bays, sharp negative bays, broad negative bays, giant pulsations (T = 270 sec), short period pulsations (T = 9 sec), are the results obtained at Syowa Station in 1959, and the local time distribution of the activated area for equivalent current system (bottom) responsible for bay disturbances is obtained by the data at 22 stations around the north polar region.

geomagnetic latitudes. Fig. 10 represents the statistical distribution pattern of activated area responsible for sharp negative bay, broad negative bay and positive bay groups on a map viewed from the geomagnetic north pole.

The world-wide pattern of distribution of the activated area strongly confirms the local time dependence of disturbances obtained at Syowa Station, showing that, the positive bay, sharp negative bay and broad negative bay occur most probably in the evening, around midnight and in the morning respectively. The change in occurrence frequency with respect to geomagnetic latitudes are also derived from the same data, as

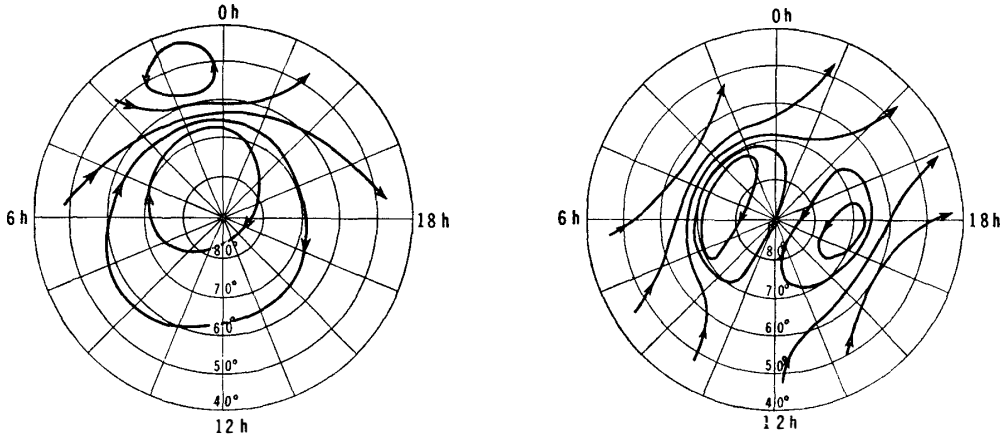

Fig. 8

(a). The typical equivalent current system of dipole type, responsible for a sharp negative bay disturbance (2022 GMT Jan. 13, 1958).

(b). The equivalent current system responsible for a broad negative bay and positive bay disturbances. The electrojet in the auroral zone in early morning is responsible for a broad negative bay and that in the evening is responsible for a positive bay (1330 GMT June 16, 1958).

illustrated in Fig. 11. There is found an appreciable difference of distribution occurrence as seen in the figure, between the negative bay and positive bay, namely, the later shows a maximum around 65° in geomagnetic latitude a little lower than that of negative bay, while no significant difference is found between two groups of negative bay. The spatial distribution of the activated area will be referred to later again in more detail in connection with the ionospheric and auroral patterns of disturbance.

4. Geomagnetic pulsations

Apart from so-called polar elementary disturbances, geomagnetic pulsation is one of the most outstanding phenomena at the stations around the auroral zone[34,35]. The observational studies on world-wide characteristics of pulsations, however, have long been not so fruitful, due to the difficulty of collection of world-wide data which make possible a reliable world-wide analysis for such rapid variations. In recent year, as a result of the greatly increased number of continuous observation, certain definite types of pulsations have been recognized, and some systematic classification has been attempted[36,37]. The great increase, however, in the amount of data has sometimes only served to show in some cases that, in reality, there exist so many different types or variations that the confusion of nomenclatures may occur. To obviate such confusion, only the period of oscillation will be taken into consideration for the classification

Table 3. List of stations.

Station	Abbreviation	Geographic		Geomagnetic	
		Lat.	Long.	Lat.	Long.
Resolute Bay	RB	74.41N	94.55W	82.9	289.3
Baker Lake	BL	64.18N	96.05W	73.7	315.1
Leykjavik	LY	64.11N	21.42W	70.2	71.0
Churchill	CH	58.45N	94.2 W	68.7	322.7
Point Barrow	PB	71.18N	156.46W	68.6	241.0
Tromso	TR	69.40N	18.57 E	67.2	116.8
Kiruna	KI	67.50N	20.25 E	65.3	115.9
College	CO	64.51N	147.50W	64.7	256.5
Murmansk	MU	68.58N	33.05 E	64.1	126.5
Sodankyla	SO	67.22N	26.39 E	63.7	120.0
Lerwick	LR	60.08N	01.11W	62.5	88.6
Dombas	DO	62.04N	09.07 E	62.3	100.1
Sitka	SI	57.03N	135.20W	60.0	275.4
Eskdalmuir	ES	55.19N	03.12W	58.4	82.8
Lovo	LO	59·21N	17.50 E	58.2	105.8
Dourbes	DU	50.06N	04.26 E	52.0	87.7
Yakutsk	YA	62.01N	129.40 E	51.0	193.8
Moscow	MO	55.29N	37.19 E	50.8	120.5
Fredericksburg	FR	38.12N	77.22W	49.6	349.9
Sverdlovsk	SV	56.44N	61.04 E	48.5	140.7
Lvov	LV	49.54N	23.45 E	48.1	105.9
Irkutsk	IR	52.28N	104.02 E	41.1	174.4

of pulsations in this paper.

Jacobs and Sinno[38,39], by their analysis of rapid-run data from 17 observatories, distributed in northern America and the Pacific, have concluded that, almost all kinds of pulsations except for short *pc*, may be represented by overhead equivalent current a little similar to that of elementary storms. It must be noted in their conclusion, however, that the small phase differences between H-and D-components have been neglected, though the polarity of the horizontal component is not always exactly linear.

Examples of the equivalent current system are shown in Fig. 12. As evident in the figure, the activated area of the current system is located around the auroral zone, and the counter current lines over the polar regions and the low latitudes hardly seem to close in the ionosphere; these open-ended current contours may be extended to the outer atmosphere. It may be worthwhile to note that the current system shows a remarkable shear within a narrow belt along the auroral zones. That is, when the current flows eastward over, Baker Lake or Point Barrow in the morning, for example, it flows simultaneously westward over Fort Churchill or College, with the same order of magnitude, though the two pairs of stations (BL-FC and PB-CO) are situated closely to each other with a difference of only five degrees in geomagnetic latitude. Thus it is

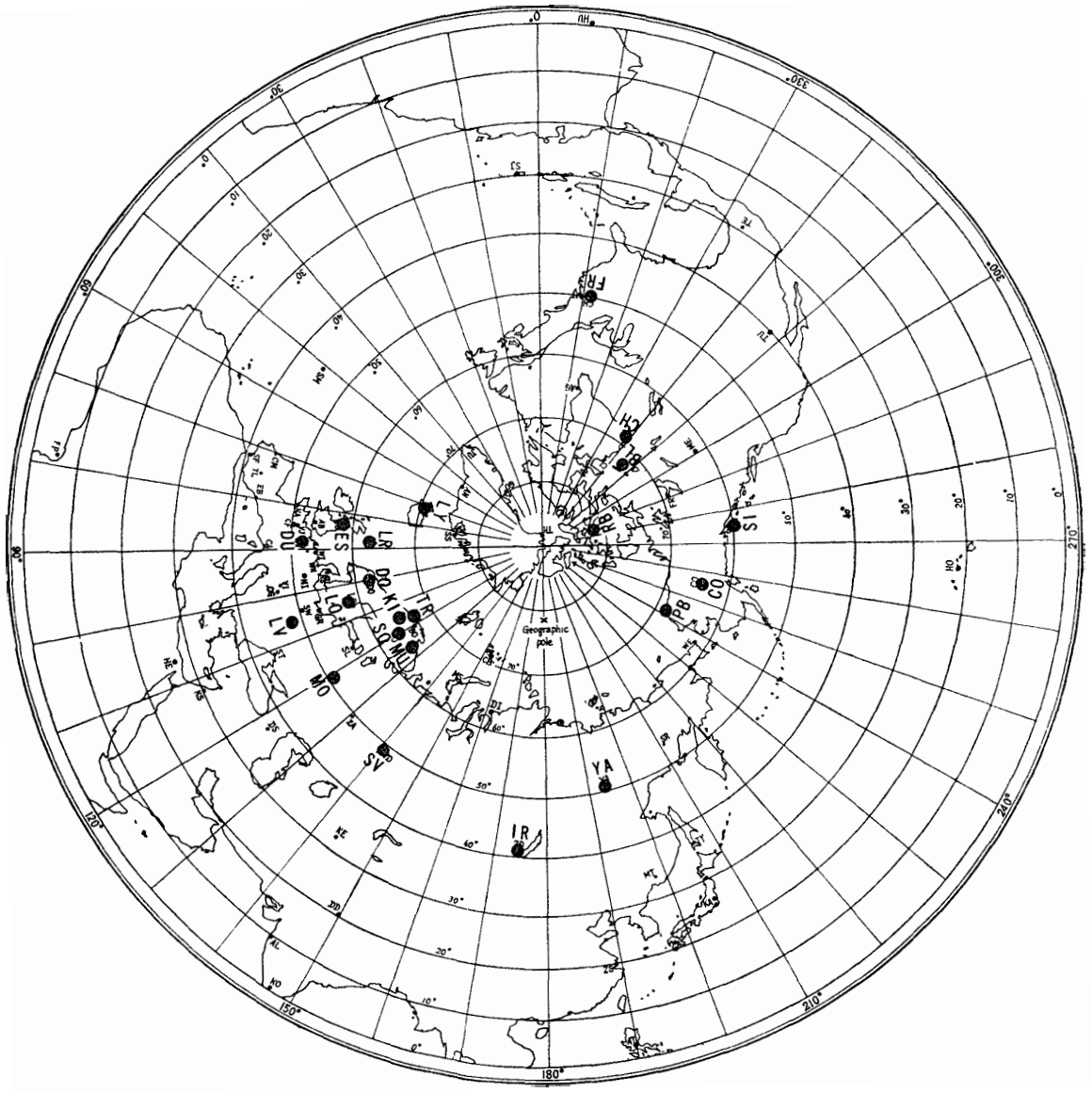

Fig. 9. Distribution of magnetic observatories whose data are used in this analysis.
RB: Resolute Bay, BL: Baker Lake, LY: Leykjavik, CH: Churchill, PB: Point Barrow, TR: Tromsö, KI: Kiruna, CO: College, MU: Murmansk, SO: Sodankylä, LR: Lerwick, DO: Dombas, SI: Sitka, ES: Eskdalemuir, LO: Lovö, DU: Dourbes, YA: Yakutsk, MO: Moscow, FR: Fredericksburg, SV: Sverdlovsk, LV: Lvov, IR: Irkutsk.

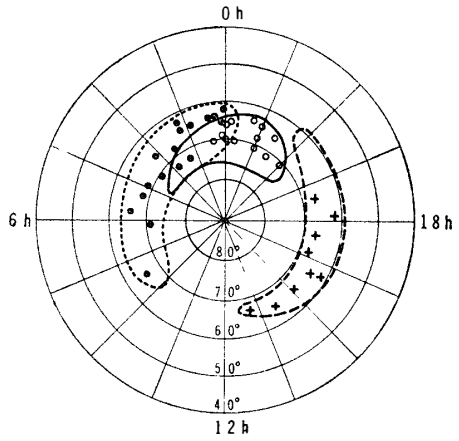

Fig. 10. The distribution pattern of the activated area of equivalent current system responsible for sharp and broad negative bay disturbances and positive bay disturbances. ○: sharp negative bay, ●: broad negative bay, +: positive bay.

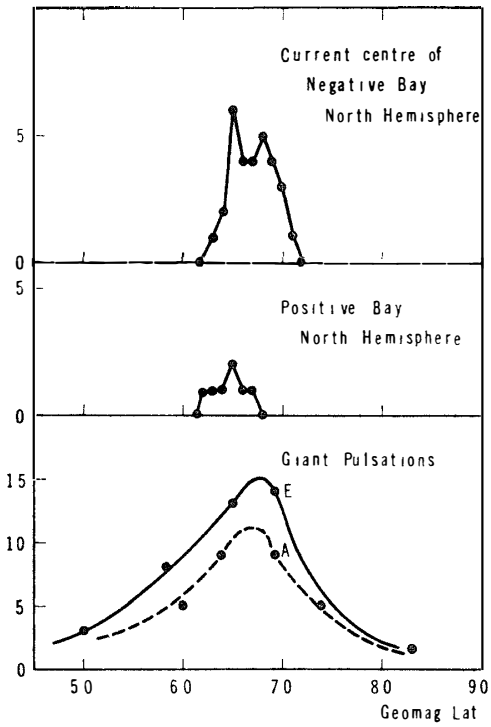

Fig. 11. Latitude distribution of occurrence frequencies of activated area for negative and positive bay disturbances and giant pulsations.
A: America Zone, E: Europe Zone.

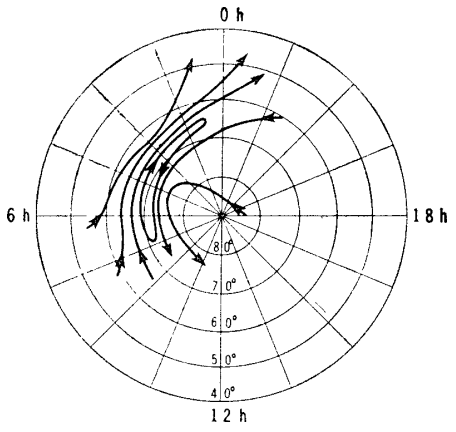

(a). A typical example of equivalent current system responsible for giant pulsation (about 1200 GMT Jan. 11, 1958).

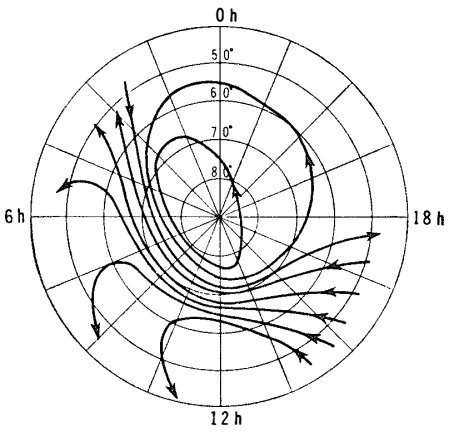

(b). The mean equivalent current system for giant pulsations in the north polar region (Jan.–June, 1958).

Fig. 12.

found that the equivalent current system for long period pulsations observed around the auroral zone is characteristically different from that of polar elementary disturbances in this point. It seems likely, therefore, that the physical origin of such a kind of pulsations generally is entirely other than that of polar elementary storms.

There still remains also a fundamental problem concerning the frequency spectrum of pulsations which seems to be important for the classification of pulsation phenomena. In another words, it is important to know whether or not the period distribution pattern, obtained at certain stations distributed widely in geomagnetic latitudes, shows the same maxima at certain periods fixed, or, whether or not the period of maximum occurrence changes continuously with latitude. It may include one of the most fundamental problems on characteristics of geomagnetic pulsations, because it may essentially concern the mechanism of their origination.

In this paper, however, this problem will not be extended further, and the frequency spectrum obtained at Syowa Station in 1959 only is shown in Fig. 13. It is to be

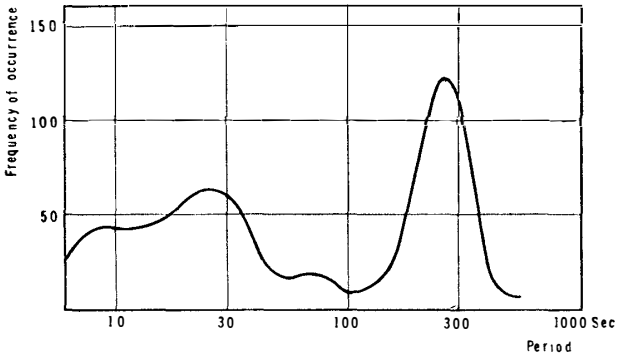

Fig. 13. Period distribution of geomagnetic pulsations observed at Syowa Station (Feb.–July, 1959).

noted here that the occurrence frequency shows three maxima at T = 290 sec, T = 27 sec and T = 9 sec respectively, which will be called in this paper for convenience, *Pg*, *Pm* and *Ps* meaning respectively giant pulsations, moderate period pulsations and short period pulsations.

5. Distributions of geomagnetic pulsations

In Fig. 7 are shown the diurnal changes of the occurrence frequency of geomagnetic pulsations *Pg*, *Pm* and *Ps*, at Syowa Station in 1959 together with those of bay disturbances. The maximum occurrence is seen around a few hours before local noon for both *Pg* and *Pm* in the same manner as the origin of them may be attributable to the same physical mechanism. On the other hand, *Ps* occurs most probably at about 6hLT, significantly different from the time favourable for *Pg* and *Pm*. These results are in good agreement with the results obtained by JACOBS and SINNO.

In the preceding paragraph, it has been already shown that the equivalent current system responsible for geomagnetic pulsations is represented by a pattern a little similar

to that for a polar elementary storm. The current is also concentrated around the auroral zone so that the activated area may be defined in like manner as in the case of polar elementary storms. The most prominent pulsations at Syowa Station, as visible in Fig. 13, is *Pg* which has a maximum occurrence at the period of about 5 min. The double amplitude of *Pg* at Syowa is about 100γ in average, but it sometimes amounts up to several hundred gammas during severe storms.

In order to investigate the world-wide features of pulsations, it is desirable to use rapid-run magnetogram records. Unfortunately, however, magnetic stations operating rapid-run recording are not well distributed over the world. A reasonable coverage, of course, is given by ordinary magnetograph anywhere in the world, but the normal recording speed of 20mm/hour is in sufficient for reliable analysis of geomagnetic pulsations except *Pg*. The discussion on the activated area and their statistical distribution in this paper, therefore, will only concern the *Pg*.

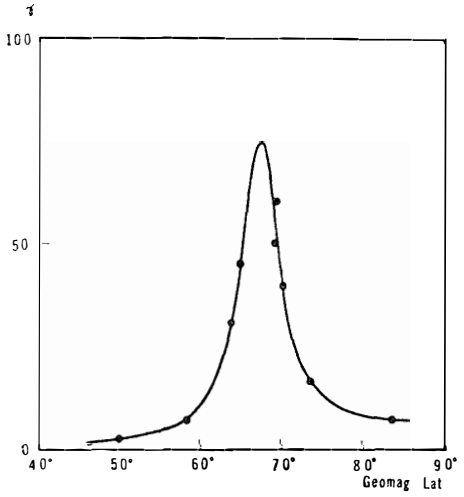

Fig. 14. Latitude distribution of the double amplitude of giant pulsations.

The data used for the investigation of polar elementary storms are used also for this purpose. At first the latitude dependence of the double amplitude was examined, then the local time inequality was odtained. The results are shown in Figs. 14 and 15. The mean curve shows a maximum double amplitude at 67° in geomagnetic latitude and falls sharply towards both middle and high latitudes. The local time inequality is much more moderate than latitude dependence as may be expected from the local time distribution of occurrence frequency. The world-wide occurrence pattern is also obtained as shown in Fig. 16, which seems to confirm the statistical results mentioned above. Special reference should be made here to the whole distributions pattern, which seems to be al-

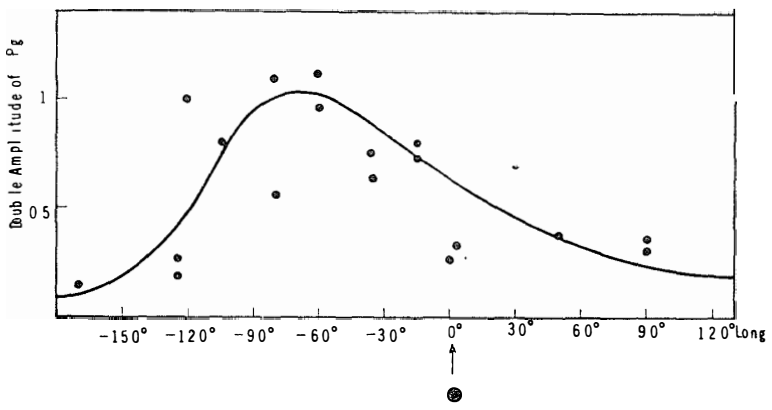

Fig. 15. Local time dependence of the relative amplitude of giant pulsations along the auroral zone.

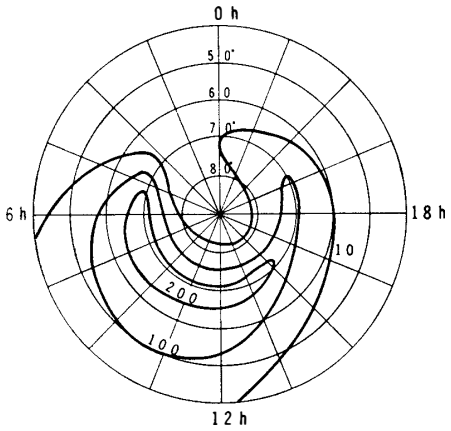

Fig. 16. The world-wide pattern of the occurrence frequency of giant pulsations.

most contrary to those of the polar elementary storms, being concentrated in the morning-daytime site in the auroral zone. This fact may be an evidence which suggest that this kind of *Pg* has generally quite a different origin other than those of the polar elementary storms.

6. Summary of Chapter I

In the preceding paragraphs, the mean features of bay disturbance and *Pg*, with special reference to the distributions pattern and equivalent current system, were examined. It is perhaps useful to re-arange here again the principal features of them, for the convenience of inter-comparison with the other disturbance phenomena.

a. The local time dependence

The polar elementary disturbances are divided into three groups, *i.e.*, positive, sharp negative and broad negative bay groups. The positive group occurs in the evening, and the activity is generally less than the sharp negative group. The sharp negative group is concentrated around midnight, and its activity is highest among the three, while the broad negative group is distributed widely from midnight to forenoon with the activity almost the same as those of positive group. *Pg* is distributed also in wide range in local time, with a maximum occurrence around a little before noon in the auroral zone.

b. Latitude dependence

These four kinds of disturbance are all concentrated around the auroral zone, with a little difference in geomagnetic latitude. The latitude of maximum occurrence of *Pg* is highest among the four and is about 67°Φ. The latitude of maximum occurrence of sharp and broad negative groups follow it, situated about 66°Φ, whereas positive bay group has the lowest latitude of occurrence of about 65°Φ.

c. Equivalent current systems

The equivalent current systems responsible for the bay groups are essentially equal to each other. They can be characterised by an activated area, where the current flows concentrated in a certain directions along the auroral zone. The average width of the activated area is about 300–400 km, and the mean linear dimension in the most elongated direction is about 1000–3000 km. The type of the current system is of dipole-like or of superposition of doublet current, which may be expressed on a spherical sheet by a current function as

$$J = \frac{\mu_0}{2R} \cot\frac{\Theta}{2} \sin A \quad \text{..... (1-1),}$$

where, R and μ_0 represent respectively, radius of the sphere and dipole moment of the electric doublet.

The doublet electrojet along the auroral zone is quite favourable for considering that the origin is the induced current in the lower ionosphere. That is to say, the electric current is induced, for example, by dynamo-action of the earth's upper atmosphere under the action of magnetic field in the high conductive region of activated area, and the return current closes in low latitudes and in the polar cap.

On the other hand, the current system responsible for *Pg* is essentially different, though apparently it seems similar to that for bay disturbances so far as the latitude of their maximum occurrences are concerned. The most outstanding characteristic of the current system is a strong shear of current within a narrow band along the auroral zone in the morning. It sometimes is revealed in a complete opposite change of magnetic horizontal vectors, observed at the two stations situated closely in both sides of the auroral zone. Then, if the current system is formulated quite perfunctorily on a shell in like manner as that for the bay disturbances, it may be given for example by

$$J = \frac{\mu_0}{2R} \cot\frac{\Theta}{2} \sin^2 A \quad . \quad . \qquad (1\text{-}2).$$

This particular type electrojet is quite improbably due to simple dynamo-action. This may be one of the most serious reasons to consider that the origin of this kind of *Pg* is essentially other than that of polar bay disturbances. The problem will be discussed more fully later again. In this paragraph, *Pm* and *Ps* are not referred to, because of the difficulty in the collection of rapid-run data well distributed for the world-wide analysis of these pulsations.

Finally, the prevailing period of pulsations and its latitude dependence is noted. The period apparently becomes long with latitude increaces, as shown in Fig. 17. This statistical result is in agreement with that abtained by OBAYASHI[40] from the data of certain individual pulsation at the stations distributed in North America.

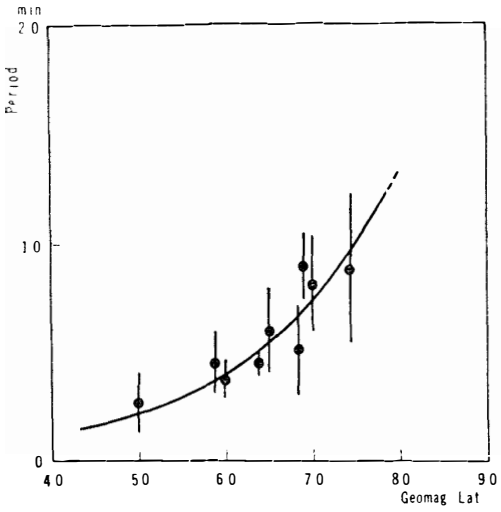

Fig. 17. Latitude dependence of the prevailing period of giant pulsations.

7. Relationship with the other disturbance phenomena

Almost all of the geomagnetic disturbances in high latitudes, as stated above, are concentrated aong the auroral zone. This fact seems to suggest that the origins of these disturbances are connected directly with the auroral display. The local time dependence of their occurrence, however, is so markedly different from each other that they may be considered to have different origins. It may be significant to study the relations of these phenomena with ionospheric disturbances and auroral displays, for the investigation of their physical origin, and it is important therefore, to note here the problems which will be connected with those in later chapters.

If the disturbance phenomena, as generally believed, are due to the invasion of corpuscular stream into the earth's atmosphere, what is the physical cause of the difference between sharp and broad negative bay and positive bay? Is it due to the kinds of impinging particles or due to the energy spectra or is it due to the receiving conditions of the ionosphere? Perhaps the condition of these three factors causes a complicated feature in the disturbance phenomena as being practically observed. These differences among the disturbances, and consequently perhaps among the origins can hardly be known only from the investigation of geomagnetic disturbances. In the next chapter, the ionospheric phenomena in the polar region will be dealt with in connection with geomagnetic disturbances shown in the present chapter.

II. POLAR IONOSPHERIC DISTURBANCES

1. Introduction

The occurrence of ionospheric disturbances associated with the polar magnetic disturbances are noticeable in all the *D*, *E* and *F* regions. Among them, the *F* region phenomena have long been studied by many investigators[40–44]. One of the most outstanding effects of an ionospheric storm over the earth so far reported, is a variation of the critical frequency $foF2$ and the height $h'F2$. Since they are parameters tabulated by ionospheric observatories, their changes have been widely studied with fruitful results[45–49]. It has been concluded from their results, that the ionospheric *F*2 storms are mostly due to the drift motion of electrons under the action of electric field which may be a cause of magnetic disturbances also, through the electric current in the lower ionosphere.

It is obvious because of the reason that the distribution of electrons in *F*-region is largely affected by electric field in the lower *E*-regions, that the disturbances which take place in the *F*-region directly, may sometimes be completely masked by the effect of *E* region. Therefore, it may be considered that the *F*-region phenomena, though suitable for the detection of electric field there, are unprofitable for the direct detection of disturbances which take place there.

On the other hand, the occurrence of a ionospheric storm in the lower ionosphere, which is clearly marked in the auroral zone by a decrease in the intensity of reflected waves, may be regarded as the direct disturbance itself. The effect is often so serious that the echo of high frequency signals disappears completely (ionospheric blackout). The study of the ionospheric absorption and blackout has also been carried out by many investigators[19,50–54] as well as of *F*-region phenomena, and the world-wide patterns of occurrence have been discussed. Recently STOFFREGEN, DERBLOM and OMHOLT[55], by their special observation of *D*-regions ionization with the aid of a powerful ionosonde during auroral displays, attained the conclusion that, a heavy simultaneous ionization in the lowest part of *D*-region takes place in the auroral displays.

The *E*-region phenomena, compared with the above two regions, is not so clear, though they have been known to be closely connected with auroral display[19,56,57]. However, from the standpoint of polar magnetic disturbances, the *E*-region phenomena are obviously the most important, since the *E*-region is likely to be responsible for magnetic disturbances, as a carrier of the most part of ionospheric electric current,

In this chapter, therefore, discussions will be mostly concerned with the *E*-region phenomena especially in high latitudes.

2. Night increase in *foEs*

The *foEs* increases generally in the auroral zone simultaneously associated with bay disturbances and auroral displays especially in night time. For example, at Syowa Station, the amount of bay disturbances associated with anomalous increase in *foEs* is about 80% as seen in Fig. 18, and the rest of the bays of about 20% are associated

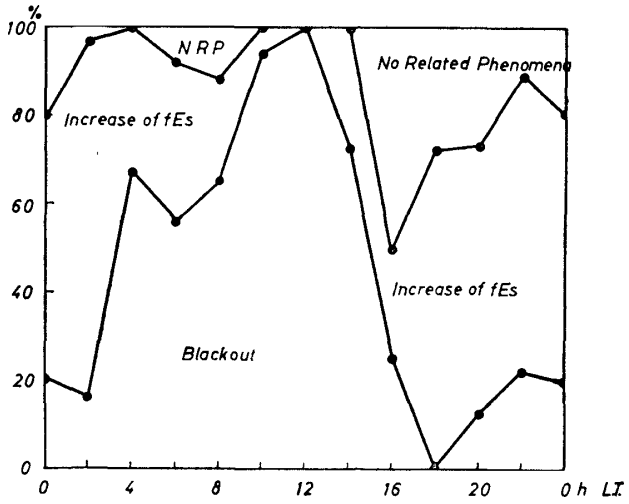

Fig. 18. The percentage of bay disturbances which are associated ionospheric balckout and increase in *foEs*. A considerable change of the percentages is found with respect to local time.

with blackout at night. Hence it is evident that the anomalous increase in *foEs* in the auroral zone are connected statistically at least with bay disturbances.

In order to study the correlation in more detail, a world-wide pattern such as used in Chapter I in the case of bay disturbances seems to be useful. The ionospheric data at Syowa, Campbell, Godley Head and Rarotonga were examined for this purpose.

The local time dependence of *foEs,* was first examined for the data at the four stations and the results are shown in Fig. 19. It can be pointed out from the figure

Table 4. List of stations.

Station	Geographic		Geomagnetic	
	Lat.	Long.	Lat.	Long.
Syowa	69.00S	39.35E	−69.7	77.4
Campbell	52.33S	169.09E	−57.4	253.1
Godley Head	43.34S	172.48E	−48.1	252.8
Rarotonga	21.12S	159.46E	−20.9	273.7

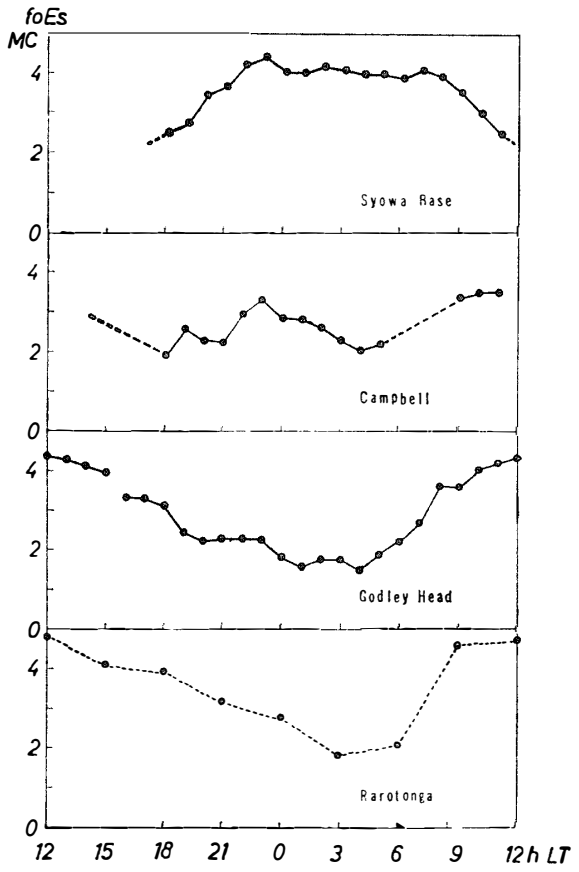

Fig. 19. The local time variation of mean *foEs* at four stations.

that, in high latitude, *foEs* shows a broad and flat maximum at night, whereas in middle and low latitude, the values of *foEs* in daytime are higher than those at night. The flat maximum seems to include three minor peaks around 20h, 0h and 6h LT, which seem to correspond respectively to the positive bay, sharp negative bay and broad negative bay groups in polar magnetic disturbances. *Es* in low latitudes, as already mentioned, almost contrary to that in high latitudes, takes its maximum value of critical frequency around noon[58,59]. It is evident from these facts that the origins of *Es* in high latitudes and in low latitudes are irrelevant with each other.

In order to see the feature of world-wide pattern of *foEs,* the results shown in Fig. 19 were reproduced in a world-wide map viewed from the magnetic pole in Fig. 20. where the pattern is projected in the north hemisphere for the convenience of its comparison with the pattern of geomagnetic disturbances which was obtained for the northern polar region in Chapter I. The world-wide distribution of *foEs,* as clearly seen in the figure, is characterized by a marked maximum area along the auroral zone at night, quite similar with the distribution of activated area of polar geomagnetic disturbances.

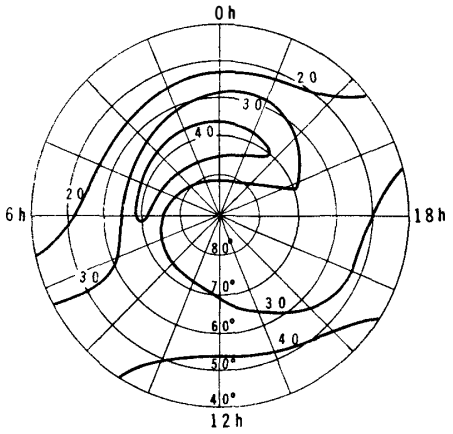

Fig. 20. World-wide pattern of mean *foEs* (July–Dec., 1958).

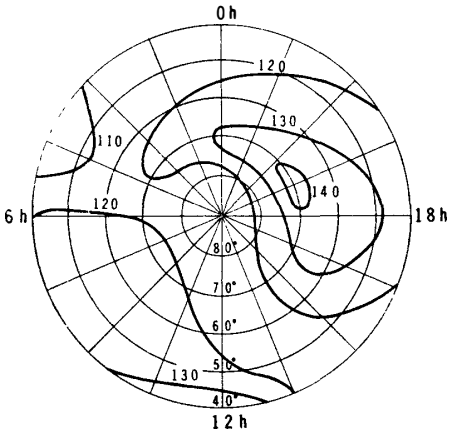

Fig. 22. World-wide pattern of mean *h'Es* (July–Dec., 1958).

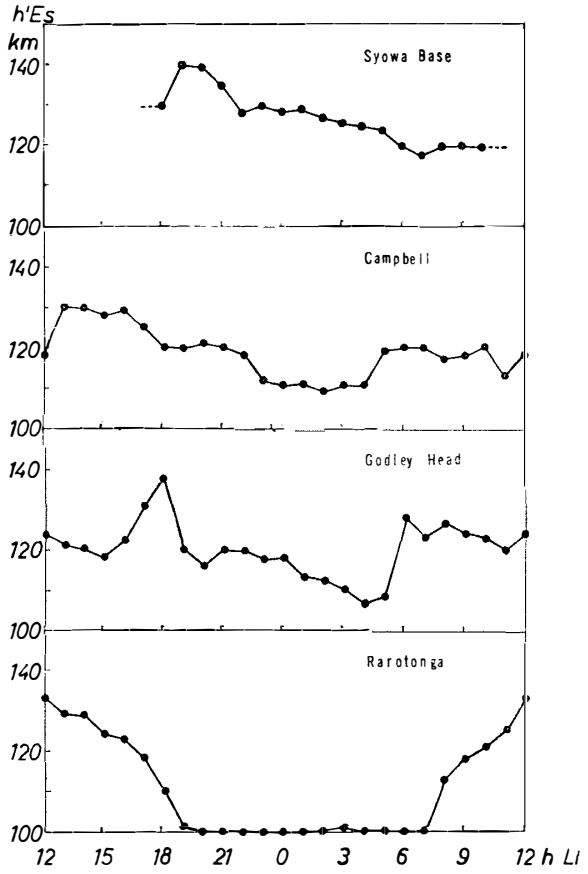

Fig. 21. The local time variation of mean *h'Es* at four stations.

3. Altitude distributions of *Es*

One may notice that there is a systematic altitude variation of *Es* layer or cloud with respect to lacal time, if *h'Es* values are examined through 24 hours in high latitudes. The features are shown in Fig. 21, where the curves represent the time change in mean vaue of *h'Es* at the four stations. Though the curves are not very smooth, being based on the data of half a year, the results obviously show that the changing mode of the altitude is roughly semi-diurnal. That is to say, the maximum height of about 140 km appears in the evening with another minor peak of 120 km at about 5 h, and the height gradually and monotonously fall throughout the night and day, attaining minimum height of about 110 km in the early morning, and in the afternoon respectively. In middle latitudes, the general tendency is conserved though the changing mode is fairly modified. The result can be reproduced in like manner as that of *foEs* in a world-wide pattern as shown in Fig. 22. The remarkable feature evident in the figure seems to be the dependence of *h'Es* upon the distance from the auroral zone, as well

as on the local time. There appears a tendency for $h'E$ to be a decreasing function of colatitude θ outside of the auroral zone.

A question may arise here, whether or not the pattern is seriously affected by the retardation effect in *D*-regions. The reliability of the results, however, may be easily confirmed since the electron content is only of the order of 10^4 electrons/cc even in the extreme case during auroral displays, and in fact, the effect of electron content of 10^4/cc in the *D*-region only produce an error of height of only a few per cent of the real height.

The spatial distribution of $h'Es$ of course should be related with the other disturbances phenomena, *i.e.*, geomagnetic disturbances and auroral displays, and the problem will be referred to again later in more detail.

4. f_{min} and ionospheric blackout

Recently STOFFREGEN and others have shown by their observation at Uppsala and at Lycksele, Sweden, that a simultaneous heavy ionization takes place in *D*-region during auroral displays. One of their results of main importance is a concentration of blackout region in the morning side of the auroral zone. Their conclusion may be confirmed in the case of bay disturbances in the auroral zone, by using the data at Syowa Station, since, as already seen in Fig. 18, the bay disturbances in morning-daytime are mostly accompanied with blackout, amounting up to almost 70% of bay disturbances which occur in the morning. The time of switch from $foEs$ increase to blackout, simultaneously associated with bay disturbances, is about 2h LT. It does not mean, however, that the magnetic disturbances are completely associated with blackout after transition time. Sometimes they are accompanied by increase in $foEs$ as well as blackout.

Thus, it may be concluded that, the ionospheric phenomena associated with polar magnetic disturbance take place at the two levels in the ionosphere, namely in the *E*-region and in the *D*-region, in the early morning in the auroral zone. The same

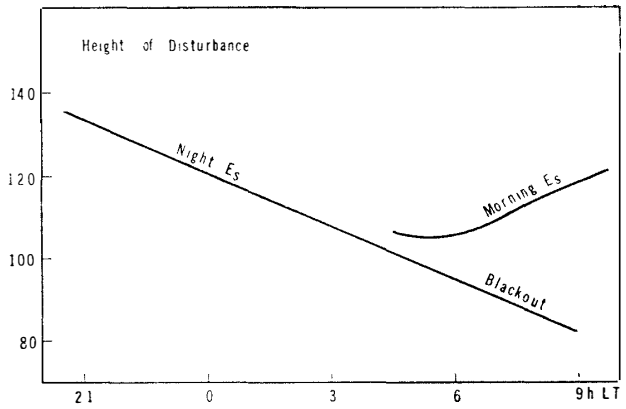

Fig. 23. A schematic illustrations of the change in disturbance height throughout the night in the auroral zone.

conclusion may be applicable to the ionospheric phenomena in the evening. But in the evening, the occurrence probability of blackout is so scarce that the dual structure of the disturbance phenomena mentioned above is not so remarkable as seen in the early morning. It is worthwhile to note that the height of *Es* layer or cloud, falling continuously throughout the night, seems to attain at about 80–90 km level, if it continues to fall in the morning. The level may be identical with that where anomalous ionization causes blackout.

The feature is schematically illustrated in Fig. 23. These facts are likely to suggest that, if the anomalous ionization is due to the impinging corpuscular stream, its penetration depth must be dependent on local time. From this point of view, the dual structure of disturbance is perhaps due to th penetration of impinging corpuscles which covers effectively both *D* and *E*-regions.

5. Night *E* layer

There are found sometimes a stable ionization in the *E*-region on the ionogram, obtained at the auroral zone in night time, which will be called night *E* layer. The morphology of night *E*, however, is not sufficiently clear yet to warrant discussion on the wold-wide pattern, but some important characteristics are evident. Namely night *E*, even in its most developed stage with high critical frequency, does not correlate appreciably with geomagnetic and auroral phenomena. This seems one of the most outstanding nature of night *E*. The behaviour of night *E* is quite curious compared with *Es* which shows a characteristic increase in the critical frequency associated with bay disturbances, because the difference of the behaviour between night *E* and *Es* is not attributable to the difference of ionospheric conductivity, since the rate of ionization should not considerably differ with each other. It may be due to the change in electric field, which may be responsible for an induced current or may be due to the shape of the pattern of ionized area. There is, however, no evidence which supports the above considerations at present, and further investigation is desirable.

6. Effective height of disturbances

As has been discussed already, the change in height of *Es* and the occurrence of blackout may be shown in a schematical variation of disturbance height both in space and time. It must be examined whether or not the altitude variation is attributable to the change in receiving conditions of ionosphere. But it may be readily approved that such a large altitude variation amounting up to about 30 km through the night is unlikely due to the change in the receiving conditions of the ionosphere only, since the amount of the change is comparable with the scale height there. On the other hand, if it is due to the change in penetration depth of impinging corpuscles, there still remain a problem, *i.e.,* why does the penetration depth (or the incident energy) distributes in such a manner as seen in Fig. 22.

7. Morphological inter-relation between polar magnetic disturbances and ionosheric disturbances

It may be convenient here to re-arrange the results obtained in the preceding sections, for the purpose of connecting them with the problems which will be brought out in the next chapter. At first, it must be mentioned that the three kinds of bay disturbances, namely positive bay, sharp negative bay and broad negative bay groups are likely to correspond with three maxima in *foEs* in night time in the auroral zone. Special reference must be taken on the fact that two kinds of ionospheric phenomena, *i.e.*, increase in *foEs* and blackout, are associated with bay disturbances which take place in the morning. On the other hand, geomagnetic pulsations seem to have no such appreciable corresponding phenomena as those which bays have, but their occurrence is concentrated in the morning when blackout is observed most frequently.

In concluding, some problems to be discussed later are set forth here. They may be summarized as follows; Is there any evidence of any altitude distribution of auroral phnomena as such that seen in the height of *Es*? Are there any corresponding phenomena of aurorae which are connected with the three kinds of magnetic bay disturbances and three peaks in *foEs* at night? Is the altitude distribution of *Es* certainly due to the kinds of and or the engergy of the impinging corpuscles? What are the spatial dispersion of incoming flux density of corpuscular stream? What is the true physical cause of the difference found in the correlation of ionization with magnetic variation between *Es* and night *E*? These problems will be dealt with in later serial.

III. AURORAL DISPLAYS

1. Introduction

The study of aurorae is of great importance in the investigation of the upper atmosphere, especially of the upper atmosphere disturbance phenomena in high latitudes. Spectroscopic observations of the auroral height in particular yield valuable information regarding not only the composition and temperature of the upper atmosphere but also the physical mechanism of auroral displays and magnetic storms. A study of the form and the geographical distribution of the aurorae is also very helpful in investigating the nature and the origin of the charged particles, the entry of which into the high atmosphere may be the cause of the magnetic storms and also of the auroral displays. It is satisfying to note that the visual, photographic and spectrographic methods of studying the aurorae, the new radar method has now been added. It is to be noted that the recent development of rocket and space probe made it possible to measure directly the physical nature of the aurorae, and new information is now being accumlated on the physical state in aurorae.

2. Altitude distributions

From an analysis carried out in 1937, EGEDAL[60] concluded that the height of the lower border of aurorae decreases throughout the night, this decrease occurring in the interval from three hours after sunset to 8 hours. This depression of height was found to be about 15 km, using the data by STÖRMER[61], and to be about 10 km, using the data of VEGARD and KROGNESS[62]. STÖRMER re-investigated the matter in 1948 and also examined whether there is a dependence on the distance, θ, from the magnetic axis. His results on auroral ray arc are shown in Fig. 24. Except in the case of homogeneous arc, they may give some support to the conclusion of EGEDAL. There appears to be a tendency for the height to be a decreasing function of for the RB form. To make clear the tendency, the result may be conveniently reproduced in a world-wide pattern of auroral height viewed from the north pole. In Fig. 25 is shown the reproduction of the results obtained by STÖRMER and BARICELLI[63] in the case of RB form.

One may notice at a glance of the figure that the pattern of the height of the lower border as the function of θ and local time is quite similar to the pattern of *h'Es*. As to the absolute height, however, there is a fairly large difference between the height

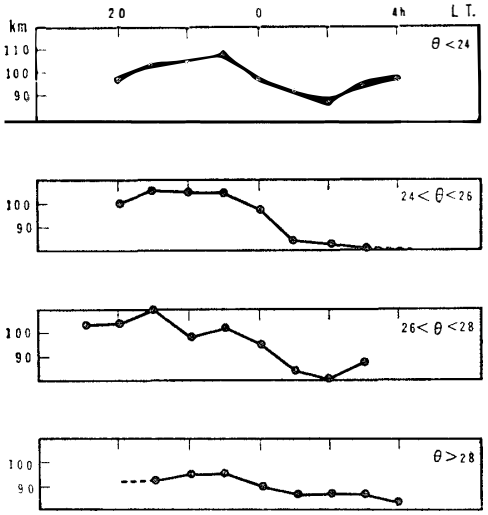

Fig. 24. The change in height of auroral (RB) lower border throughout the night at four different latitudes. θ represents the geomagnetic colatitude. After STÖRMER.

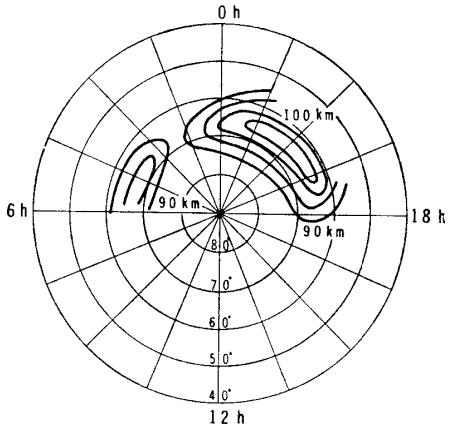

Fig. 25. The world-wide pattern of the height of auroral RB lower border reproduced from the results obtained by STÖRMER.

of the auroral lower border and *h'Es*. It is perhaps partly due to the difference of the period covered for the two sets of data, and partly may be due to the method of data reduction. Further study is desirable on the problem, but the resemblance found between the height pattern of auroral RB lower border and *h'E* may not be seriously affected by further detailed examinations.

3. Temporal distributions

Many kinds of temporal distributions have already been known especially on the diurnal, yearly and secular occurrences, etc. Among them, the diurnal occurrence only will be dealt with here, in connection with the other disturbance phenomena.

The dependence of the occurrence frequency of aurorae on local time has long been known [2,3,64–68], and it was found that the auroral frequency curve passes through the main maximum, usually an hour or so in advance of local midnight. According to VEGARD[64], the main maximum take place about 1.3 hours before magnetic midnight at the place of observation. It seems that the frequency curve obtained at Syowa, which is illustrated in Fig. 26 gives some support to this conclusion. The frequency curve at Syowa normalized for the duration of observation, however, seems to have two subsidiary maxima in the evening and in the early morning. It suggests that the three maxima may correspond to the three kinds of polar magnetic disturbance discussed in Chapter I and also to the three maxima in *foEs* in Chapter II. The results may be confirmed also by radio technique with the aid of auroral reflection of radio waves, which has such a major advantage that it is applicable throughout the full 24 hours. CURRIE *et al.*[69] and GERSON[70] reported that the phenomenon is predominantly noc-

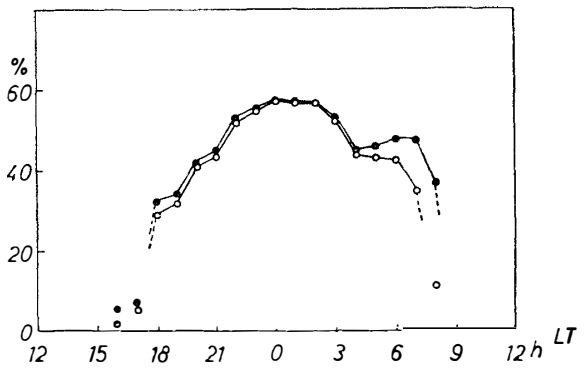

Fig. 26. Normalized probability of auroral appearance at Syowa Stations (Feb.–Nov., 1959).

turnal, though sometimes detected in early morning, as it is so in case of geomagnetic and ionospheric disturbances in the auroral zone.

4. Relative intensities and their variations in the auroral spectra

It is readily obvious from the different colour of aurorae that the relative intensities of the various spectral features are not always the same. This section is concerned with the information available on certain representative values for $H\alpha$ and 1PG of N_2 among many auroral lines and bands.

According to MEINEL[71], the maximum of the luminosity curve for $H\alpha$ lies at a slightly lower level than the maximum of the main luminosity. The intensity of the Hydrogen emissions relative to the allowed atmospheric emissions increases with decreasing latitude. The Balmer lines have a tendency to be most prominent in the early part of a display, and their intensities may be greatest, several hours in advance of the full auroral development. GARTLEIN[72] has written that the general luminescence may continue long after the Balmer lines become too feeble to be detected. A series of spectroscopic observation of importance in connection with theories of the auroral origin has been carried out by MONTALBETTI and JONES[73] at Saskatoon and Churchill. In examining their results for diurnal variation, MONTALBETTI and JONES discovered that there is a tendency for $H\alpha$ to appear strongly before midnight at Saskatoon and after midnight at Churchill. They also studied the relation between the emission of the Hydrogen lines and magnetic activity, and they found that at Saskatoon the $H\alpha$ intensity tends to increase with increase of magnetic activity, whereas at Churchill it tends to decrease. The general tendency of $H\alpha$ lines obtained at Syowa generally supports the results known so far. For example, in Fig. 27, temporal variations of the relative occurrence of $H\alpha$ is shown, which reveals itself in agreement with the result obtained by MEINEL and GARTLEIN.

On the other hand, no remarkable temporal effect of 1PG has yet been reported. This effect is, however, important in connection with mean altitude distribution of displays. This is because 1PG is observed frequently at the lowest border of aurorae,

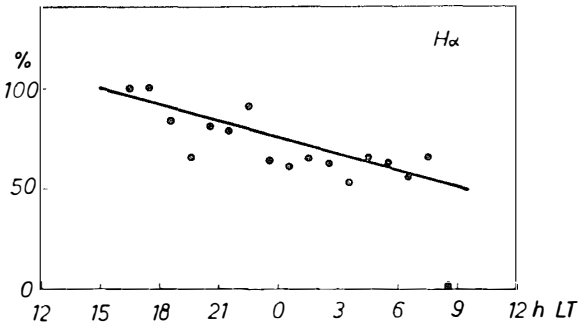

Fig. 27. Relative apprearance probability of auroral H_α line.

and the level of intense 1PG emission is consequently lower than the level for λ5577 emission, thus the intensity ratio I(1PG)/I(5577) or the relative occurrence of 1PG may represent a measure of the disturbance altitude. It means that, if the excitation agency reaches the level well below that in which the O_2—O transition takes place, there are no more observed green (λ5577) emission, and 1PG emission only predominates, since the green line is due to atomic oxygen. In reality, the relative occurrence of 1PG at Syowa Station, as shown, in Fig. 28, tends to increase considerably throughout the night. This fact may indicate that the effective height of displays decreases throughout the night, in agreement with the result from the actual observation of the height of auroral lower border.

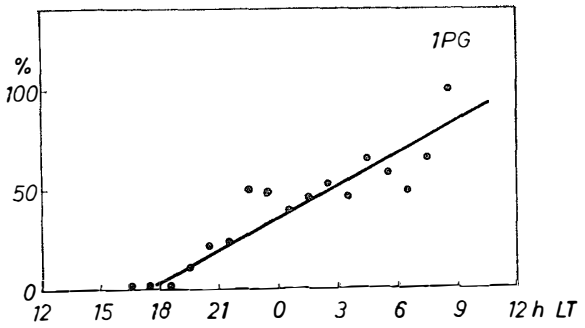

Fig. 28. Relative appearance probability of auroral 1PG.

5. Relations with magnetic and ionospheric disturbances

Much information now have been collected on geomagnetic, ionospheric and auroral disturbances phenomena. The relations among them may be discussed on the two points of view, namely, the one which concerns the world-wide distribution of intensity of disturbances and the other the spatial distribution of altitude where disturbances take place effectively. As to the intensity distribution, representative examples for geomagnetic, ionospheric and auroral phenomena, for instance, the distribution of the

activated area for bays and pulsations, *foEs* and the appearance probability of aurorae, respectively, are shown in this paper. The close relations among the phenomena in the auroral zone are already known as shown in Figs. 7, 19 and 26, and it is evident from these illustrations that the correspondence of three maxima in each phenomena at night is fairly good. The mean features of latitude dependence have also been shown in Figs. 11, 14 and 29, for the two kinds of disturbance phenomena, revealing that both concentrate around the auroral zone.

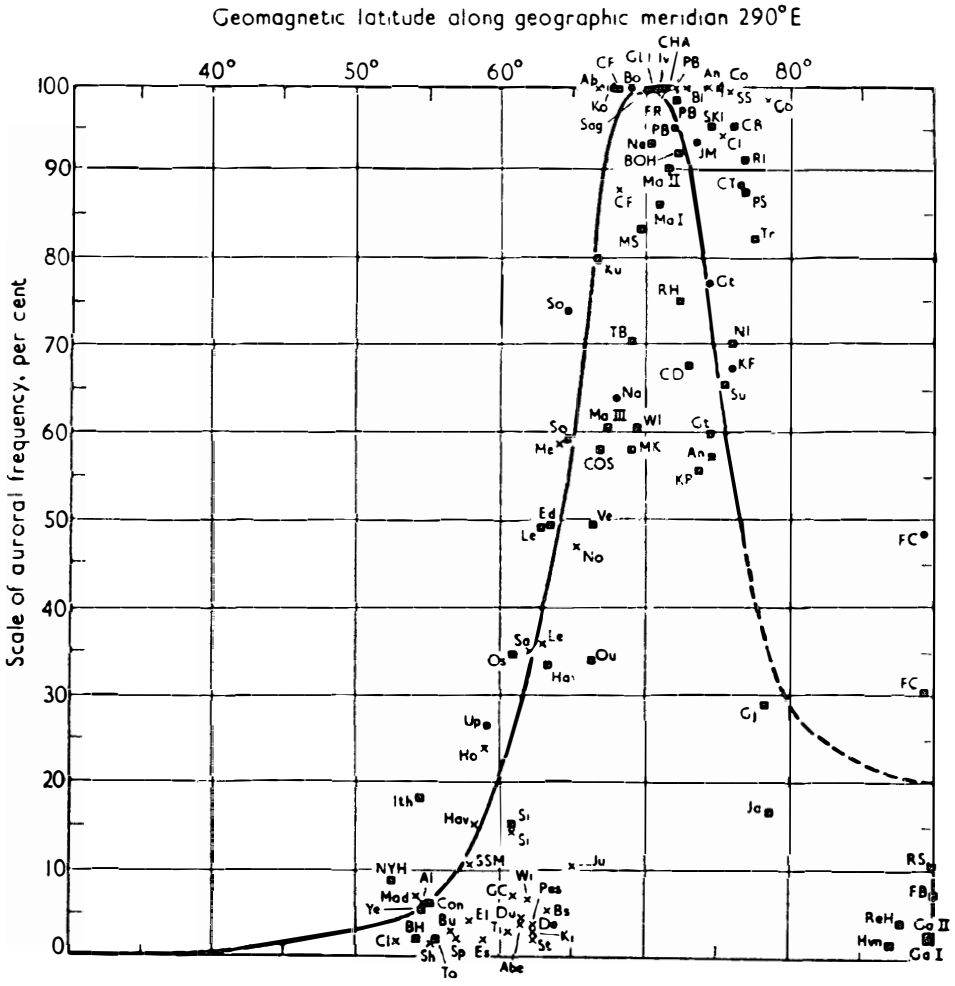

Fig. 29. Estimated average auroral percentage frequency. After VESTINE.

As to the spatial distribution of disturbance altitude, two kinds of evidence have been obtained namely *h'Es* and the auroral height. The two distribution patterns are in good agreement with some discrepancies in absolute height. A conclusion may be deduced from the fact that the disturbing agency, consequently the mean energy of impinging corpuscles, may have such a tendency that it may result in the distribution pattern as schematically reproduced in Figs. 30 and 31.

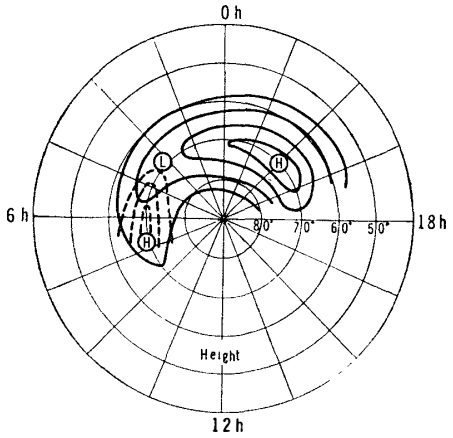

Fig. 30. Schematic pattern of disturbance height

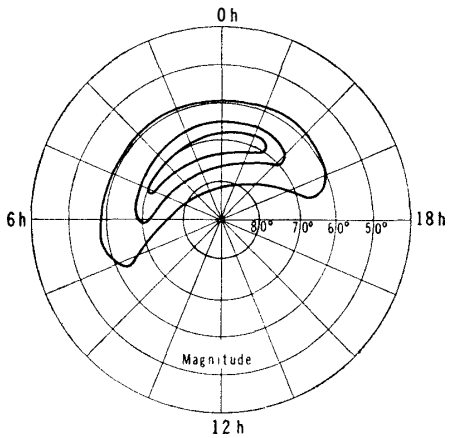

Fig. 31. Schematic pattern of disturbance intensity.

IV. BRIEF SUMMARY OF PART I

1. Summary of morphological relations

Table 5, which is based on the analysis of observational data at Syowa Station, indicates that there are undoubtedly some modifications of relations according to the height of the level where disturbance takes place, or/ and according to the activities of disturbances, and sometimes according to the local time when it occurs. The following are some among the results seen in Table 5.

Table 5. Occurrence local time of the upper atmosphere disturbance phenomena.

Local time	12	15	18	21	0	3	6	9	12
Magnetic variation		—— Positive bay ——		—— Sharp negative bay ——		— Broad negative bay —		—— Giant pulsation	
Ionospheric disturbance				—— Es increase —— (height falls)			—— Blackout ——		
Auroral phenomena			—— Hα ——	—— 5577 —— (height falls)	—— 1PG ——				

1). Aurora in evening is very often, accompanied by an increase in *foEs* and geomagnetic positive bay of moderate activity. The altitude of the aurorae is generally much higher than the level of mean maximal intensity, and at the same time, 1PG is hardly noticeable. It is to be noted that the appearance probability of Hα line is appreciably high in the eveing. *h'Es* is also rather high being about 130 ~ 140 km.
2). The characteristic feature of the disturbance at midnight is that, intense aurora with ray structure is accompanied by sharp magnetic disturbances in which the meridian component of force changes by several hundred gammas in a few minutes. The disturbance is generally accompanied by abrupt increase in *foEs* also, with a height which ranges from 110 to 130 km. An appreciable increase of 1PG appearance is found, while the appearance probability of Hα line gradually falls.
3). Constitution of disturbances in early morning is a little more complicated. Two

ionospheric phenomena are associated with broad negative bay, namely blackout and *foEs* increase. A rise of the auroral height is also found in early morning, and the time when it takes place agree with the time of the appearance of higher *Es* in the morning. IPG also frequently appears, being consistent with the general tendendy to fall of the disturbance altitude. The blackout may be considered as the anomalous ionization in *D*-region, the height of which may be expectable as the continuation of the descending height of *Es* for the preceding period. Thus, in the morning, the disturbances seem to cover widely in altitude including in it both *D* and *E*-regions.

The relationship between auroral and magnetic activity has also been discussed partially by CHREE[2], GARTLEIN[75], BLESS *et al.*[76], MEEK[19], HEPPNER[74] and MALVILLE[68]. Their conclusions are also in general accord with those mentioned above.

For example, MEEK states that the *Es* layer becomes increasingly prominent before the advent of a positive bay, and at the advent, a bright auroral arc at an elevation usually not more than 10° and at an azimuth which is often slightly west of the magnetic north. Coincident with its appearance, he obtained spasmodic echo from the same point of the sky. There is some evidence that *D*-region absorption increases throughout the course of the bay and so does the maximum reflection from the sporadic *E* layer. The aurora usually remains approximately constant in position. It decays in intensity and becomes more diffuse as the field returns to normal.

2. Main problems left untouched in Part I

There are a number of problems still left untouched in Part I, which will be an object of consideration and discussion in Part II. They may be summarized as follows; What is the cause of different features of sharp and broad bay? How is the effect of altitude on disturbance phenomena? What is the intensity ratio among the physical quantities of the disturbance? How are the effects of impinging electrons and protons on the relationship among the disturbance phenomena? The answers to these problems will be given in Part II, successful for some but not completely so, for others.

PART II.

V. INTRODUCTION TO PART II.

1. General remarks

It is of course of great importance to investigate statistically each of the upper atmosphere disturbance phenomena, namely geomagnetic variation, ionospheric disturbances and auroral displays. In addition, the investigation of quantitative relationship among the phenomena seems to be also most essential. It is because, as already pointed out, the origin of disturbance phenomena seems to be common, being concentrated along the auroral zone in almost all cases of disturbances.

A number of incidental discussions have already been made of several relationships among the disturbance phenomena by many investigators[2-6,19,77,78]. Among them, MEEK has reached the conclusion that the *Es* layer becomes prominent during the course of bay disturbances which is usually associated by auroral displays overhead, and that, in some cases, blackout takes place of increase in *foEs* during a large bay when the field is greatly depressed with aurora overhead. At Syowa Station, in fact, an abrupt increase in auroral zenith luminosity and in *foEs* are usually observed coincident with the onset of bay disturbances.

Some examples of the set of records reproduced are shown in Fig. 32. The result shown in this figure is in general accord with the conclusion reached by MEEK and others, but it is a little but importantly different. The difference mainly concerns the time of the advent of disturbance phenomena. That is, the disturbance phenomena start simultaneously within the accuracy of observation in this case, while on appreciable time difference has been reported to exist among the onsets of the phenomena.

Generally speaking, many investigations so far carried out are qualitative descriptions of the inter-relations, and it was not until after the work of OMHOLT[56] in 1945, that a quantitative investigation began to be made. He found a correlation between the emission of the negative nitrogen bands emitted from aurorae in zenith and the maximum electron density in *Es* layer, with the aid of his simultaneous observation at Tromsö. He has pointed out also that zenith luminosity of the negative nitrogen bands may be proportional to the fourth power of the critical frequency of *Es* layer. He also referred to the recombination coefficient in the *Es* layer during aurorae and mentioned that it is greater than 10^{-7}cm^3 sec^{-1}.

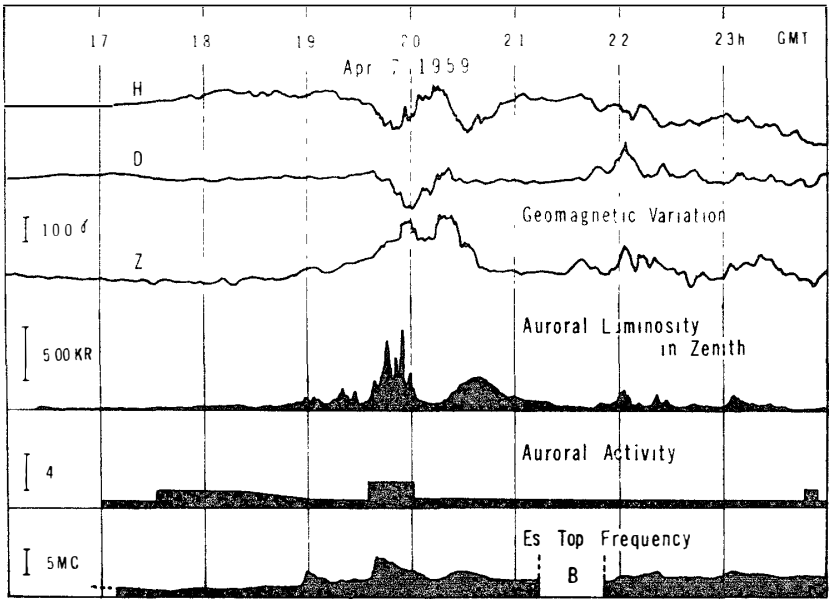
17
18
19
20
21
22
23h GMT
Apr 7, 1959
H
D
Z
100 γ
Geomagnetic Variation
500 KR
Auroral Luminosity in Zenith
4
Auroral Activity
5MC
Es Top Frequency
B

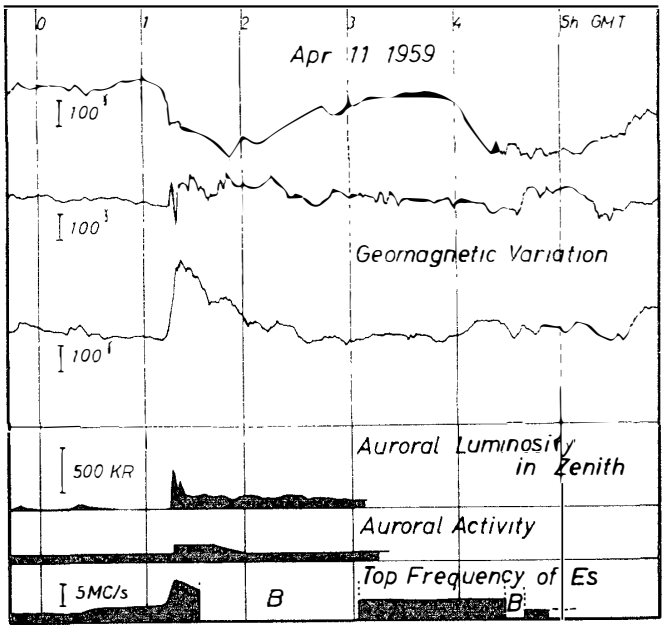
0
1
2
3
4
5h GMT
Apr 11 1959
100 γ
100 γ
Geomagnetic Variation
100 γ
500 KR
Auroral Luminosity in Zenith
Auroral Activity
5MC/s
B
Top Frequency of Es
B

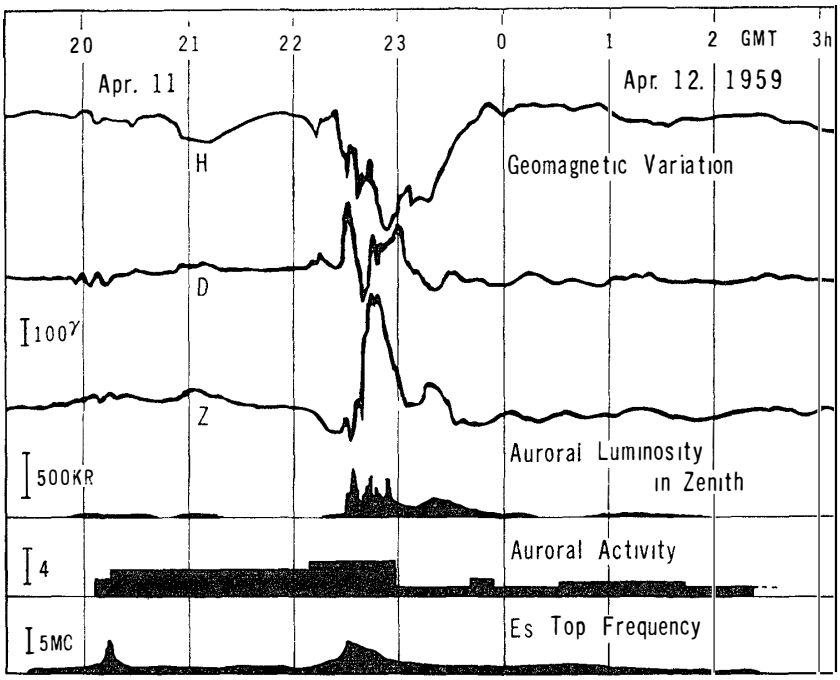

Fig. 32. Typical examples of simultaneous record sets of geomagnetic variation, auroral luminosity in zenith, total auroral activity and *Es* top frequency during upper atmosphere disturbances in the auroral zone.

Similar study has been further extended by TOHMATSU and NAGATA[79] mostly from the theoretical view-point, and by the present writer[80], based on the data at Syowa Station. On the other hand, recent developments of rocket and space probe made possible a direct observation of the physical state in aurorae, especially of the corpuscular inflow into the upper atmosphere. MCILWAIN state that the integral number energy spectrum of protons incident upon the atmosphere during the auroral displays of quiescent glow of about intensity I, is approximately $2.5 \times 10^6 \exp(-E/30)$ protons/sec cm^2 sterad, over the range 80 to 250 kev, while that of electrons equal to $2.5 \times 10^9 \exp(-E/5)$ electrons/sec cm^2 sterad over the range 3 to 30 kev. Further, he states that at least 75% of the light in some aurora is produced by nearly monoenergetic electrons with about 6 kev energy with the peak values of the electron flux of about 5×10^{10} electrons/sec cm^2 sterad.

One of the most important problems in Part II, is to investigate the quantitative relations among the phenomena on the bases of observation data, since the disturbance phenomena are attributable to the impinging corpuscles, as expectable from the results so far obtained. The study is not only helpful for the understanding of the physical state of the ionosphere during aurorae but is of importance for the complete understanding of the whole feature of earth storms.

2. Physical quantities

As visible in a schematic diagram (Fig. 33), the invasion of protons and electrons

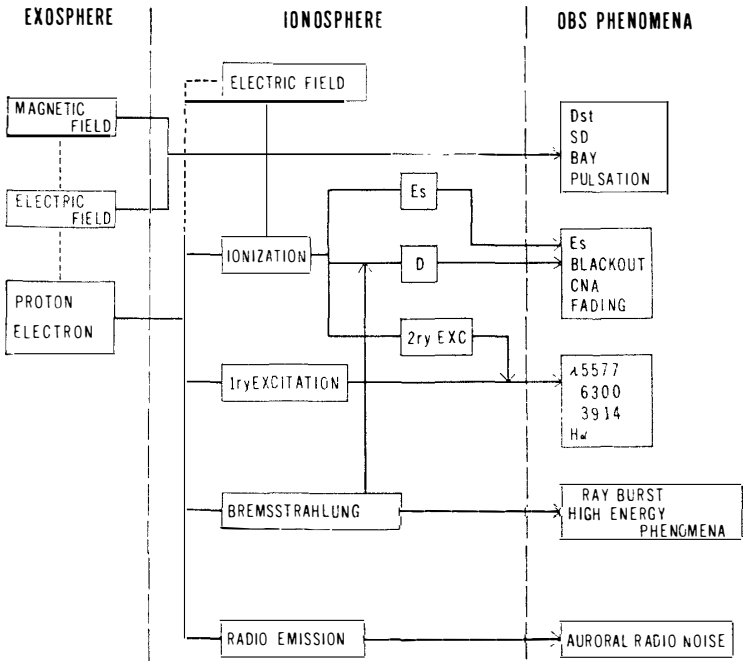

Fig. 33. Schematic illustration of the upper atmosphere disturbance phenomena, and their inter-relations.

may result in ionization and excitation of the upper atmosphere particles. Furthermore, the excess ionization in the lower ionosphere may cause an induced electric current there, which may be responsible for magnetic variations. The three kinds of information are, therefore, available for the investigation of the relationship. They are the ionization in the ionosphere which is represented, for example, by *foEs* and/or by blackout, auroral luminosity and the deviation of geomagnetic field.

Among the ionospheric phenomena, blackout is not very appropriate for quantitative investigations because of its dependence on the sensitivity of sounding apparatus. *foEs* therefore will be mainly dealt with in Part II as an indication of ionization rate.

The forbidden green line of OI (λ5577) is generally used in this paper as a representative of auroral intensity, since it is the most popular and intense among a number of the auroral spectra. 1PG and H_α line are subsidiarily referred to, as occasion demands. As to the geomagnetic variations, here will be used the deviation of horizontal disturbance vector from the expected value without disturbances. Almost all kinds of geomagnetic disturbances are included in the data for a year, namely magnetic storm, bay disturbances, giant pulsations, short period pulsations and *SSC*'s, which will be discussed later.

3. Summary of early works

As already mentioned, the different colours of aurorae indicate that the relative intensities of the various spectral features are not always the same. This paragraph is concerned with the information available on representative mean values. The discussion will be concerned also with the information on mean ionization rate. Table 6

gives summary of results on relative spectral intensity obtained by many investigators[81–86], the scale for each set being chosen so that $\cdot$I (λ5577) is unity.

Table 6. Relative intensity of auroral spectra.

Identification	Wave length	Luminosity
OI ^1S ^1D	5577	1
N_2^+ 1NG (0,0)	3914	1.1—1.9
N_2^+ 1NG (0,1)	4278	0.2—0.4
N_2^+ (NG)		1.0—2.0
O_2 Atmospheric (1,1)	7708	0.08

On the other hand, the ratio of ionization rate with excitation has been investigated by OMHOLT on his observational results obtained at Tromsö. Thus we can now estimate, with the aid of Table 6, the quantitative relations among relative intensity and furthermore the relations between electron density and auroral luminosity of certain line or band. The ratio of ionization with excitation, *i.e.*, the ratio of electron density and luminosity, is obtained also by theoretical process. Based on their calculation, for example, TOHMATSU and NAGATA[79] concluded that the ratio is given by

$$\frac{J\,(5577)}{n^2_{\max}} = 1.5 \times 10^{-10} \quad KR/(\text{electrons/cc})^2.$$

Recently, ROACH and his colleague[87–90], based on the data at College, reported that there is a general increase in auroral zenith luminosity with increase of Kp index. This relation will also be re-examined later in this paper.

VI. RELATIONS BETWEEN MAXIMUM NUMBER DENSITY OF ELECTRON IN *Es* LAYER OR CLOUD AND AURORAL LUMINOSITY IN ZENITH

1. Electron number density in *Es* and luminosity of negative group

The ionization process responsible for the increase in the *E*-regions ionization during magnetic disturbances and auroral displays may be identical with the preliminary excitation process causing the auroral luminosity in negative nitrogen bands in the aurorae (N_2^+, $B^2\sum_u^+ - X^2\sum_g^+$). The excitation of these bands is perhaps also an ionization process as pointed out by OMHOLT, namely

$$N_2(X^1\sum_g^+) + X \rightarrow N_2^+(B^2\sum_u^+) + e + X \quad . \qquad (6\text{-}1),$$

where X is the incoming particle. The fact that it is the primary electron or proton that is responsible for the excitation of $B^2\sum_u^+$ state of N_2^+ makes the problem appreciably simple. Moreover, the life time of this excited state is fortunately short enough (about 10^{-8} sec), so that the collisional deactivation need not be taken into consideration. In the case of negative bands, therefore, a simple relationship is expected to hold between the intensity and electron density in the same place, as follows. It is supposed now that the ionization rate $q(e)$ is proportional to the production rate of N_2 molecules in the $B^2\sum_u^+$ state (q'(N.G.)) such as,

$$\frac{q(e)}{q'(\text{N.G.})} = \kappa \quad \ldots\ldots\ldots\ldots\ldots\ldots\ldots \qquad (6\text{-}2)$$

Under the assumption of equilibrium state, we get for the electron density $n(e)$

$$n(e) = \left(\frac{\kappa q'(\text{N.G})}{\alpha_{\text{eff}}}\right)^{1/2} \quad \ldots\ldots\ldots\ldots \qquad (6\text{-}3),$$

α_{eff} being the effective recombination coefficient. Then, the photon number observed on the ground is given by

$$J(\text{N.G}) = \int_h q'(\text{N.G})dh = \int_h \frac{\alpha_{\text{eff}}}{\kappa} n(e)^2 dh \quad \ldots\ldots\ldots\ldots \qquad (6\text{-}4).$$

If it is assumed that, as an approximation, κ and α_{eff} are independent of height h,

eq. (6–4) may be modified as

$$J(\mathrm{N.G}) = \frac{\alpha_{\mathrm{eff}}}{\kappa} l_0 n^2(e)_{\max} \quad \text{..... (6-5),}$$

where l_0 represents the effective thickness of auroral emission. Based on the data of zenith luminosity of N.G. and ionospheric *foEs* at Tromsö, OMHOLT has obtained a linear relation between $n^2_{\max}$ and J(N.G.), which strongly suggests that the process above approximately holds in aurorae. His result is reproduced in Fig. 34, in which the value of $l_0\alpha_{\mathrm{eff}}/\kappa$ can be numerically estimated to be about 2.5×10^{-10}, the relationship being expressed empirically as $J(\mathrm{N.G.}) = 2.5 \times 10^{-10}\, n^2_{\max}$.

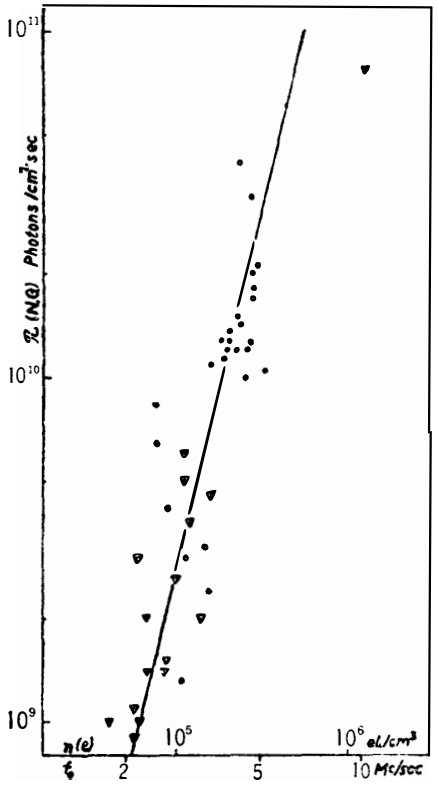

Fig. 34. The relationship between auroral NG luminosity and electron density in *Es* layer. After OMHOLT.

The above relation between J(N.G.) and $n_{\max}$ can be readily replaced by the same kind of relation between J(5577) and $n_{\max}$ with the aid of Table 6, in which is tabulated the relative intensity of auroral emissions. Then, we can presume a numerical relation as

$$J(5577) = (2.5 \sim 1.3) \times 10^{-10} n^2_{\max} \text{...} \quad \text{(6-6).}$$

The equation based on the data at Syowa Station will be discussed more extensively in next paragraph.

2. Electron number density in *Es* and luminosity of green line (J(5577))

The numerical relation between the maximum electron density in *Es* ($n_{\max}$*Es*) and the luminosity of green line (J(5577)) is already deduced from the relations among J(N.G.), J(5577) and $n_{\max}$*Es*. The relation is exmained now by the direct comparison of $n_{\max}$*Es* with J(5577) during auroral displays based on the data at Syowa Station. The period covered is from Feburary to July 1959. The photon emission of λ5577 is measured with a small area in zenith, and the ionospheric observations were carried out every fifteen minutes. The results of the observations are given in Figs. 35 and 36. In Fig. 35 is given a typical set of records during the period when critical frequencies *foEs* could be deduced from the ionospheric records, and in Fig. 36 are given the relation between the values of $n_{\max}$*Es* deduced from the measured values of *foEs* and the values of J(5577) in zenith measured simultaneously.

Although a considerable scatter appears in the points plotted, Fig. 36 gives a strong indication of the validity of eq. (6–5). No fundamental difference is found between the result of observations of NG by OMHOLT and that of green line here. The

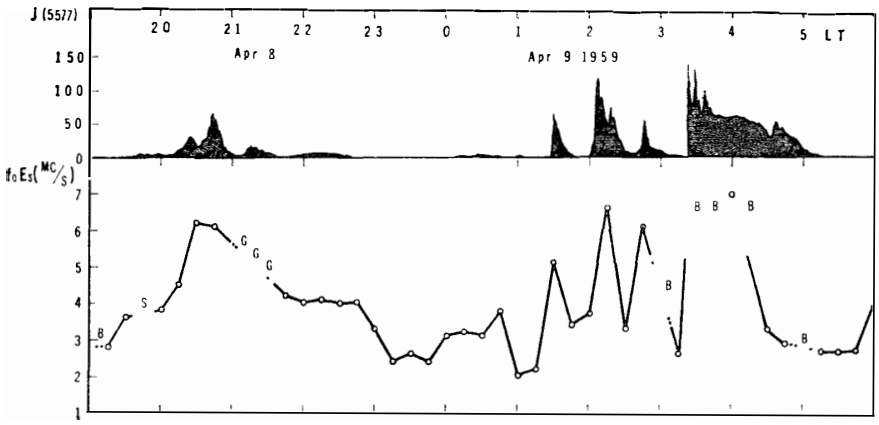

Fig. 35. The variation of the luminosity J (5577) of aurora in zenith and the critical frequency of Es layer or cloud at Syowa Station.

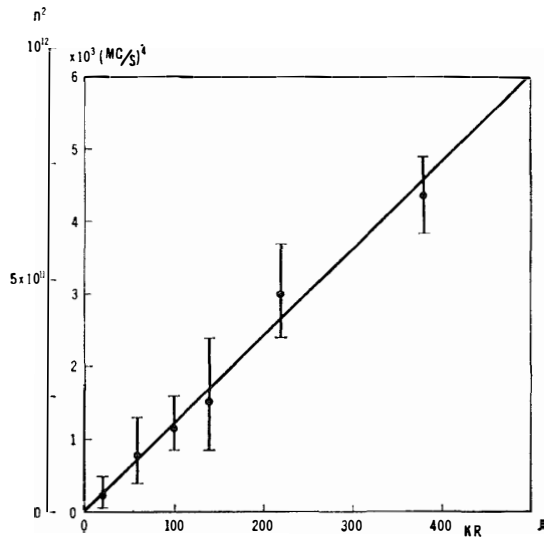

Fig. 36. The critical frequency *foEs* against the photon emission of λ5577 from the aurora in zenith.

scatter in the point plotted may be expected as due to the change in κ, l_0 and α_{eff} with respect to time and space, which may be caused by the change in ionization and excitation process. The empirical formula deduced from the result shown in Fig. 37, which connect J (5577) with $n_{\max}Es$ may be represented by

$$J(5577) = 5 \times 10^{-10} n^2_{\max} \quad \ldots\ldots\ldots\ldots \quad (6\text{-}7).$$

Surprisingly enough, it agrees with the relation in eq. (6–6), which has been deduced indirectly from the relation among J (5577), J (NG) and $n_{\max}$, with a little difference by factor 2 or 3.

From the theoretical view point, however, the relation includes some uncertainties on the excitation process of atomic Oxygen to 1S state and on its deactivation process also, because of the uncertainty of the energy distribution of secondary electrons which

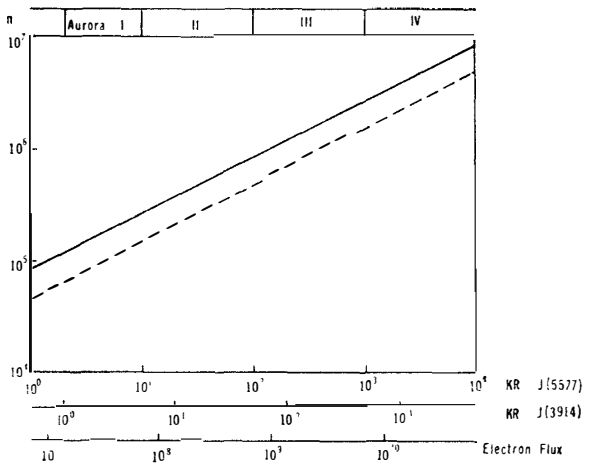

Fig. 37. The maximum eletron density in *Es* layer or clouds vs the photon emission of λ5577 from aurorae in zenith. Observed results at Syowa Station are shown with the results of theoretical consideration by TOHMATSU and NAGATA.

Relations among electron flux auroral luminosity and maximum electron density of auroral ionization.

$$J(5577)=147\pi F(\text{electron})$$
$$=1.5\times10^{-10}\cdot n^2 \quad \text{.....theoretical}$$
$$J(5577)=5\times10^{-10}\cdot n^2 \quad \text{.....observational}$$

may be responsible for λ5577 emission and because of the rather long lifetime of OI in 1S state ($\tau = 0.4$ sec). Then the numerical relation (6–7) may hold in the actual auroral displays in average, including the two effects implicitly in it. Thus we may conclude here that, in auroral displays, the luminosity $J(5577)$ and n^2_{max} is also in proportional relation, and that, if the excitation and ionization processes are always equal, the proportional constant $l_0\alpha_{eff}/\kappa$ should be universaly constant.

According to McILWAIN[11], the flux density of impinging protons and electrons during auroral displays are such as shown in Table 2. It is noted that, the flux of such a majority is electron's that we may consider as the proportional relation is mostly due to electron precipitation.

The result obtained here can be examined in theoretical consideration. TOHMATSU and NAGATA have examined the relationship between incoming flux and auroral luminosity of λ5577 and have concluded that the relation $J(5577) = 1.5 \times 10^{-10} n^2_{max}$ holds under the assumption that the most predominant process in excitation is due to secondary electrons ejected from atmospheric oxygen molecules in such a way as

$$\begin{aligned} &O(3P) + e' = O(1S) + e'' \quad E \geqq 4.17\text{eV} \\ &O(1S) = O(1P) + h\nu(5577) \end{aligned} \quad \text{..... (6-8).}$$

Their theoretical result is satisfied by the broken line drawn in Fig.37, and it seems to agree roughly with the line for observational results in the same figure.

3. Relations of incoming flux with n_{max} and $J(5577)$

From the theoretical consideration above, the production of OI excited to 1S state is known to be proportional to the incoming electron flux. The relation is given by

$$I(5577) = 147\pi F \text{ (electrons)} \quad \ldots\ldots\ldots\ldots \quad (6\text{-}9),$$

where πF represents the particle flux of incoming electrons. The relation can be readily transformed into the relationship between incoming flux and maximum density of electon in *Es* layer or cloud such as

$$\pi F \text{ (electron)} = 3.4 \times 10^{-3} n^2_{max} \quad \ldots\ldots\ldots \quad (6\text{-}10)$$

Using the relation, we can expect the mean electron flux incoming into the upper atmosphere in the auroral zone (from Fig. 20 in Chapter III), to about $10^8 \sim 10^9$ resulting in the order of luminosity which falls into the range of aurora II or III in average around midnight. The consideration may be reasonably supported by the direct rocket observations of incoming flux during auroral displays by McIlwain and others.

4. Altitude dependence and local time effect

If the proportional relationship exists between the second power of electron density (n^2_{max}) and auroral intensity $I(5577)$ anywhere in auroral forms, the height dependence of the relationship is perhaps due to the altitude dependence of the proportional constant $l_0\alpha_{eff}/\kappa$. Then, the information of auroral height must be taken into consideration. It is, however, fairly difficult to obtain the information by the observation at one station, and instead, we use as a measure of disturbance height, the height of *Es* layer or cloud.

Fig. 38 shows the dependence of the ratio of $\sqrt{I(5577)}/(foEs)^2$ with *h'Es*. In the figure, the altitude dependence does not seem remarkable, though there seems to be some tendency to increase in $l_0\alpha_{eff}/\kappa$ with increasing virtual reflection height. The effect is perhaps mostly due to increase in l_0, the effective thickness of aurora, with the increasing height of maximum disturbances, since α_{eff} is obviously the decreasing function of height. Uing the value of α_{eff} so far known, we can deduce from the altitude dependence of $l_0\alpha_{eff}/\kappa$, the altitude dependence of l_0 itself, since κ may be constant independent of height. The results is seen in Fig. 39.

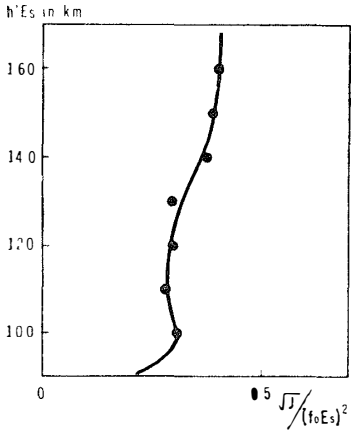

Fig. 38. Altitude dependence of $\sqrt{I}/n_{max}$. The values of $\sqrt{I}/(foEs)^2$ are plotted against the virtual height of *Es*.

Theoretically, the dependence of l_0 with altitude may be obtained from the ionization curve, if a suitable energy spectra of incoming corpuscles can be assumed. As an extreme case, in Fig. 40 are shown the ionization curve obtained by Tohmatsu and Nagata for monochromatic spectra, which may be readily reproduced in form of the relationship between l_0 and the height of maximum disturbances, as shown in Fig. 41. It is found that the curve in Fig. 41 is in general accord with the plotted points in Fig. 39.

The local time inequality of the constant $l_0\alpha_{eff}/\kappa$ is also found at Syowa Station as shown in Fig. 42,

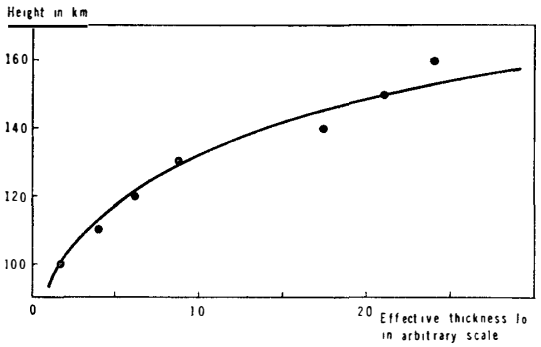

Fig. 39. Relative thickness of auroral displays against the virtual height of *Es*.

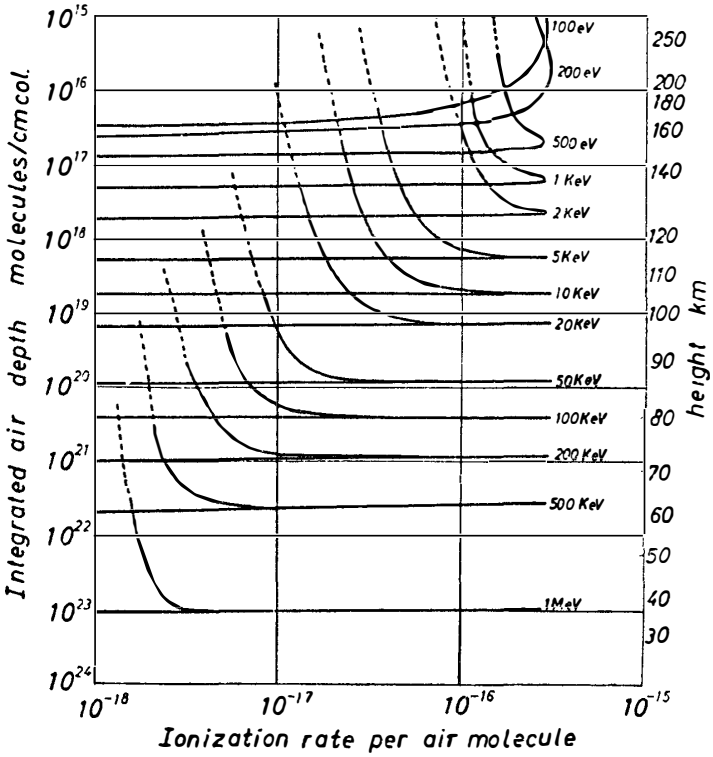

Fig. 40. Ionization rate versus height by fast electrons (ion pairs/electron-air molecule). After Tohmatsu and Nagata.

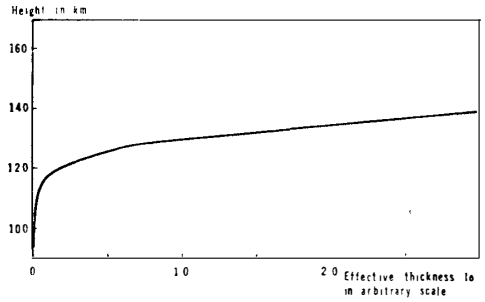

Fig. 41. Estimated thickness of auroral displays versus height, in such a limitting case as the energy of incoming electrons is monochromatic.

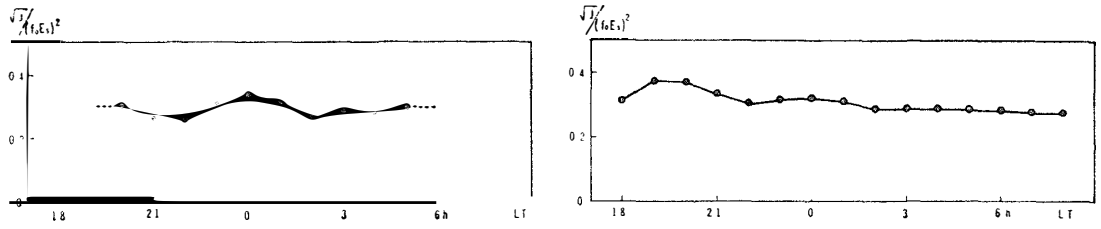

(a) (b)

Fig. 42

(a). Local time variation of $\sqrt{J}/n_{max}$ observed at Syowa Station

(b). Local time variation of $\frac{l_0\alpha_{eff}}{\kappa}$ estimated from the local time change in $h'Es$.

in which is shown the observed value of the ratio $\sqrt{J}/n_{max}$, compared with the values $l_0\alpha_{eff}/\kappa(h)$ obtained by $h'Es$, showing that they are in good agreement with each other. It may concluded, from the result, that the apparent change in $\sqrt{J}/n_{max}$ with local time or with latitude of observation are mostly due to the altitude dependence of $l_0\alpha_{eff}/\kappa$, and that the altitude dependence of $l_0\alpha_{eff}/\kappa$ is most essentially responsible for almost all systematic deviation of $\sqrt{J}/n_{max}$ values from those in the case of isolated bays.

5. Some discussions on the relationship

As stated above, the change in the constant $l_0\alpha_{eff}/\kappa$, of course, considerably scattered in the actual observation, and the change is perhaps due to 1) the kinds of incident particle, 2) the energy spectra of each kind of streams, *i.e.*, the difference of ionization and excitation mechanism, and 3) the mechanism of electron dissipation. The emission of λ5577 may be due to exciation by electron. It is, of course, partly due to incoming protons, but the excitation by secondary electrons caused from primary protons may be estimated far less than the effect of those from primary electrons. It may be concluded, therefore, that the change in ratio of electron flux with proton flux does not affect seriously the auroral luminosity both in λ5577 and NG, though the ratio changes a little with local time, as seen in Chapter III.

From the auroral luminosity curve obtained by HARANG[91], l_0 is found to be 25–30 km for a mean auroral intensity. Adopting 30 km for l_0 and 1 for κ, we get 2×10^{-7} cm^3 sec^{-1}. This is somewhat a higher value than usually accepted for the normal E layer, which is 3×10^{-8} cm^3 sec^{-1} [92]. This value is, however, valid only for daylight conditions. For example, the recombination coefficient for the E-region is generally given by

$$\alpha_{eff} = \alpha_{dis}(A^+) + \alpha_{rad}(A^+) + \sum\lambda(B^-)\{\alpha_m(B^-A^+) + \alpha_3(B^-A^+)\}. \quad (6\text{-}11),$$

where the first and the second terms are coefficients of dissociative and radiative recombination of electrons with A^+ ions, while α_m and α_3 in the third term represent the coefficient of mutual neutralization and three body collision between positive A ions and negative B ions. A is a representative of any atoms and molecules in the upper

atmosphere, and B represents atoms and molecules of oxygen. As the relative concentration of the different positive ions, A^+ may well be different in the two cases (photon ionization and corpuscular ionization), we may easily explain the different value of α_{eff} between those usually accepted and obtained in this paper, as was suggested by OMHOLT.

It should be pointed out also that the values of electron densities given here are mean values over a considerable volume of aurora, though aurorae showing complex structure may include small volumes of considerably higher electron densities. It seems that the numerical relation (6–7) holds between the mean values of n_{max} over a considerable volume of aurora and the auroral luminosity of λ5577 under the statistical conditions of α_{eff} in the aurorae, which may be due to the incoming electrons of a statistical energy spectrum. The relation of n_{max} with luminosity may be extended to other spectra of aurorae with the aid of Table 6.

VII. RELATIONS BETWEEN AURORAL ZENITH LUMINOSITY OF λ 5577 AND GEOMAGNETIC VARIATIONS.....I

1. General remarks

The echo patterns of ionospheric sounding during magnetic disturbances are often very complex. Furthermore, the echo often disappears during severe disturbances, giving information about neither the effective electron density nor the effective disturbance height. Therefore, for the investigation of inter-relations, it seems convenient to replace n_{max} by $\triangle \boldsymbol{H}$ the horizontal magnetic disturbance vector, which may be useful information even in the most severe disturbances.

It should be noted in the replacement, however, that proportionality not always holds between the magnitude of magnetic variations and increases in ionization.

Generally speaking, the variation of magnetic field observed in certain stations is a summation of two kinds of variations. The one is due to the electric current in the lower ionosphere with the direct origin there, and the other is perhaps propagated from the earth's exosphere where it originates. The former is believed to be generally represented by bay disturbances, and the later may include geomagnetic pulsations. The situation may be shown as

$$\triangle \boldsymbol{H} = \triangle \boldsymbol{H}_i + \triangle \boldsymbol{H}_e \quad \text{(7-1)}.$$

where i and e mean that the part is of ionospheric origin and of exospheric origin respectively. As seen already in preceding sections, the interest in this paper mostly concerns $\triangle \boldsymbol{H}_i$, the variation of ionospheric origin, for the investigation of physical interaction and relation among various kinds of disturbance phenomena in the auroral zone. It seems therefore that the most important problem now is to expect the relationship between the number density of changed particles in the ionosphere and magnetic variation of ionospheric origin.

The magnetic variation of ionospheric origin may be expressed in the general form as

$$\triangle \boldsymbol{H}_i = \frac{1}{4\pi} \int \frac{n' \{(\sigma') \boldsymbol{E}\} \times \boldsymbol{r}}{r^3} dV \quad \text{(7-2)}.$$

where n', σ' and $\boldsymbol{E}$ represent respectively effective number density of electrons, specifis conductivity for a ion pair and electric field. In the formula, we can hardly expect

simple relation between $n_{\max}$ and $\triangle \boldsymbol{H}_i$. When the electric current in the aurora of simple form is concerned, however, the situation may be considerably simplified. For example, if the electric current in aurorae may be considered as a line current of infinite length, then in the first approximation in its simple form of displays, $\triangle \boldsymbol{H}_i$ may be connected with $n_{\max}$ in the following relation as

$$|\triangle \boldsymbol{H}_i| = \frac{n_{\max}}{2\pi h} |(\bar{\sigma}')\cdot \boldsymbol{E}| \, d_0 l'_0 \quad \cdots\cdots\cdots\cdots\cdots \quad (7\text{-}3),$$

where d_0 and l'_0 are effective width and thickness of current layer. Postulating l'_0 in eq. (6–10) equal with l_0 in eq. (7–8), we get

$$|\triangle \boldsymbol{H}_i| = \sqrt{\frac{\kappa l_0}{\alpha_{\text{eff}}}} \frac{d_0}{2\pi h} |(\bar{\sigma}')\boldsymbol{E}| \sqrt{J} \quad \cdots\cdots\cdots \quad (7\text{-}4),$$

we can expect therefore a simple relation as $|\triangle \boldsymbol{H}_i| \backsim \sqrt{J}$, if $(\bar{\sigma}') \cdot \boldsymbol{E}$ is independent on $n_{\max}$ *i.e.*, on $\sqrt{J}$. It must be noted that the eq. (7–3) is deduced from a line current approximation. If the area where electric current concentrates is of a certain with, for example, if it is a long ellipse, the relation is considerably modified, and the relation (7–3) is found to hold in the extreme case where the ellipticity e tends to unity.

A simple consideration on the shape of the area of heavy concentration has led to the conclusion that $\triangle \boldsymbol{H}_i$ should be proportional to $n_{\max}$ for the range of $\frac{1}{\sqrt{1-e^2}} \gg \frac{\bar{n}'_{\max}}{n_0}$ while it is proportional to $\frac{1}{\sqrt{1-e^2}}$ if $\frac{1}{\sqrt{1-e^2}} \ll \frac{\bar{n}'_{\max}}{n_0}$ is satisfied. The validity of eq. (7–3) or eq. (7–4), therefore, means that the condition $\frac{1}{\sqrt{1-e^2}} \gg \frac{\bar{n}'_{\max}}{n_0}$ to be satisfied at least in the case of isolated bay disturbances. The discussion above concerns only a stationary state of auroral displays and electric current. In the investigations of the correlations, however, the transient phenomena also must be taken into consideration. For example, the set-up of polarization field E_p in the auroral forms is shown by[70]

$$\boldsymbol{E}_p = \frac{\bar{n}_0 - \bar{n}'_{\max}}{n_0} \left(E_{\perp}^0 + \frac{h_i - h_e}{t_i - t_e} E_{\parallel}^0 \right) \left[1 - \exp\left(- \frac{\sigma_1'}{\varepsilon} \right) \right]$$

where

$$t_{e,i} = \nu_{e,i}/m_{e,i} \, (\nu_{e,i}^2 + \omega_{e,i}^2)$$
$$h_{e,i} = \omega_{e,i}/m_{e,i} \, (\nu_{e,i}^2 + \omega_{e,i}^2) \quad \cdots\cdots\cdots\cdots\cdots \quad (7\text{-}5).$$

The characteristic time $\tau \left(= \frac{\varepsilon}{\sigma_1'} \right)$ in the lower ionosphere is found to be the order of 1 second or its fraction, revealing itself far less than the other characteristic time, for example, of electron dissipation and the duration of bays and giant pulsation, verifying the stationary treatment to be appropriate. Here must be also examined the time change of electron number density in aurora. Since the characteristic time τ_e for electron dissipation is obtained as

$$\tau_e = \frac{e-1}{n_0 \alpha_{\text{eff}}} \quad \cdots\cdots\cdots\cdots\cdots \quad (7\text{-}6),$$

the numerical value of τ_e is obtained to be order of 10 sec, which is also small enough

compared with the duration of ordinary upper atmosphere disturbances so that the change in bay disturbances and giant pulsations can be regarded as stationary phenomena. The stationary relations between $|\triangle H_s|$ and J(5577) will be dealt with in the next paragraph as an example of the simple but most essential case.

2. Relations between geomagnetic variation and auroral zenith luminosity (J(5577)) in the case of bay disturbances

From the two sets of record of a photometer for the systematic recording of OI λ5577 luminosities and of geomagnetic three components which were put into service at Syowa Station in February 1959, the isolated bays (sharp usually) out of the data for 1959 and the corresponding sharp increase in λ5577 zenith luminosity are examined first. The coincidence of the onsets of the two phenomena, as well as of their peaks, is good, as seen in Figs. 32 and 43.

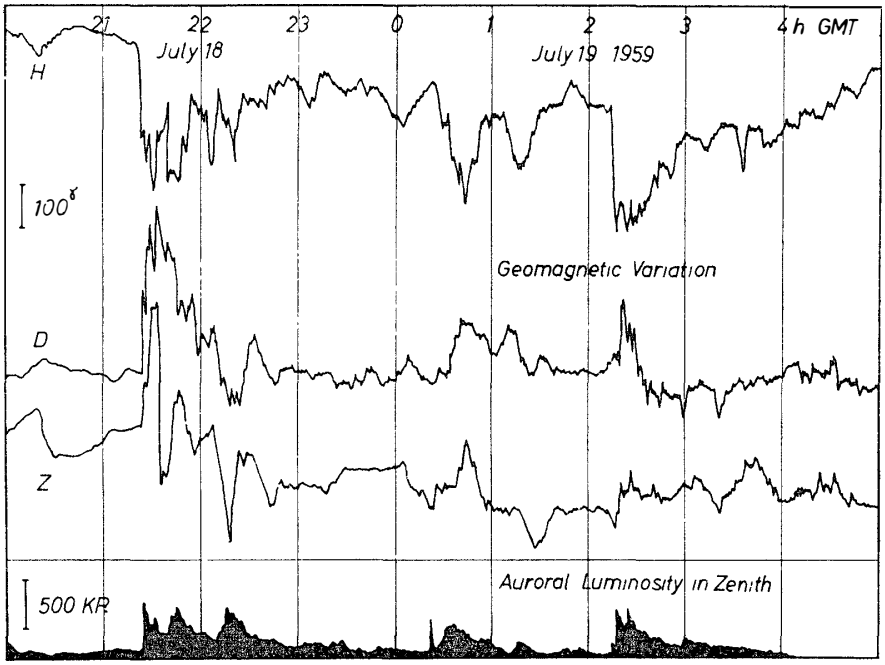

Fig. 43. Geomagnetic variations and coincident change in auroral λ5577 luminosity in zenith.

The original records were read for each peak of variations for J(5577) and $\triangle H$. Fig. 44 is a representation of the relationship between the peak value of $\triangle H$ and the corresponding peak value of J(5577) in the case of bay disturbances. The difference between the relationships of J(5577) with negative bay and with positive bay is somewhat appreciable but not so large as will be shown later, and therefore both negative and positive bays are plotted without any discrimination.

Although a little scatter is visible in the points plotted, the figure shows a strong indication of validity of eq. (7–4). That is, the straight line in Fig. 44, which is

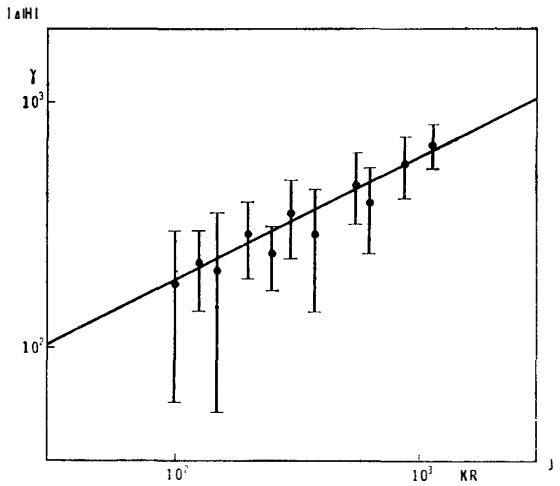

Fig. 44. The magnitude of the geomagnetic horizontal disturbance vector against the auroral λ5577 luminosity in zenith, in the case of bay disturbances.

decided by an ordinary method of least square, is expressed as

$$J(5577) = 3 \times 10^{-3} |\triangle \boldsymbol{H}|^2 \quad \cdots\cdots\cdots\cdots\cdots \quad (7\text{-}7),$$

in general accord with eq. (7–4).

Here is thus established the relation of $|\triangle \boldsymbol{H}|$ with J. The conclusion from Fig. 44 and eq. (7–7) is that the magnitude of magnetic variation increases as the luminosity $J(5577)$ increases, with such a numerical relation that $J(5577)$ is almost proportional to the 2nd power of $|\triangle \boldsymbol{H}|$. Strictly speaking, however, the power factor is found to be 2.2. The fact indicates that the relation is not a simple one as discussed in 7–1, and that the factors in eq. (7–4) *eg.* $\boldsymbol{E}$ and/ or the shape factor which has been neglected in the consideration above is slightly dependent on $J(5577)$, in other words on the activity of disturbances.

3. Altitude dependence of the relationship

The numerical relation between $|\triangle \boldsymbol{H}|$ and $J(5577)$ has been already established in section 7–2, but it was noted to be an universal one. As evident from eq. (7–4), the relation is a weighted mean with respect to altitude. Here, the altitude dependence of the relation will be referred to and will be given some discussions.

The data available for investigations of altitude dependence are restricted to those for excellent conditions, because the sounding echo often disappears in severe storms. Therefore, the amount of data useful for this purpose is so limited that strict discussions on the altitude dependence are fairly difficult to make. Fig. 45 shows the change in $|\triangle \boldsymbol{H}|/(foEs)^2$ which may be proportional to $|\triangle \boldsymbol{H}|/\sqrt{J}$ with respect to the virtual height of *Es* cloud or layer. The values $|\triangle \boldsymbol{H}|/\sqrt{J}$ show a maximum at the level of 120 km and falls toward both the levels below and above showing the level of 120 km to be most efficient for magnetic disturbances.

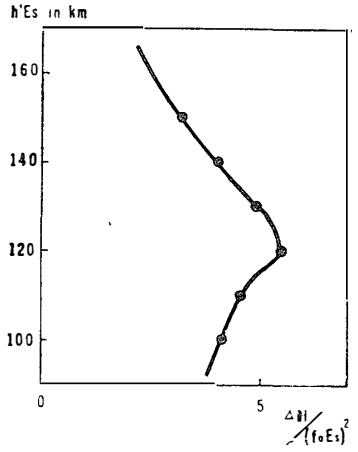

Fig. 45. The altitude dependence of $|\triangle \boldsymbol{H}|/(foEs)^2$, in the case of bay disturbances.

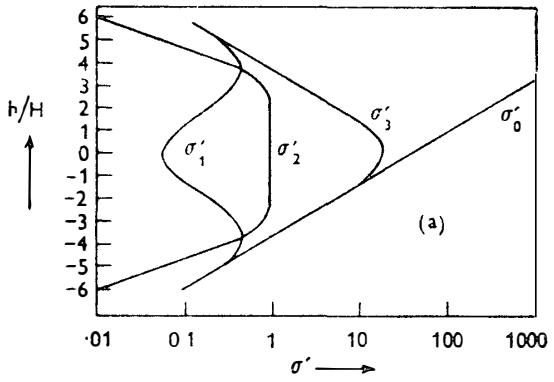

Fig. 46. The conductivities σ'_0, σ'_1, σ'_2 and σ'_3 per ion pair. After RATCLIFFE. The altitude is scaled in unit of scale height H.

The altitude dependence may be tentatively interpreted as follows: Among the factors in eq. (7–4), κ and $\boldsymbol{E}$ does not depend on height in principle and d_0 may be regarded to be independent of h, since the average relations are concerned. Among the rest, however, l_0 and α_{eff} are essentially dependent on the disturbance height. One may suppose, thus, the factor $\sqrt{\frac{l_0}{\alpha_{\mathrm{eff}}}}\frac{|(\sigma')|}{h}$ is perhaps responsible for the altitude dependence of $|\triangle \boldsymbol{H}|/\sqrt{J}$ There still remains a question about the value of (σ'), the effective conductivity per ion pair. Since the magnitude of Hall, Transverse and Cowling conductivities at different heights show considerably different values as shown in Fig. 46, the altitude dependence of $\sqrt{\frac{l_0}{\alpha_{\mathrm{eff}}}}\frac{|(\sigma')|}{h}$ is largely affected by the kind of conductivity appropriate for the factor. For example, it should be noted that the scale for σ_3' is smaller than that for σ_1' and σ_2' by a factor of 10. Among them in the present case, σ_3' is found to be available for substituing σ', being postulated as a line current approximation in the auroral forms. In Fig 47, the estimated value of the factor are plotted as functions of height for a mean auroral display in which l_0 is substituted by the numerical values obtained in 6-2. Comparing the result with that in Fig. 45, one may reach the conclusion that the altitude dependence of $|\triangle \boldsymbol{H}|/\sqrt{J}$ may be almost due to the product of $\sqrt{\frac{l_0}{\alpha_{\mathrm{eff}}}}$ $(\propto l_0)$, the increasing function of height, and $\frac{(\sigma_3')}{h}$, the decreasing function of height, resulting in a peak of the product at the level of about 110 km. Complications arise here because the level height of the maximum value of this estimation is a little less than the observed one. To interpret the fact, however, we can readily

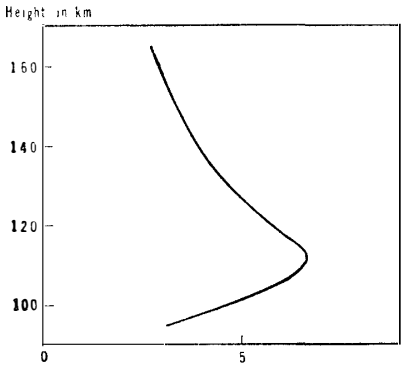

Fig. 47. Estimajed $|\triangle \boldsymbol{H}|/\sqrt{J}$ versus height.

suppose that it is due to the validity of the replacement of σ_3' for σ', and that σ' in fact is well reduced from σ_3' at the level concerned since σ' in reality falls between σ_3' and σ_1', with a slight upward shift of the height of the maximum value.

The numerical value of $\boldsymbol{E}$, substituted in the above consideration is 10^{-3} volt/m, which is not far from the values generally accepted for the electromotive force caused by the dynamo action in the lower ionosphere.

4. Local time inequality of the relationship

On examining the ratio $|\triangle \boldsymbol{H}|/\sqrt{J}$ by means of the ratio $|\triangle \boldsymbol{H}|/(foEs)^2$, one may notice a little but systematic local time dependence of the value as well as its altitude dependence. In Fig. 48, are plotted the value at different local time. The ratio, as seen in the figure, shows a minimum in the evening and tends to increase throughout the night. The situation may be formulated, the altitude dependence of

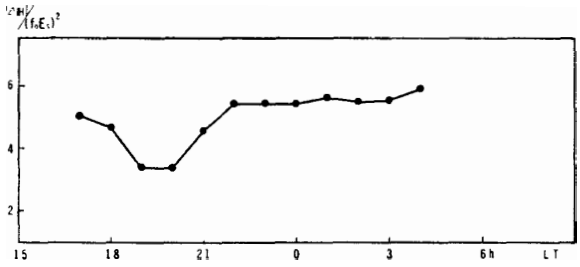

Fig. 48. Local time variation of $|\triangle \boldsymbol{H}|/\sqrt{J}$ at Syowa Station.

$\sqrt{\frac{l_0}{\alpha_{\text{eff}}}}\frac{|(\sigma_3')|}{h}$ being taken into consideration, as follows;

$$|\triangle \boldsymbol{H}|/\sqrt{J(t)} = A(h), \text{ and } h = h(t) \quad \text{..... (7-8),}$$

where $$A(h) = \sqrt{\frac{l_0(h)}{\alpha_{\text{eff}}(h)}} \cdot \frac{\sigma_3'(h)}{h} \quad \text{..... (7-9).}$$

The left hand side of eq. (7–8) is illustrated in Fig. 48, obtained from the numerical values of $\triangle \boldsymbol{H}$ and *foEs*, while the right hand side can be estimated by the numerical value of eq. (7–9) by the height change of *Es* layer, which is shown in Fig. 21. The later, as shown in Fig. 49, is in good agreement in general tendency with the values in Fig. 48. This fact may be an obvious proof that the altitude dependence is essentially the cause of the apparent local time dependence of $|\triangle \boldsymbol{H}|/\sqrt{J}$ This fact may also indicate that the local time dependence is mostly due to the disturbance altitude only and it needs no effect of any other particles than electrons. The effect of incoming protons participating in the relationship among the disturbances may be thus regarded as far less than that of electrons.

It seems worthwhile to note here the conclusions reached in this chapter. One of the most important results is the numerical relation between the magnitude of geomagnetic disturbance vector and auroral zenith luminosity of λ5577, which is given

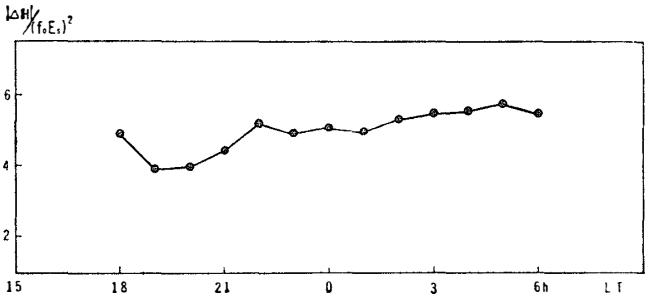

Fig. 49. Local time variation of $|\triangle H/\sqrt{j}|$ estimated from the local time change in $h'Es$.

by the empirical relation (7–7), assuming stationary state. This relation appears to be reasonable, being postulated a line current approximation in the auroral forms. A little altitude dependence of the relation, is also noted, and this has been shown to be interpreted as the altitude dependence of α_{eff}, l_0 and (σ'). The altitude dependence is one of the modifications of the relation (7–7), which will be dealt with in the next chapters more extensively, where the concept of alternative phenomena will be taken into consideration, as well as stationary ones.

VIII. RELATIONS BETWEEN $|\triangle \boldsymbol{H}|$ AND $J(5577)$..... II

1. Severe storms and auroral luminosity

In the preceding chapter, the relation between $J(5577)$ and $|\triangle \boldsymbol{H}|$ in isolated bay disturbances has been examined, and this relation is shown to be the most simple but essential one in the case of stationary and simple formed disturbances. Here, the same kinds of relations between peak values of $J(5577)$ and the corresponding peak values in $|\triangle \boldsymbol{H}|$ of bay type disturbances during severe storms will be examined. It is noted here that there is no reason to expect the validity of eq. (7–7) even statistically, because there is no evidence for the independence of $\boldsymbol{E}$ and d_0 upon J, *i.e.*, upon the activity of disturbances during severe storms.

The relationship is given in Fig. 50. The line drawn to represent the mean relation

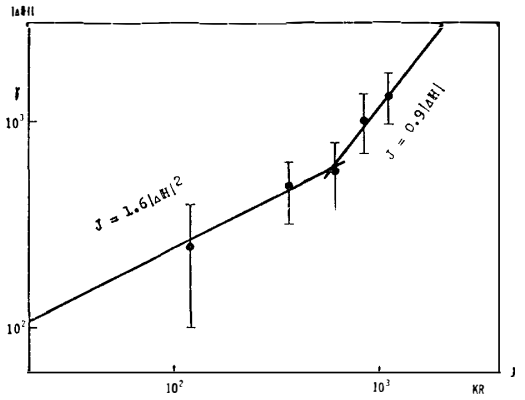

Fig. 50. The magnitude of horizontal disturbance vector of geomagnetic field versus auroral λ5577 luminosity in zenith, in the case of bay type variations in severe storms.

consists of two parts of different feature, which indicate that simple proportionality of $|\triangle \boldsymbol{H}|$ with $\sqrt{J}$ does not hold. Namely $|\triangle \boldsymbol{H}|$ in low-activity is related with J such as $|\triangle \boldsymbol{H}| \propto \sqrt{J}$ as in the case of isolated bays with a little difference in the proportionality constant, but the relation of high activities is far from eq. (7–7). The proportionality of $|\triangle \boldsymbol{H}|$ with $\sqrt{J}$ itself seems to fail for the period of high activity. The empirical

formula in this case may be represented, as

$$J = 1.6 \times 10^{-3} |\triangle \boldsymbol{H}|^2 \quad , \quad \text{at} \quad |\triangle \boldsymbol{H}| < 700\gamma \quad \cdots\cdots\cdots \quad (8\text{-}1),$$

$$J \simeq 0.8 \sim 0.9 |\triangle \boldsymbol{H}| \quad , \quad \text{at} \quad |\triangle \boldsymbol{H}| > 700\gamma \quad \cdots\cdots\cdots \quad (8\text{-}2).$$

The relation (8-1), compared with the eq. (7-7), may indicate that the assumption of independence of $\boldsymbol{E}$ and d_0 upon J, is valid also storms less than 700γ of the magnitude of disturbance horizontal vector. The difference of the proportional constant between eq. (7–7) and eq. (8–1) may be therefore due to the mean change in d_0, the effective width of the current band, in other words due to the integration effect in eq. (7-2) in Chapter VII. On the other hand, the relation (8-2) may be difficult to be interpreted unless an assumption is taken into consideration that $\boldsymbol{E}$ is also dependent on J(*i.e.*, $n_{\max}$), since no significant difference of the other factors cannot be expected to exist between the two ranges of disturbances. If $\boldsymbol{E}$, the electric field, is only responsible for the modification of the relation, one may easily obtain the relationship between $\boldsymbol{E}$ and J(5577) or $n_{\max}$, as

$$E = 6.5 \times 10^{-2} \sqrt{J} \cdot E_0 \quad \cdots\cdots\cdots\cdots\cdots \quad (8\text{-}3).$$

Summarizing the considerations above we get empirical relations of $(\triangle \boldsymbol{H}/\sqrt{J})^2$ in storms with that in bay disturbances, such as

$$\left(\frac{|\triangle \boldsymbol{H}|}{\sqrt{J}}\right)^2_{\text{storm I}} = c_1 \left(\frac{|\triangle \boldsymbol{H}|}{\sqrt{J}}\right)^2_{\text{bay}}, \quad |\triangle \boldsymbol{H}| < 700\gamma \quad \cdots\cdots \quad (8\text{-}4).$$

$$|\triangle \boldsymbol{H}|_{\text{storm II}} \cdot \left(\frac{E_0}{E}\right)^2 = \left(\frac{|\triangle \boldsymbol{H}|}{\sqrt{J}}\right)^2_{\text{bay}}, \quad |\triangle \boldsymbol{H}| > 700\gamma \cdots\cdots \quad (8\text{-}5).$$

$$c_1 \simeq 2$$

The relations will be discussed in more detail later in connection with the other evidence of the electric field $\boldsymbol{E}$

2. *SSC** and auroral luminosity

Of all sudden commencements of magnetic storms, which took place during IGC, when the simultaneous observation of magnetic field and auroral luminosity at Syowa Station was carried out. about 80% of them occured in the day time or during stormy weather without corresponding observation of auroral zenith luminosity. Of the remainder. some were missed and some were inappreciable at the station, so only three sets of data are listed in Table 7. It is found, however, in the records of the three cases, that there is a strong evidence for the geomagnetic *SSC** to be related directly with auroral activity. For example, a record is reproduced in Fig. 51, where the coincidence of negative kick in *SSC**, with the peak of luminosity curve in zenital aurora is found to be almost complete. This fact seems to suggest that *SSC** has its origin, *i.e.*, the equivalent current system responsible for, in the low ionosphere, in like manner as in case of day disturbances. The value of $(|\triangle \boldsymbol{H}|/\sqrt{J})^2$ in this case is quite similar to that of bay disturbances or storms though the mean value of the ratio may

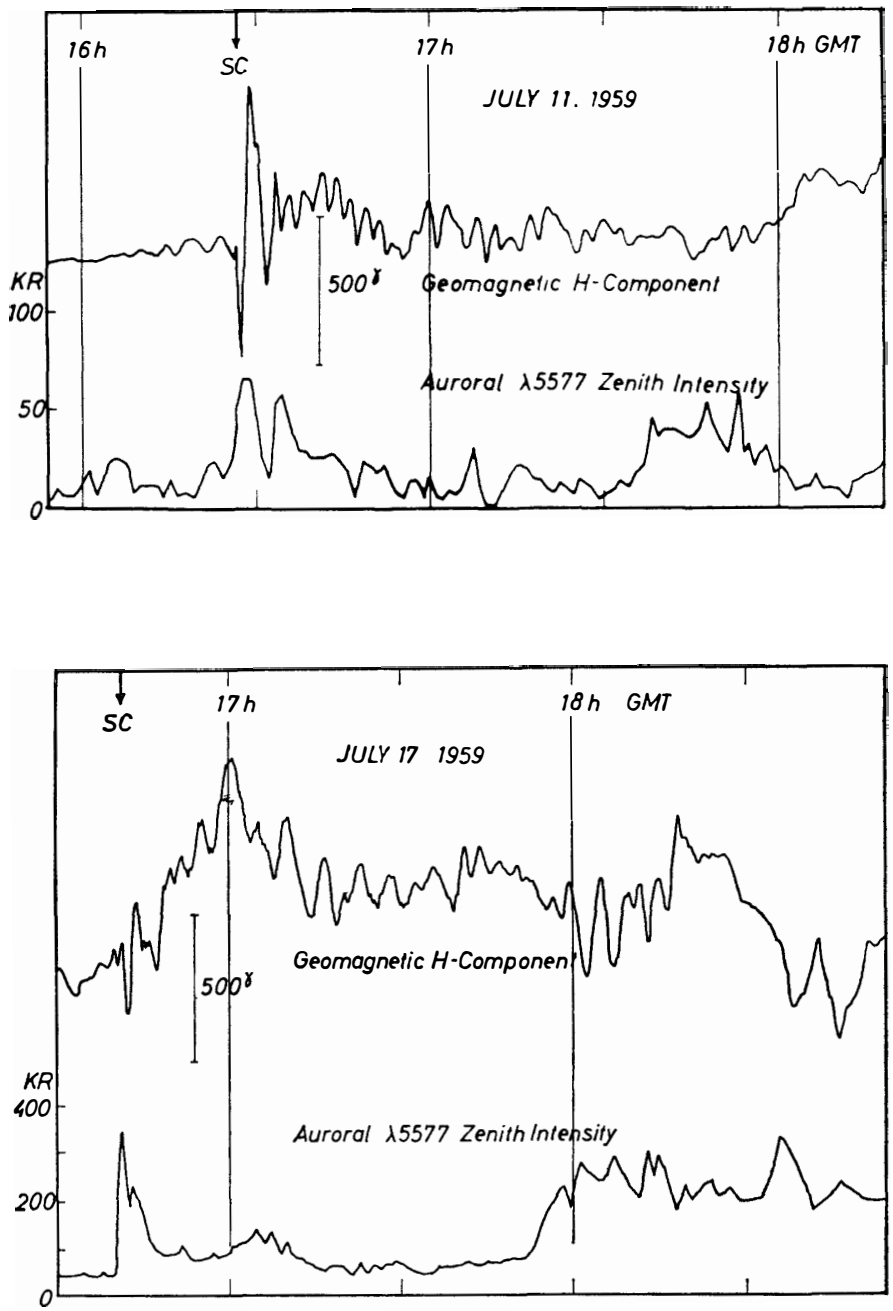

Fig. 51. Examples of geomagnetic record of *SSC** associated with increase in auroral luminosity λ5577 in zenith.

Table 7. Relation between auroral zenith luminosity and geomagnetic variation.

Disturbances	$J/\lvert\triangle \boldsymbol{H}\rvert^2$ (KR/γ^2)	Remarks
Isolated Bay (average)	3×10^{-3}	
Storm (average)	1.6×10^{-3}	$\lvert\triangle \boldsymbol{H}\rvert < 700\gamma$
*SSC**	3×10^{-3}	1828, Apr. 9, 1959
	0.4×10^{-3}	1626, July 11, 1959
	1.4×10^{-3}	1638, July 17, 1959

only be slightly significant owing to the paucity of available data. This fact also seems to be an evidence that the phenomena to be of ionospheric origin, as has been already pointed out by NAGATA and others[94, 95] by an equivalent current system concentrated in the polar region (Fig. 52).

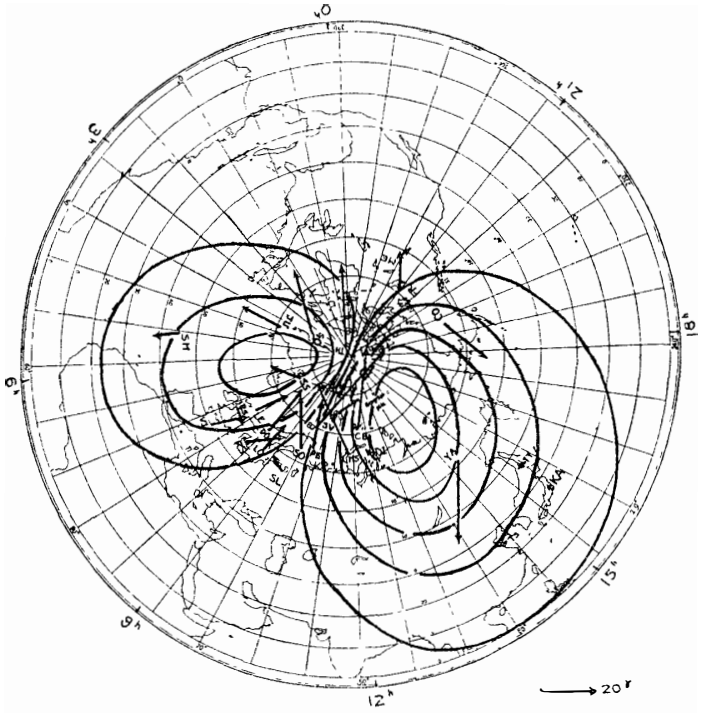

Fig. 52. Equivalent current system for preliminary reverse kick of *SSC** at 0625 GMT on May 29, 1933. After NAGATA and ABE

3. Geomagnetic pulsation and auroral luminosity

Three kinds of geomagnetic plusations were found to be dominant at Syowa Station, on both rapid-run magnetogram and induction magnetogram. The main periods of them are as seen in Fig. 13, 9 sec, 27 sec and 270 sec, which have been called, short period pulsation, intermediate period pulsation and giant pulsation respectively. In this paragraph, the relationship between J (5577) and $\lvert\triangle \boldsymbol{H}\rvert$ in short period pulsation as

well as giant pulsation will be dealt with.

Generally speaking, geomagnetic pulsations are mostly concentrated in the morning-daytime site in the auroral zone as seen in Fig. 16 in Chapter I, and therefore it is fairly difficult to find out whether or not they are associated with simultaneous auroral pulsations.

In some cases, however, when *Pg* occur in dark time, there are found sometimes corresponding auroral pulsations in λ5577 in zenith, while in some other cases no appreciable auroral pulsations associated with magnetic pulsations can be found, even for the most striking pulsations. Examples of the geomagnetic pulsation with or without the coincident auroral pulsations are shown in Fig. 53. On examining the giant pulsa-

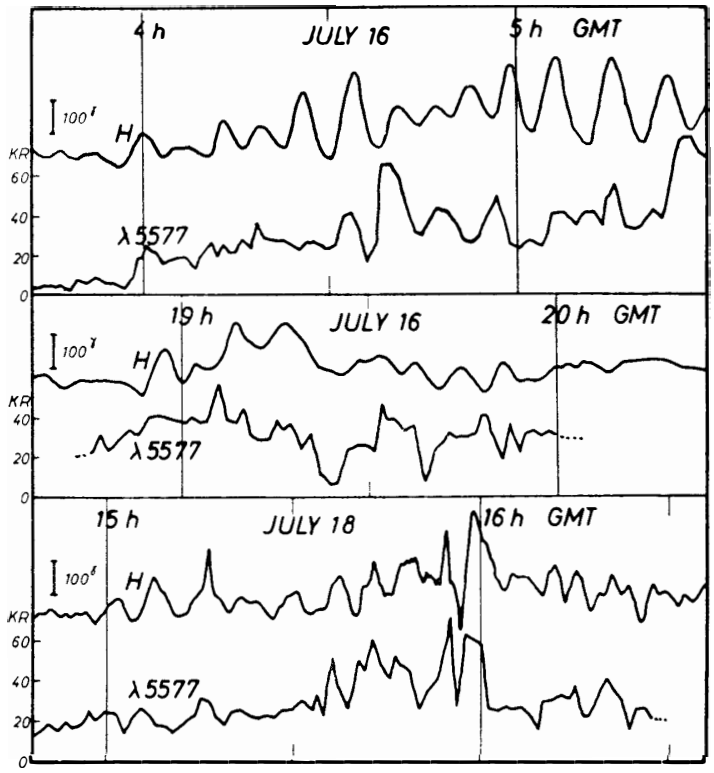

Fig. 53. Geomagnetic giant pulsations and associated auroral pulsations in zenith.

tions, one may find that there are two groups of them, according ways of relating them with the auoral pulsations. The existence of the two groups definitely different from each other, can be clearly indicated in $(J_1/|\triangle H_1|)$ diagram, as shown in Fig. 54, where the suffix means the quantity to be the pulsative fraction of each disturbance.

The points plotted with some scatter are obviously found to be concentrated into two groups, the one showing a close correlation between $|\triangle H_1|$ and J_1, the other not showing this. These will be called hereafter *Pg*I and *Pg*II respectively. It must be noted, here on examining only geomagnetic features, that no remarkable characteristic difference is found between the two groups. The amount of data, much less than that of bay disturbances, seems to prevent us from a complete understanding of the

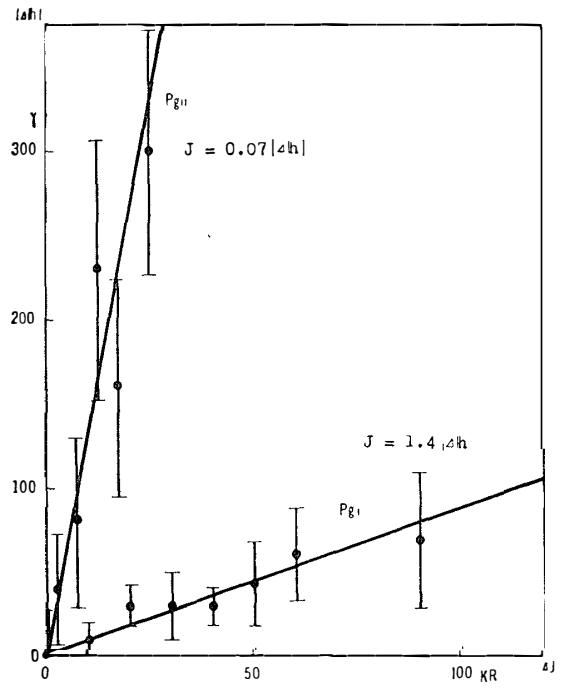

Fig. 54. Double amplitude of geomagnetic giant pulsations against that of auroral λ5577 pulsation in zenith.

characteristic of the two groups, though there may be some appreciable evidences which suggest that there is a systematic change in the base line value of each quantity, $|\triangle \boldsymbol{H}_0|$ and J_0, which the pulsative fraction $|\triangle \boldsymbol{H}_1|$ and J_1 are superposed. In fact, the mean value of $J_1/|\triangle \boldsymbol{H}_1|$ is obtained to be about $1.4^{KR}/\gamma$ for Pg_I, while it is about $0.07^{KR}/\gamma$ for Pg_{II}, corresponding to each mean value of about 200γ and 50γ. It can also be proved easily that $J_1/|\triangle \boldsymbol{H}_1|$ of the pulsations of Pg_I is nearly equal to $dJ_0/d|\triangle \boldsymbol{H}_0|$ of the base line value, a differential form of the relation which has been already obtained in the case of bay disturbances. The salient points of discussion above may be seen in Fig. 55.

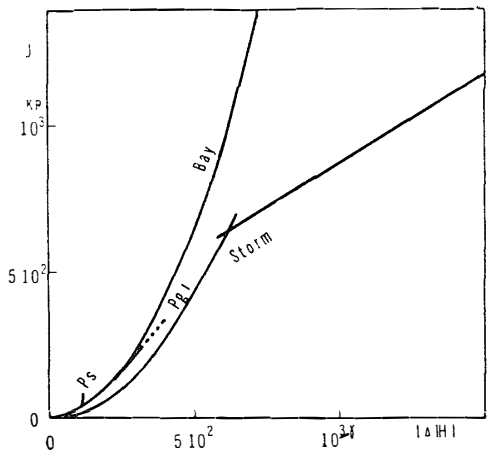

Fig. 55. Inter-relation among the $|\triangle \boldsymbol{H}|-J$ relationships for bay, storm, giant pulsation and short period pulsation on $|\triangle \boldsymbol{H}|-J$ diagram.

On the other hand, if the relation $\sqrt{J_0}/|\triangle \boldsymbol{H}_0| = \text{const.}$ holds universally for all Pg, the minimum value of $(dJ_0/d|\triangle \boldsymbol{H}_0|)$ for Pg of 100γ of double amplitudes, is about $0.3^{KR}/\gamma$, which is proved to be definitely larger than the observational value of $(J_1/|\triangle \boldsymbol{H}_1|)$ for Pg_{II}, being taken into consideration the non-linear characteristics.

From the results mentioned, a conclusion may be derived, namely the Pg_I is mainly of ionospheric origin, whereas Pg_{II} is unlikly

due to the electric current in the lower ionosphere. The result may be important, because it indicates that some part of *Pg* may be of ionospheric origin in contrast to the general belief that they are of exospheric origin. *Pg*ı is perhaps due to periodic ionization with simultaneous excitation in the lower ionosphere as well as the bay disturbances. The physical cause of the periodic ionization is not clear enough at the present stage of the research, though it may be due to the periodic change in incoming flux. Hence it is desirable to develop the study further in order to clarify this point.

4. Short period pulsation and auroral luminosity

It is found occasionally, that the short period pulsation is directly associated with auroral pulsation of the same period at Syowa Station. An example of change in double amplitudes is given in Fig. 56 in which the parallelism of the changes is found

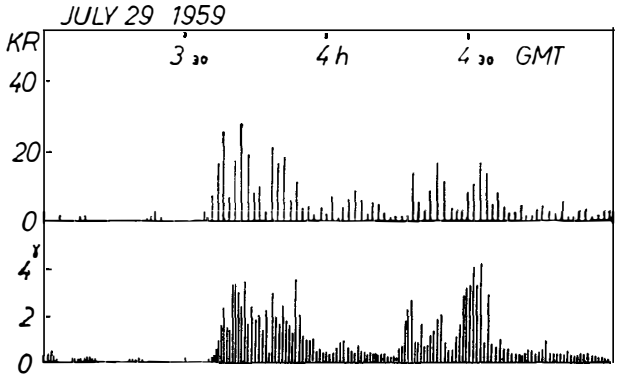

Fig. 56. The time variation of the double amplitude of geomagnetic and auroral pulsations of short period (T ≒ 9 sec).

to be remarkably good. The short period pulsation (the periods ranging from 5 to 12 sec) can no more be considered as stationary phenomena, since its period is comparable with some characteristic time in the lower ionosphere, *e.g.* the time of electron dissipation in this region. In this case, therefore, several "impedance" effects which augment the value $J_1/|\triangle H_1|$ must be taken into account. Among the effects, the electron dissipation and setting up of polarization field seem to be most important, since the excitation life time of λ5577 is about 0.4 sec being far less than the other characteristic time. The later which is a minor effect compared with the former has been already discussed in 7–1. Hence the former will be examined here in connection with the observational result.

The ratio of the pulsative fraction of disturbances in $|\triangle H|$ and $J(5577)$ for short period pulsation are plotted in Fig. 57, where we can see that $(J_1/|\triangle H_1|)$ is anomalously larger than the value both for *Pg* and bay disturbance (Table 8). Moreover, the value being about 6.7, is proved to be appreciably larger than $(dJ_0/|d|\triangle H_0|)$ at the corresponding value of $|\triangle H_0|$ (about 120γ). In fact, this actual value of $(J_1/|\triangle H_1|)$ is

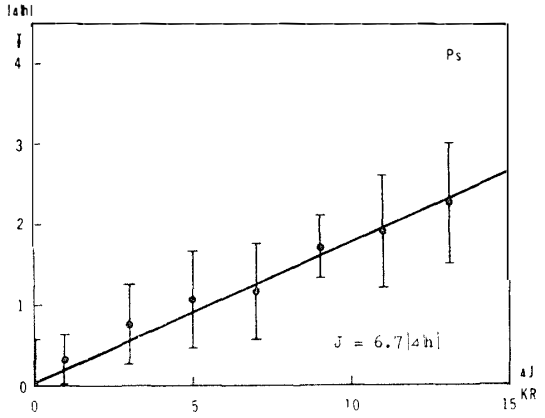

Fig 57. Double amplitude of geomagnetic short period pulsations versus associated auroral pulsations of λ5577 in zenith.

Table 8. Relation between auroral zenith luminosity and geomagnetic variation

Disturbances	$J/\lvert\triangle \boldsymbol{H}\rvert$ (KR/γ)	Remarks
PgI	1.4	T=270 sec
PgII	0.07	
Ps	6.7	T=9 sec $\lvert\triangle \boldsymbol{H}_0\rvert \sim 120\gamma$
$\mathrm{d}J_0/\lvert\mathrm{d}\triangle \boldsymbol{H}\rvert$	1.2	-200γ
min $\mathrm{d}J_0/\lvert\mathrm{d}\triangle \boldsymbol{H}\rvert$ for Pg	0.3	-50γ

high enough for suggesting that the time constant in the ionosphere takes an important role for the remarkable augmentation of the value. We now proceed to calculate the impedance effect by which the ratio $(J_1/\lvert\triangle \boldsymbol{H}_1\rvert)$ may change considerably. For convenience sake it is postulated here that the other conditions except time factor are equal to those of Pg, and that the change in $(J_1/\lvert\triangle \boldsymbol{H}_1\rvert)$ is only due to the difference of the periods between Pg and Ps.

Being thus postulated, the time change in n and J may be given respectively such as

$$\frac{\mathrm{d}J}{\mathrm{d}t} = Q' \cdot n'(\mathrm{M})\, \pi F - \eta J \quad , \qquad (8\text{-}6)$$

$$\frac{\mathrm{d}n_e}{\mathrm{d}t} = Q \cdot n(\mathrm{M})\, \pi F - \alpha_{\mathrm{eff}} n_e^2 \quad . \qquad (8\text{-}7)$$

$$\frac{Q'}{Q} = K \quad . \qquad (8\text{-}8),$$

where $n'(\mathrm{M})$, $n(\mathrm{M})$, πF, and η represents respectively, the number density of neutral atoms of Oxygen, the number density of neutral atoms and molecules responsible for ionization, incoming flux of electrons and effective decreasing factor of excited Oxygen atoms due to λ5577 emission.

The left-hand side of eq. (8–6) can be eliminated since the decay time of luminosity is short enough for considering that the luminosity follows coincidently with the change in incoming flux. We get therefore

$$J = \frac{Q'}{\eta} n'(\mathrm{M})\, \pi F \quad \text{..... (8-9).}$$

If bay and *Pg* are concerned, the left-hand side of eq. (8–7) is also neglected, resulting in the relation

$$n_e^2 = \frac{Q}{\alpha_{\mathrm{eff}}} n(\mathrm{M})\, \pi F \quad \text{..... ..... (8-10).}$$

Substituting πF in eq. (8–10), eq. (8–9) is then modified to a form such as already discussed in Chapter VII as

$$J = K \frac{\alpha_{\mathrm{eff}}}{\eta} \frac{n'(\mathrm{M})}{n(\mathrm{M})} n_e^2 \quad \text{..... (8-11),}$$

which may hold for the equilibrium state. However, if there occurs a quick change in incoming flux as

$$\pi F = \pi F_0 (1 + k \sin \omega t) \quad \text{..... (8-12),}$$

where $k \ll 1$, a small perturbation term n_1 defined as

$$n_e = n_0 + n_1 \quad \text{..... (8-13),}$$

is found to be given by

$$n_1 = \frac{KQ\, n(\mathrm{M})\, \pi F_0}{\sqrt{\omega^2 + 4\alpha^2_{\mathrm{eff}} n_0^2}} \sin(\omega t - \delta) \quad \text{..... (8-14),}$$

$$\tan \delta = \frac{\pi}{\alpha_{\mathrm{eff}} n_0 T} \quad \text{..... (8-15).}$$

Then we get from eqs. (8–9) and (8–14),

$$\frac{J_1}{n_1} = \sqrt{1 + \frac{\omega^2}{4\alpha_{\mathrm{eff}}^2 n_0^2}} \cdot \frac{dJ_0}{dn_0} \quad \text{..... (8-16).}$$

Therefore, if it is supposed that the simple relation $|\triangle \boldsymbol{H}| \propto n$ is satisfied in this case, the relation of amplitude between zenith auroral luminosity and magnetic change in short period pulsation can be given as

$$\frac{J_1}{|\triangle \boldsymbol{H}_1|} = \sqrt{1 + \frac{\omega^2}{4\alpha_{\mathrm{eff}}^2 n_0^2}} \cdot \frac{dJ_0}{d|\triangle \boldsymbol{H}_0|} \quad \text{..... (8-17)}$$

This equation can be transformed into

$$\frac{J_1}{|\triangle \boldsymbol{H}_1|} = 6 \times 10^{-3} \sqrt{1 + \frac{\omega^2}{4\alpha_{\mathrm{eff}}^2 n_0^2}} \cdot |\triangle \boldsymbol{H}_0| \quad \text{..... (8-18),}$$

with the aid of eq. (7–7).

On substituting each numerical value for $J_1/|\triangle \boldsymbol{H}_1|$, ω and $\triangle \boldsymbol{H}_0$, we get $\alpha_{\mathrm{eff}} n_0 =$

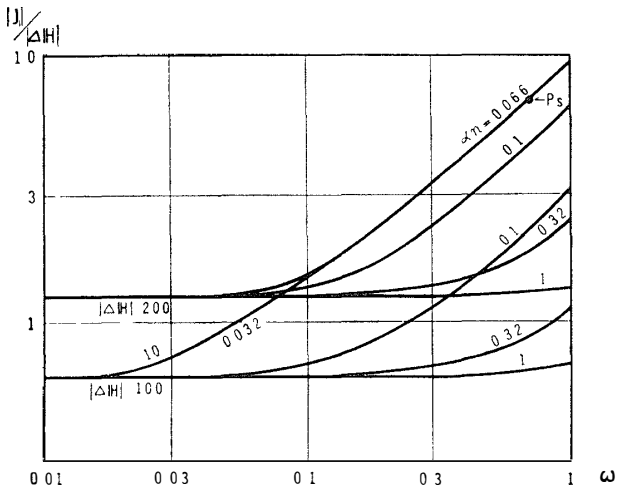

Fig. 58. Dependence of $J_1/|\triangle \boldsymbol{H}_1|$ on $|\triangle \boldsymbol{H}_0|$ and on the period of pulsations.

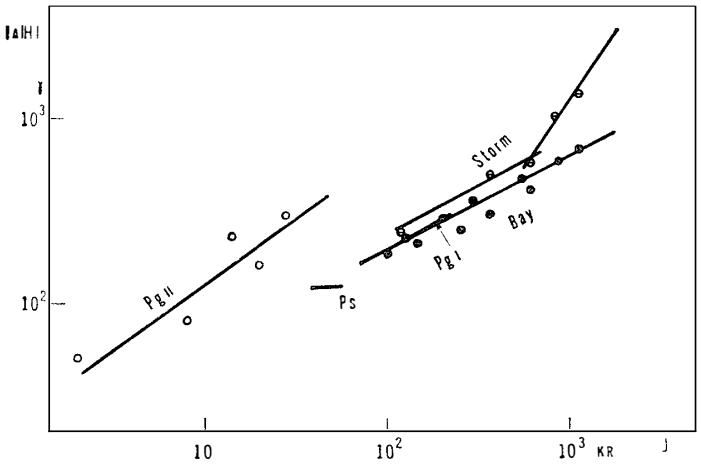

Fig. 59. General aspect of $|\triangle \boldsymbol{H}| - J$ relationship.

0.076 and $\alpha_{\text{eff}} = 1.5 \times 10^{-7}$ (Fig. 58). The effective recombination coefficient thus estimated, which is little higher value than that generally accepted for this region of ionosphere, is in agreement with the value obtained in 6–5. From the results stated above, it is concluded that the short period pulsation is due to the pulsation of incoming flux, and that the apparent change in ratio $J_1/|\triangle \boldsymbol{H}_1|$ is attributable to the fact that the characteristic time of luminosity decay is short enough compared with the change in flux, while that of electron dissipation is comparable to it. In Fig. 59 are summarized the relationship between $|\triangle \boldsymbol{H}|$ and $J(5577)$ for various kinds of magnetic disturbances which have been dealt with in this chapter.

5. Latitude dependence of the relationship

Another kind of information on $|\triangle \boldsymbol{H}|/\sqrt{J}$ has been obtained by ROACH and

others[87–90] from the data collected from station mainly distributed in North America. They have estimated, the median value of luminosity for different Kp indices, at four stations, College, Thule, Rapid City and Fritz Peak, and have found a general increase in J with increase of Kp. Their results can be summarized and reproduced for convenience of our purpose. For direct intercomparison of their results with those in the present paper, we need to replace their relation, J-Kp by J-A, where A represents the equivalent amplitude. In Fig. 60 the results reproduced in which we can see $A/\sqrt{J}$ to have a

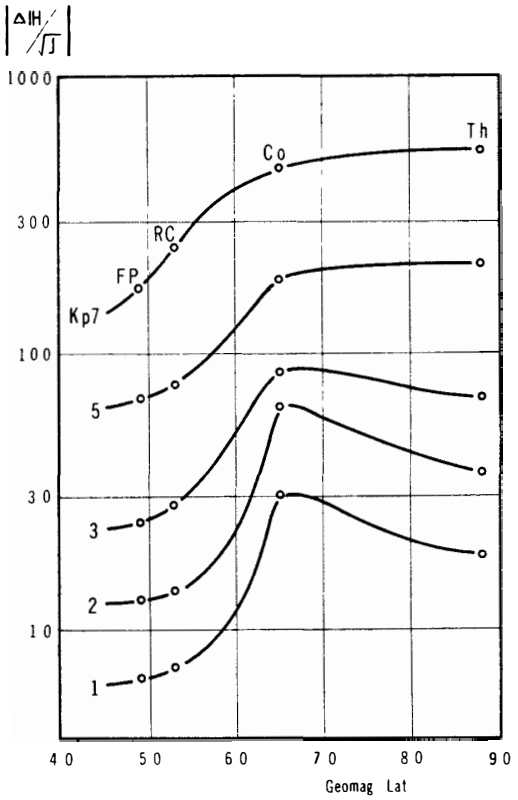

Fig. 60. Reproduction from the results by ROACH *et al.* $A/\sqrt{J}$ versus geomagnetic latitude.

maximum at the auroral zone for smal' activities. During high activities, however, $A/\sqrt{J}$ seems to tend to increase as a whole, and at the same time, the value around polar cap becomes highest. This is perhaps partly due to the integration effect on $|\triangle H|$ and partly due to the change in electric field, since there is no reason, apriori, that it remains constant during severe magnetic storms.

In the next chapter, we will proceed to examine the change in the relationship between $|\triangle H|$ and J, with a reference to the effect of electric field.

IX. VARIATIONS OF THE RELATIONSHIP BETWEEN $|\triangle \boldsymbol{H}|$ AND J

1. Altitude dependence

In Chapters VII and VIII, the observational results on the relationship between $|\triangle \boldsymbol{H}|$ and J are discussed, and it has been pointed out that the relationship is most simple, being statisfied by a proportionality of $|\triangle \boldsymbol{H}|$ with $\sqrt{J}$, in the case of isolated bay disturbances. There are found, however, also considerable fluctuation or deviation from this simple relation for other magnetic variations as discussed in Chapters VII and VIII. Hence, of the relations that were previously referred to occassionally, that which was given in eq. (7–2) is the most general. Since the integral of this equation depends directly on the mode and extension of the equivalent current system, it seems to be more convenient to write eq. (7–2) in terms of deviation from the "standard" relation by some factors, which include implicity the effect of the integral as well as the effect of the impedance for rapid variation. In terms of these "deviation factors", the magnitude of geomagnetic disturbance in horizontal vector becomes

$$|\triangle \boldsymbol{H}_s| = \frac{|\boldsymbol{E}|l_0|(\sigma)'|}{2\pi h}\sqrt{\frac{\kappa}{\alpha_{\mathrm{eff}}\, l_0}}\, d_o A_s \cdot A_t \cdot \sqrt{J} \qquad \cdots\cdots \text{(9-1)},$$

where

A_s = Integration factor

A_t = Inpedance factor.

In the case of isolated bays, $|\triangle \boldsymbol{H}|/\sqrt{J}$ seems to remain approximately constant. In reality, however, the relationship is complicated even for isolated bays, and the proportionality should be considered to be satisfied in statistical meaning, in such a limiting case where both A_s and A_t in eq. (9–1) approach to unity. To give an explicit form of altitude dependence factor as well as A_s and A_t, we need here some considerations on the factors in eq. (9–1). The value κ must essentially remain constant since the ionization and excitation process have been postulated. $|\boldsymbol{E}|$, the intensity of electric field is readily found to be approximately independent of altitude in aurora, because the parallel conductivity is estimated to be far from the transverse conductivities. Then, if d_o is statistically independent of the mean altitude of disturbance, we get a factor A_h, which is a function of height only, such as

$$A_h = \sqrt{\frac{l_0}{\alpha_{\text{eff}}}} \cdot \frac{(\sigma')}{h} \quad \text{..... (9-2),}$$

which has been already discussed in Chapter VII.

It must be noted here that, though each factor in eq. (9–2) is a function of height, A_h as a whole shows such a little dependence on height, that the altitude dependence may be negligible on the examination of the relationship without special interest on height dependence.

2. Effect of integration

Apart from altitude dependence of $|\triangle \boldsymbol{H}|/\sqrt{J}$ there are considerable differences of the value between isolated bays and bay type variations in severe storms, as seen in Table 7. One of the most outstanding difference between the two disturbance phenomena may be that of linear scale of disturbed area. We can suppose, therefore, that the integration factors A_s may be an important factor in this case. From eq. (8–1), we get a numerical value approximately constant for A_s at the range of $|\triangle \boldsymbol{H}|$ well below 700γ, such as,

$$A_s \fallingdotseq 1.4, \quad |\triangle \boldsymbol{H}| < 700\gamma \quad \text{..... (9-3).}$$

On the other hand, at the range exceeding 700γ, the change in the relationship seems unlikely to be attributable to only the integration factor A_s. It is perhaps due to the change in E, as

$$\frac{E}{E_0} = 6.5 \times 10^{-2}\sqrt{J}, \quad |\triangle \boldsymbol{H}| > 700\gamma \quad \text{..... (9-4).}$$

We now proceed here to seek the physical origin from which A_s may be derived.

Since J have been measured in a small area in zenith, the ratio $|\triangle \boldsymbol{H}|/\sqrt{J}$ may change with change in effective width of auroral displays, which may be one of the integration effects on $|\triangle \boldsymbol{H}|/\sqrt{J}$. In fact it is readily found that the magnitude of magnetic change may be modified by such a factor, in the simple case of a uniform current band of 2s in width, as

$$A_s = \frac{2h^2}{d_0} \log\left(\frac{s + \sqrt{h^2 + s^2}}{h}\right) \quad \text{..... (9-5)}$$

Fig. 61 shows the effect of broadening of the display band, where A_s is found to amount to 2, corresponding to the change in the effective width from 100 km to 300 km. In this case, if the observation point deviates from the centre of the current band, the derivation of course results change of $|\triangle \boldsymbol{H}|/\sqrt{J}$. The factor A'_s which is given by

$$A_s' = \log\left[\frac{(s - x) + \sqrt{h^2 + (s - x)^2}}{\sqrt{h^2 + (x + s)^2} - (s + x)}\right] \Big/ \log\left[\left(\frac{s + \sqrt{h^2 + s^2}}{h}\right)^2\right] \quad \text{(9-6),}$$

where $x =$ deviation, is, however, not be much effective in actual cases, being approximately equal to unity with a deviation less than some fractions of the current width.

Apart from the effects, there still remains a problem on the change in effective conductivity in the auroral forms. The numerical values of σ' have been equalized to σ_3' in the discussion above, but there are some reason to consider the approximation to

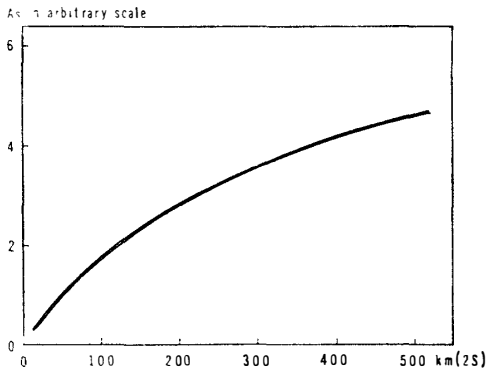

Fig. 61. Change in $|\triangle H|/\sqrt{J}$ by the broadening of auroral band.

be sometimes quite incorrect. It is because that the activated area, though obviously long along the direction of auroral zone, may not always be approximated to the line current of infinite length. The problem of examining the linear dimension of disturbance area and its shape seems, therefore, to be one of the most important problem not only because it is directly connected with the incoming mechanism of the corpuscular stream, but because it may offer a clue to the investigation of the electric field impressed in the lower ionosphere during auroral displays, through a comparison of the order of magnitude of σ observed with expected value of σ' in actual disturbances.

3. Impedance effect

Magnetic pulsations of short period which are sometimes observed at dawn have been already discussed in some detail in connection with the corresponding auroral pulsation, in Chapter VIII. From eq. (8–17), we can get the factor A_t for the pulsative fraction of $|\triangle H|$ namely $|\triangle H_1|$, as

$$A_t = 1\Big/\sqrt{1+\frac{w^2}{4\alpha_{\mathrm{eff}}{}^2 n_0{}^2}} \quad \cdots\cdots\cdots\cdots\cdots \quad (9\text{-}7).$$

There should be, of course, a characteristic phase difference expected form eq. (8–15) between auroral and geomagnetic plusations, as well as the difference in amplitude. Unfortunately, however, the apparatuses used at Syowa Station have been of insufficient resolving power for such a short time delay as the phase of the short period pulsations. It is desirable to confirm the presumption of the phase delay, which may be a strong indication that the short period pulsation is a modification of bay type variation of ionospheric origin, owing to a periodic incoming of corpuscular stream.

4. Change in electric field

From the result obtained by ROACH *et al.*, which is reproduced in Chapter VIII, it has been pointed out that $A/\sqrt{J}$ depends on Kp as well as on latitude. In addition, it has been found in Chapter VIII that, the feature of $|\triangle H|/\sqrt{J}$ at the range of $|\triangle H|$ above 700γ is quite different from that in the other cases. The curious feature of $|\triangle H|/\sqrt{J}$ which seems to depend on J has been already interpreted tentatively by the change in electric field during an auroral disturbance. We can hardly reach other conclusions, since there is neither physical reason nor observational evidence for proving that other factors may differ in such a way as seen in Fig. 50, at the two ranges of $|\triangle H|$ below and above 700γ The result seems to be strongly supported by other kinds of facts obtained

at the auroral zone. That is the change in drift velocity of electron in the lower ionosphere with increasing magnetic activity[96–100]. According to CHAPMAN[101], the drift speed of electrons in the E region remains approximately constant around 80 m/sec at the value of Kp below 5 while it abruptly tends to increase with increase of Kp, corresponding to Kp above a critical value (Fig. 62).

By the eq. (8–3), we are able to obtain the ratio of the additional electric field intensity E to that in quiet state E_0, as one of the modification factors to the "standard" relationship, such as

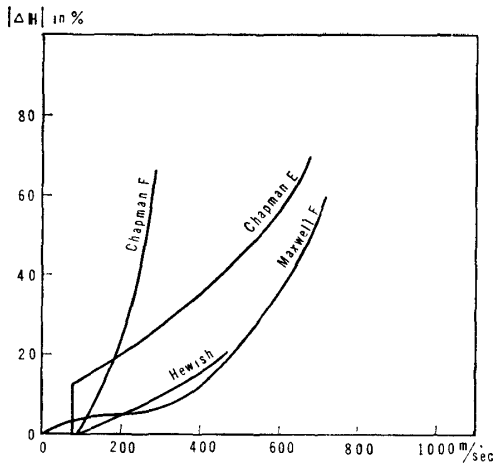

Fig. 62. Drift velocity of electrons versus geomagnetic activity.

$$\frac{E}{E_0} \fallingdotseq 9 \times 10^{-2} |\triangle H|_{\text{in}\%} \quad \cdots\cdots\cdots\cdots\cdots\cdots \quad (9\text{-}8).$$

$|\triangle H|$ is expressed here in this equation, by degree of variation that establishes K of 9 for the station concerned to be 100 per cent, for the convenience of comparison with the data at various stations.

By CHAPMAN's data on the drift velocity, the value of E/E_0 during severe storms above $Kp = 5$ may also be estimated since E seems to be proportional to the drift velocity. The relation is found to be in general accord with eq. (9–8) with a little difference in the proportionality constant as given by

$$\frac{V_d}{V_{d0}} = \frac{E}{E_0} \fallingdotseq 12 \times 10^{-12} |\triangle H|_{\text{in}\%} \quad \cdots\cdots\cdots\cdots\cdots \quad (9\text{-}9),$$

where V_d = drift velocity during severe storms

V_{d0} = drift velocity during small disturbances

and E_0 may be estimated to be about 5×10^{-3} volt/m.

Generally speaking, the change in electric current in the lower ionosphere which is responsible for magnetic variation may be attributable partly to the increase in conductivity and partly to that in electric field.

If the electric field is constant, and if the geomagnetic change is regarded consequently to be only due to the increasing conductivity in the ionosphere, there may be no reason to expect the increase in drift speed with increasing activity. We may conclude therefore from the result also that the electric field in the auroral forms may change, at the activities over $Kp = 5$ at least. The existence of a knee point around $Kp = 5$, which is seen in Fig. 62, may suggest that, the electric field is approximately independent on activity for small activities, whereas it is impressed abruptly for severe activities above $Kp = 5$. The feature of $|\triangle H|/\sqrt{J}$ in high activity may be thus attributable to the effect of increasing electric field, together with the increase in conductivity.

5. Geomagnetic chage of exospheric origin

There have been found a characteristic variation of geomagnetic field named *Pgii*, which have no corresponding auroral phenomena (very little if they have). It is clear in Fig. 59 or in Tables 7 and 8, that almost all geomagnetic variation, *e.g.*, the isolated bay, storms, *Pgi*, short period pulsations and *SSC**s belong to one group which satisfies the relation $|\triangle \boldsymbol{H}| \propto \sqrt{I}$, with or without some modifications except *Pgii*. Then we may conclude, therefore, that the relation (7–7) is one of the criteria for examining whether or not a certain kind of geomagnetic variation is of ionospheric origin.

According to this, the group of *Pgii* which shows a value well deviated from the eq. (7–7), as shown in Fig. 59, may be regarded as the change of other kind, which may have its origin well beyond the earth upper atmosphere, for example, in exosphere, judging from its small value of the luminosity compared with corresponding variation of geomagnetic field.

X. INTERPRETATIONS AND DISCUSSIONS

1. Disscussions on the morphological characteristics

The main feature of the upper atmosphere disturbance phenomena obtained in Part I in this paper, seems to be of profound significance from the two physical viewpoints, namely 1) the change in intensity and/or occurrence frequency of disturbance phenomena and 2) the distribution of altitude of the level where they mostly take place. It is because the former, which may be represented by the distribution pattern of *foEs* as well as by that of the occurrence probability of activated area, indicates directly the intensity of incoming flux, while the later which is represented by *h'Es* concerned with the energy spectra of the flux.

The discussion above may be applicable for both protons and electrons in incoming corpuscular streams. In reality, however, the effect of incoming proton may be negligible on the auroral luminosity because of its less abundance in the incoming stream, unless a special reference is taken into account on H_α, H_β etc., in auroral spectra. On the other hand, magnetic activity is not a direct indication of incoming flux, because the activity may be modified by some factors, the height, the changing rate and the electric field, etc. In Chapters VIII and IX these problems have been discussed in some detail, and it has been pointed out that the most essential change in the relationship between $|\triangle \boldsymbol{H}|$ and J for isolated bay disturbances, is the change in terms of height. Out of the inter-relations thus established among $|\triangle \boldsymbol{H}|$, J, and n through their altitude dependences, we have arrived at a conclusion that the disturbance phenomena in the auroral zone may be regarded as the effect of the incoming electrons, which have different energy spectra at different local times and at different latitudes. In the evening, it penetrates into the level of about 140 km, corresponding to the initial energy of about 500 ev $\sim$ 1 kev, while in the early morning the effective penetration height is about 90–100 km which corresponds to the initial energy of about 5 kev–30 kev. The origin of such a remarkable change in energy of incoming electrons may be one of the most important problems in connection with the physical mechanism of acceleration of the electrons in the outer atmosphere. At the present stage of research, however, the information on the problem is still insufficient for establishing the acceleration mechanism. It may be worthwhile to note here that the appearance of H_α line in auroral spectra precedes generally the appearance of the other lines or bands. It means that the electron precipitation is generally preceded by proton invasion, which may result

in an electric charge separation near the auroral zone and its break-down throughout the night. Some papers on electrostatic field on the surface of the earth have stated that the field changes considerably during displays, but the fact is not yet well established and further investigation is certainly desirable.

The fall in the mean altitude of auroral displays with decreasing latitude, as seen in Figs. 22 and 25, is perhaps due to the broadening of the auroral zone during the severe disturbance accompanied by a characteristic fall of mean display altitude. It is because, at the area far outside of the auroral zone, the auroral displays observable are severe, while in the auroral zone even the weak and high aurorae can be observed. This consideration leads us to the conclusion that the storminess of disturbances is not only due to the flux density of impinging corpuscles, but considerably due to the broadening of the energy range of the incoming corpuscles. It may be supported by the fact that severe disturbances frequently are associated with ionospheric black-out. The general feature, discussed above, may be schematically illustrated in Fig. 63.

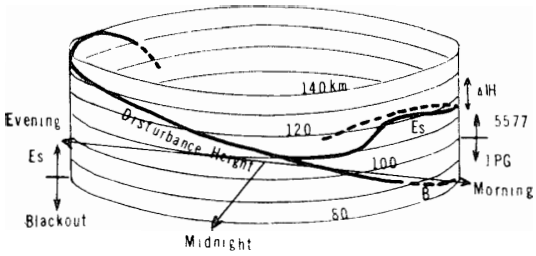

Fig. 63. Schematic illustration of upper atmosphere disturbance phenomena around the auroral zone.

2. Discussions on the inter-relations

Briefly speaking, the inter-relations among disturbances phenomena may be summarized in simple formulae (6–7) and (7–7), in Chapters VI and VII, which seem to be supported by theoretical consideration. The relations may be a direct proof of the magnetic disturbance phenomena to be of ionospheric origin. Even the existence of many factors which modify the "standard" relations, does not affect the conclusion for the magnetic disturbance of ionospheric origin except *Pg*II. The situation has been already illustrated in Fig. 33, where the physical causality with each other of the disturbance phenomena are shown in a simple schematic diagram. It may be mentioned now that the relationship among $foEs$, $|\triangle H|$ and auroral zenith luminosity of λ5577, their altitude effect being taken into consideration, have been numerically established with a primary disturbing agency of incoming electron stream. The discussion above seems to give us some aspect of the disturbances in the earth's atmosphere though the amount of data is not yet sufficient for establishing a complete understanding of the earth storms. The aspect reached is that, if electron precipitates into the upper atmosphere in the auroral zone, regardless its origin, it excites the atoms and molecules of the upper atmosphere with simultaneous ionization in the lower ionosphere. The

additional ionization results in the increase in electric conductivity and then the additional electric current flows in the lower ionosphere under the action of electric field. Therefore, if a disturbance takes place in the ionosphere, a rather simple relationship may be expected to hold among the magnitudes of the disturbance phenomena, whereas if a disturbance can not be regarded as of ionospheric origin, it may be associated with no considerable phenomena in other kinds of disturbances. There still remain, however, many problems unsolved, *e.g.* the night E layer, auroral emissions other than $\lambda 5577$, electric field impressed, etc. all of which are of importance for the complete understanding of the earth storms. We tentatively proceed here to consider that possibility of electric field $\boldsymbol{E}$ out of the problems mentioned above. As already noted in Chapter VIII, the electric field impressed in the lower ionosphere during magnetic disturbances depends apparently on magnetic activity. The feature of the dependence is found to be quite different at the different ranges of activity, above or below a critical value of $Kp = 5$. The critical value of $Kp = 5$ is in good agreement with the critical value of $\triangle \boldsymbol{H} = 700\gamma$ at Syowa Station, which has been found as shown in the feature of the relationship between $\triangle \boldsymbol{H}$ and J in severe magnetic storms in Fig. 50, or 59. The drift speed of charged particles in the lower ionosphere should be proportional to the electric field impressed. Substituting $\boldsymbol{E}$ in eq. (7–4) by the numerical values shown in Fig. 62, we may estimate the $\triangle \boldsymbol{H}$-J relation in the case of severe storms for the range above $\triangle \boldsymbol{H} = 700\gamma$. The estimated values of $\triangle \boldsymbol{H}/\sqrt{J}$ are found to be in good agreement with the observations, as seen in Fig. 64. This fact suggests that additional

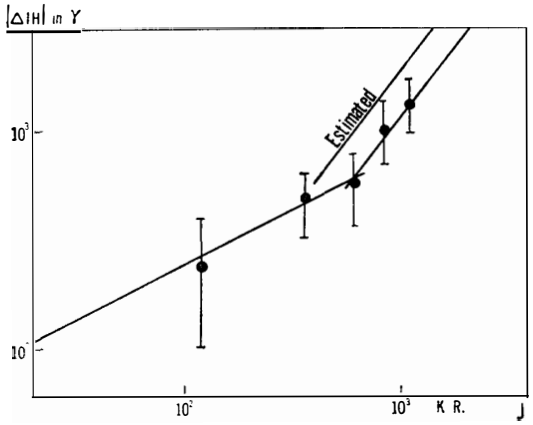

Fig. 64. $\boldsymbol{H} - \mathrm{J}$ relation for severe storms estimated from the drift velocity of dectrons in the lower ionosphere.

electric field may be impressed during severe disturbances of the range over Kp = 5, while below the critical value the electric field remains constant regardless of its origin. What is the physical cause of the additional e.m.f. other than that of dynamo-action in the lower ionosphere? It is improbable that it is due to the increase in wind speed in the lower ionosphere, since the drift speed of charged particles measured by doppler rader[102,103], is comparable with the sound velocity there, and it is quite unlikely that the mass motion exists with a velocity well beyond the sound velocity. It may, therefore, be

quite natural to attribute the e.m.f. to the electric field impressed by net charge separation far from the earth's surface, for example, around cavity surface, transfered near to the surface along the magnetic lines of force. If the field exists, it should of course affect the precipitation of corpuscles, because its potential is of comparable order with the energy of incoming corpuscles. The electric field may be also the cause of the difference of energy of incoming electrons at the different local time in the auroral zones. This has been discussed in the preceding chapter.

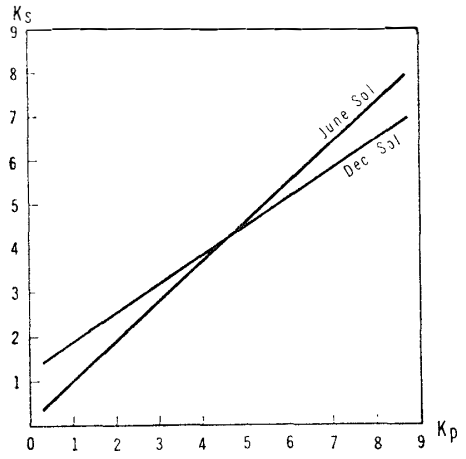

Fig. 65. K at Syowa Station versus Kp.

It must be noted here that there is another evidence for suggesting the existence of a critical value of Kp[104]. It is deduced from comparing K values at Syowa Station with Kp. In reality, one may readily find at a glance of Fig. 65 that the seasonal changes of K value are quite different between the two ranges of K below and above $K = 4.5$. The discussions above may then be briefly summarized now as follows; the small disturbances may be mostly due to the anomalous ionization and excitation in the lower ionosphere under the influence of e.m.f. which is roughly constant, while the severe disturbances may be due to both the anomalous ionization and additional electric field which may be impressed in the lower ionosphere perhaps from the cavity boundary.

XI. CONCLUSION

Throughout the present study, the relationship among the upper atmosphere disturbance phenomena as well as their morphological characteristic was examined in detail, especially with respect to the numerical inter-relations and their spatial distributions. The analysis was carried out by means of the world-wide data so far available, so as to examine the world-wide distribution comprehensively. At the same time, the simultaneous records of each phenomenon at Syowa Station were examined as numerically as possible. The systematic nature of ionospheric and geomagnetic disturbances associated with auroral displays as well as the numerical inter-relations among them is one of the most interesting results, though its physical explanation is not yet satisfactory. It has been suggested that the electric field may be introduced as an important factor to interpret the morphological feature of disturbances and $|\triangle \boldsymbol{H}|$-$J$ relation during high activity. The disturbing agencies, the incoming protons and electrons into the auroral zone, have been also studied to see which is the main agency responsible for the polar disturbances. It has been proved by the observational result that electrons mainly participate in causing the disturbances of such systematic features.

Summarizing the present results, the important conclusion obtained in various problems mentioned above are described as follows;

i) General aspect

The general aspect of the morphology of geomagnetic and ionospheric disturbances and auroral displays in high latitudes shows very systematic features with respect to geomagnetic latitude and local time. The altitude of the level where disturbances take place, as well as the intensity of disturbances, is the most important factor in determining the feature of disturbances. The average characteristic of the world-wide pattern of the disturbance phenomena, *i.e.*, ionospheric and geomagnetic disturbances and auroral displays, are so similar to each other, that they can be regarded to be derivatives of common physical origin even if viewed from only this standpoint of the similitude.

ii) Relationship among the disturbances

There appears to be a strong evidence for the existence of numerical correlation in the magnitude of horizontal disturbance vector of geomagnetic field $|\triangle \boldsymbol{H}|$, the anomalous ionization in the E-region $n_{\max}$ and auroral zenith luminosity of $\lambda 5577$. The close relationship is also a proof for indicating the existence of common physical origin, and they are all found attributable to the anomalous ionization with simultaneous

excitation of the upper atmosphere particles by incoming of electrons (500 ev–30 kev) into the auroral zone. It appears probable that the incoming protons as well as electrons also contribute to detemining the inter-relations. The effect has been neglected, however, in the present paper since there is no observational evidence for the importance of its role.

Though there appears to be some characteristic deviations from the "standard" relationship, they are reasonably explained by integration factor A_s in some cases and by time factor A_t in others. The electric filed E is regarded also as responsible for the deviation in the case of severe magnetic disturbances. Thus the relationship among the disturbance phenomena, with some physically reasonable modifications, is understood to be the numerical relations among the physical quantities expected in the process of energy partition from incoming stream to the upper atmosphere particles.

An exceptional disturbance is *Pg*II, a kind of giant pulsation. It seems essentially to differ from the other geomagnetic variations, since it has no (or inappreciably small) related phenomena in both ionospheric and auroral activity. This may be one of the evidences for proving that *Pg*II is not of ionospheric origin. It must be noted here that the "standard" relationship which is regarded to hold in the case of isolated bay disturbances, may be useful for a criterion to judge whether or not some upper atmosphere variations belong to those of ionospheric origin.

iii) Energy of incoming corpuscles

The local time dependence of the energy spectra of electron stream impinging into the auroral zone, is estimated from the height of the disturbance level in the ionosphere. The appreciable daily change in the level height from 140 km in evening to 110 km in early morning correspond to the change in initial energy of electrons from 500 ev to 10 kev, if fall of disturbance height throughout the night is only due to the change in kinetic energy of incoming particles. The ionospheric blackout which are frequently observed in the morning may be then attributable to the high energy corpuscles probably abundant in the stream precipitating in the morning side of the auroral zone. The flux density is estimated from the observational results to be of the order of 10^8–10^9/cm^2 sec sterad for the ordinary disturbances.

In connection with the local time change in the disturbance height the altitude dependence of the numerical inter-relations among the disturbances is a problem of great importance. There appear to exist some characteristic heights of the level, where certain phenomena may especially predominate compared with the other kinds of phenomena associated. In fact, for example, the level of height about 120 km is found to be more effective for magnetic disturbances than the other levels. Also IPG emission in auroral spectra appreciably predominates below the height of about 100 km, above which it is almost completely masked by intense green line emission of λ5577.

iv) Electric field in aurorae

There are some evidences for the existence of additional electric field, other than that by dynamo-action in auroral forms, though the direct observational proof[105,106] is not yet satisfactory. This existence is suggested in the present paper by three observational results, namely by the anomalous feature of $|\triangle H|$-J relation in the case of severe magnetic disturbances, by increase in drift velocity of electrons in the lower ionosphere with increasing activity, and by the different behaviour of seasonal change

in K indices at their different magnitudes.

The conclusions reached in the present study, although not all complete way, likely provide some information on the mechanism of polar earth storms. In concluding, it is perhaps important to note some problems of great importance which still remain unsolved in the present study. Among them, the physical origin of the world-wide distribution pattern of the corpuscular energy, the origin of the electric field which is found to be impressed in the ionosphere during severe disturbances and the origin of *Pg*II with its mechanism of propagation towards the earth's surface, may be the most fundamental problems, which are directly connected with the origin and the mechanism of the earth storms.

It is desirable to extend the study further on these problems in order to give us a new knowledge towards a complete understanding of the earth storms.

Acknowledgements

All of the present work has been carried out under the direction of Prof. T. NAGATA. In concluding, the author wishes to express his most hearty gratitude to Prof. T. NAGATA for his constant guidance since the very beginning of the author's study of the upper atmosphere throughout the Antarctic Research Expeditions. He also wishes to thank Dr. T. RIKITAKE of the Earthquake Research Institute, the University of Tokyo for his kind encouragement and advice for preparing the upper atmosphere observations at Syowa Station. The writer cordially acknowledges the valuable discussions and advice rendered by Dr. N. FUKUSHIMA. Some of the ionospheric and auroral data used in the present study were kindly made available by Mr. N. WAKAI, Radio Research Laboratory, and by Mr. J. NAKAMURA, College of General Education, Tokyo University, to whom the author is very grateful. He is also indebted to all members of the third wintering party at Syowa Station for their fruitful discussions and comments. The writer's hearty thanks are due to Mr. H. MAEKAWA for his kind assistance in preparing this paper. Finally, he acknowledges the valuable discussions and criticisms given by all of his colleagues in Prof. NAGATA's Laboratory, Messrs. N. MATUURA, T.TOHMATSU, R. MAEDA, M. OSHIO, A. NISHIDA, S. KOKUBUN and E. KANEDA.

References

1) C. Störmer: Arch. Sci. Phys., a, **24**, 5, 113, 221, 317 (1907).
2) C. Chree: Proc. Phys. Soc., **39**, 389 (1927).
3) A. W. Lee: Met. Office Professional Note, No. 56, Roy. Soc. London (1930).
4) F. T. Davies: Terr. Mag., **40**, 267, 456 (1935).
5) B.W. Currie and H.W. Edwards: Terr. Mag., **41**, 265 (1936).
6) J. M. Stugg: "British Polar Year Exp. Fort Rae, 1932–33", **1**, 127, Roy. Soc. (1937).
7) K. Birkeland: Arch. Sci. Phys., **1**, 497 (1896).
8) A.B. Meinel: Astrophys. Journ., **113**, 50 (1951).
9) G.W. Gartlein: Nature, **167**, 277 (1951).
10) L.R. Davis, O.E. Berg and L.H. Meredith: Rep. 1st International Space Res. Symp., Nice (1960).
11) C.E. McIlwain: Journ. Geophys. Res., **65**, 2727 (1960).
12) T. Obayashi and Y. Hakura: Journ. Radio Res. Labor., **7**, 27 (1960).
13) T. Obayashi and Y. Hakura: Rep. Ionos. Res. Japan, **14**, 427 (1960).
14) J.A. Van Allen, G.H. Ludwig, E.C. Ray and C.E. McIlwain: Jet Propulsion, **28**, 588 (1958) etc.
15) V.I. Krassovsky, Y.M. Kushnir, G.A. Vordovsky. G.F. Zokharov and E.M. Svetlisky: Artificial Satelites of the Earth, No. 2. 82, Publ. Akad. Nauk. SSSR, Moscow (1958) etc
16) J.A. Van Allen and L.A. Frank: Nature, **183**, 430 (1959); Nature, **184**, 219 (1959).
17) P. Rothwell and C.E. McIlwain: Journ. Geophys Res., **65**, 799 (1960).
18) R.L. Arnoldy, R.A. Hoffman and J.R. Winkler: Journ. Geophys, Res., **65**, 1361 (1960).
19) J.H. Meek: Journ. Geohys. Res., **58**, 445 (1958).
20) H.W. Wells: Terr. Mag. **52**, 315 (1947).
21) J.P. Heppner, E.E. Byrne and A.E. Belon: Journ. Geophys. Res., **57**, 121 (1952)
22) W. Stoffregen: Journ. Atoms. Terr. Phys., **13**, 167 (1958).
23) S. Chapman: Proc. Roy. Soc., A, **95**, 61 (1918).
24) S. Chapman and V.C.A. Ferraro: Terr. Mag., **36**, 77, 171 (1931); **37**, 147 (1932)
25) S. Chapman and J. Bartels: *Geomagnetism,* Oxford (1940).
26) E.H. Veetine and S. Chapman: Terr. Mag., **43**, 261 (1938).
27) L. Harang: Terr. Mag, **51**, 353 (1946).
28) H.W. Newton: Mon. Not. Roy. Astr. Soc. Geophys. Suppl., **5**, 159 (1948).
29) T. Nagata: Journ. Geophys. Res., **55**, 127 (1950).
30) E.H. Vestine: Trans. Washington Meeting, ATME, IUGG, 360 (1940).
31) N. Fukushima: Journ. Fac. Sci. Univ. Tokyo, sec. II, **VIII**, part V, 293 (1953).
32) Y. Kato and S. Akasofu: Sci. Rep. Tohoku Univ., Ser. V, **7**, 103 (1956).
33) J.W. Dungey: *Electrodynamics of the Outer Atmosphere, The Physics of the Ionosphere,* 229, Phys. Soc. London (1955).
34) M. Eschenhagen: Terr. Mag., **2**, 105 (1897).
35) G. Angenheister: Terr. Mag., **25**, 26 (1920).
36) V.A. Troitskaya: IAGA Symposium, Utrecht (1959).
37) A.G. Kalashnikov: Proc., IAGA Symposium, Utrecht (1959).
38) J.A. Jacobs and K. Sinno: Sci. Rep., No. 2 Contract No. AF19(604), 4068, Geophys. Lab., Univ. British Columbia (1960).
39) J.A. Jacobs and K. Sinno: Journ. Geophys. Res., **65**, 107 (1960).
40) T. Obayashi: Journ. Radio Res. Lab., **6**, 375 (1959).
41) L.V. Berkner and S.L. Seaton: Terr. Mag., **45**, 393 (1940)
42) H. Uyeda and Y. Arima: Rep. Ionos. Res. Japan, **6**, 1 (1952).

43) E.V. Appleton and W.R. Piggot: Nature, **165**, 130 (1950); Journ. Atoms. Terr. Phys., **2**, 236 (1952).
44) N. Fukushima and T. Hayashi: Rep. Ionos. Res. Japan, **6**, 133 (1952).
45) T. Obayashi, S. Suzuki and Y. Fujii: Mem. Wakkanai Radio Wave Obs., **2**, 15 (1951).
46) K. Sinno: Rep. Ionos. Rep. Japan, **7**, 7 (1953).
47) D.F. Martyn: Proc. 2nd Meeting Mix. Comm. Ionosphere, 49 (1951).
48) J.H. Meek: Journ. Geophys. Res., **57**, 117 (1952).
49) T. Nagata and T. Oguti: Rep. Ionos. Res. Japan, **7**, 21 (1953).
50) E.V. Appleton: Proc. Roy. Soc., A, **162**, 451 (1937); Quar. Journ. Roy. Met. Soc., **65**, 324 (1939).
51) J.C. Seddon, A.D. Picker and J.E. Jackson: Journ. Geophys. Res., **59**, 513 (1954).
52) B. Landmark: Journ. Atoms. Terr. Phys., **12**, 79 (1958).
53) J.P. Heppner: Defence Research, Board, Canada Rep., DR 135 (1958).
54) K. Davies: Journ. Geophys. Res., **65**, 2285 (1960).
55) W. Stoffregen, H. Derblom and A. Omholt: Journ. Geophys. Res., **65**, 1699 (1960).
56) A. Omholt: Journ. Atoms. Terr. Phys., **7**, 73 (1955).
57) R.W. Knecht: Journ. Geophys. Res., **61**, 59 (1956).
58) E.K. Smith: Natl. Bur. Standards, Circ., **582** (1956).
59) J.A. Thomas and E.K. Smith: Journ. Atoms. Terr. Phys., **13**, 295 (1959).
60) J. Egedal: Meteorologie, **13**, 301 (1937).
61) C. Störmer: Terr. Mag., **18**, 133 (1913); **20**, 1, 158 (1915); **21**, 45, 153, 157 (1916).
62) L. Vegard and Krogness: Geofys. Publ. (Oslo), **1**, No. 1 (1920).
63) C. Störmer: Geofys. Publ., **4**, No. 7 (1926); Z. Geophys., **6**, 463 (1930); *The Polar Aurora*, Clarendon, Oxford (1955).
64) L. Vegard: Phil. Mag., **23**, 211 (1912).
65) B.W. Currie and H.W. Edwards: Terr. Mag., **39**, 293 (1934).
66) H.T. Stetson and C.F. Brooks: Terr. Mag., **47**, 21 (1942).
67) B.W. Currie: Canad. Journ. Phys., **33**, 773 (1955).
68) J.M. Malville: Journ. Geophys. Res., **64**, 1389 (1959).
69) B.W. Currie, P.A. Forsyth and F.E. Vawter: Journ. Geophys. Res., **58**, 179 (1953).
70) N.C. Gerson: Proc. Roy. Soc., B, **68**, 408 (1955).
71) A.B. Meinel: Mem. Soc. Roy. Sci. Liège, **12**, 203 (1952).
72) C.W. Gertlein: Mem. Soc. Roy. Sci. Liège, **12**, 195 (1952).
73) R. Montalbetti and A.V. Jones: Journ. Atmos. Terr. Phys. **11**, 43 (1957).
74) J.P. Hepner: Journ. Geophys. Res., **59**, 329 (1954); **60**, 29 (1955).
75) C.W. Gartlein: Ann. Geophys., **15**, 31 (1959).
76) R.C. Bless, C.W. Gertlein, D.S. Kinbell and C. Sprague: Journ. Geophys. Res., **64**, 949 (1959).
77) A.B. Meinel, B.J. Negaard and J.W. Chamberlain: Journ. Geophys. Res., **59**, 407 (1954).
78) D. Barbier: Ann. Geophys. **14**, 334 (1958).
79) T. Tohmatsu and T. Nagata: Rep. Ionos. Space, Res. Japan, **14**, 301 (1960).
80) T. Oguti: Rep. Ionos. Space Res. Japan, **14**, 291 (1960).
81) D.R. Bates: Proc. Roy., A, **196**, 217 (1949); Mon. Roy. Astr. Soc., **112**, 614 (1952).
82) A. Omholt: Journ. Atoms. Terr. Phys., **5**, 243 (1954).
83) D.M. Hunten: Journ. Atoms. Terr.Phys., **7**, 141 (1955).
84) M.H. Rees: Journ. Atmos. Terr. Phys., **14**, 325 (1958).
85) W.B. Murcray: Journ. Geophys. Res., **64**, 995 (1959).
86) L.W. Wallace and R.W. Nicholls: Journ. Atoms. Terr. Phys., **7**, 101 (1955).
87) F.E. Roach and M.H. Rees: Journ. Geophys. Res., **65**, 1489 (1960).

88) F.E. Roach: Journ. Geophys. Res., **65**, 1495 (1960).
89) J.W. McCaulley, F.E. Roach and S. Matsushita: Journ. Geophys. Res., **65**, 1499 (1960).
90) F.E. Roach, J.W. McCaulley, E. Marovich and C.M. Purdy: Journ. Geophys. Res., **65**, 1503 (1960).
91) L. Harang: Geophys. Publ., **16**, No. 6 (1946).
92) A.P. Mitra and R.E. Jones: Journ. Geophys. Res., **59**, 391 (1954).
93) K.D. Cole: Aust. Journ. Phys. **13**, 484 (1960).
94) T. Nagata and S. Abe: Rep. Ionos. Res. Japan, **9**, 39 (1955).
95) J.A. Jacobs and T. Obayashi: Geofis. pura e appl., **34**, 21 (1956).
96) C.G. Little and A. Maxwell: Journ. Atoms. Terr. Phys., **2**, 356 (1952).
97) A Maxwell and C.G. Little: Nature, **169**, 746 (1952).
98) A. Hewich: Porc. Roy. Soc., A, **214**, 494 (1952).
99) A. Maxwell and M. Dagg: Phil. Mag., **45**, 551 (1954).
100) A. Maxwell: Proc. Roy. Astr. Soc., London, **3**, 65 (1954); Rep. Phys. Soc. Conf. Cambridge, 166 (1955).
101) J.H. Chapman: Canad. Journ. Phys., **31**, 120 (1953).
102) K.L. Bowles: Journ. Geophys. Res., **59**, 553 (1954).
103) B. Nichols: Journ. Atoms. Terr. Phys., **11**, 292 (1957).
104) T. Oguti: Antarctic Record (Rep. Japanese Antarctic Res. Exp.), No. 11 (1960).
105) K.L. Sherman: Trans. Geophys. Union, **15**, 141 (1934).
106) J. Scholz: Gerlands Beitr. Geophys., **44**, 145 (1935).

(Manuscript received September 27, 1962)